

Electronic Differential System for Electric Vehicles

March 2023

Matthew Youngman (PM), Nathaniel
Owen, Sam Berry, Henry Wong, Finlay
Sanderson, Christian Garry

Project ID: GLIKR1

Project Supervisors:
Grant Ingram
Ken Ridgeway

Final Design Report - GLIKR1: Electronic Differential

Matthew Youngman (PM), Nathaniel Owen, Sam Berry, Henry Wong, Finlay Sanderson, Christian Garry

March 2023

Executive Summary

Since their invention in 1827, mechanical differentials have been the dominant engineering solution for controlling wheel torque distribution in vehicles. Although effective in their function, mechanical differentials are heavy and inefficient. With the rapid growth of the electric vehicle market, demand from drivers and governing bodies for improved range and efficiency in electric vehicles has increased drastically. This has pressured car manufacturers to seek lighter and more efficient systems, and this report presents a solution in the form of an electronic differential.

The designed electronic differential will be integrated into a multi-motor electric vehicle to control the torque delivered to each wheel individually, with the system having the capacity to function on both 2 or 4 wheel drive vehicles. It will be implemented using a bespoke Electronic Control Unit (ECU) and a designed Variable Frequency Drive (VFD), with one VFD per motor. These will be self-contained units sold to car manufacturers on contract based employment.

The ECU determines the torque distribution by building a model of the current vehicle dynamics using sensor signals, conditioned for reliability to a signal to noise ratio of 66dB. Comparison of this model with the driver demands provides full user control, and an undetectable sliding mode yaw rate controller corrects the non-linear dynamics within 0.45s. Computation on the ATSAME54P20A-VAO microcontroller has a reduced latency of 12ms for fast response.

Communication of the required torque distribution to the VFDs provides means of actuation of the motors. Application to an 800V system, as well as regenerative braking integration improves power losses up to 25%. Driver preferences for regenerative braking scaling and differential type enhances the user experience.

Final calculations place the mass of the electronic differential at 2.5kg, which represents around 4% of the mass of a standard mechanical differential. The majority of this mass consists of the housing

for the ECU and VFDs, which have been comprehensively stress tested to ensure they are fit for purpose. This reduced mass demonstrates the value that this system can add to the differential market, as this solution simulates the function of a mechanical differential whilst reducing the weight of the overall vehicle. Current estimates suggest that this weight reduction can lead to an increase of 4.2% in electric vehicle driving range.

Initial debt financing will be £1 million, at a predicted 12% interest rate. Current forecasts estimate a net profit of over £2 million by the end of the third year of operation, with roughly 7,000 sales per year at the end of this period.

Executive Summary	2
List of Tables	5
List of Figures	5
Nomenclature	8
1 Introduction	9
2 Product Decomposition	11
3 Technical Summary	12
3.1 Integration into vehicle	13
3.1.1 Communication	13
3.1.2 Interrupt System	14
3.2 Electronic Control Unit	15
3.2.1 Microcontroller	16
3.2.2 AUTOSAR Software Architecture	17
3.2.3 Connector	18
3.2.4 CAN Transceiver	18
3.2.5 Signal Conditioning	19
3.2.6 Voltage Regulating Circuits	21
3.2.7 Protection Circuits	22
3.2.8 Thermal and Mechanical Considerations	23
3.2.9 Future-Proofing	23
3.3 Control Algorithm	23
3.3.1 Overarching Control Structure	24
3.3.2 Vehicle State Models	25
3.3.3 Stability Control Module	27
3.3.4 Torque Distribution Module	31
3.3.5 Regenerative Braking	32
3.3.6 Adjustable Regenerative braking - No Pedal Depression	34
3.4 Housing, Fixing and Casing of the Electronic Control Unit	35
3.4.1 Location	35
3.4.2 Stress Analysis	36
3.4.3 Material Choice	40
3.4.4 Fixing	40
3.5 Variable Frequency Drive	42
3.5.1 Variable Frequency Drive Circuit	42

3.5.2	Control Signal Generation	43
3.5.3	Electronic Control Unit Signal Minimisation Circuit	44
3.5.4	Printed Circuit Board	45
3.6	Housing, fixing and casing of the Variable Frequency Drives	45
3.6.1	Variable Frequency Drive Cooling	46
3.6.2	Shedding force analysis	50
3.7	Connections	53
4	Design for Manufacture	54
4.1	Manufacture of Casing	54
4.2	Aluminium Fin Heat Sink	55
4.3	PCB Manufacturing	55
5	Design for Sustainability	56
6	Final Product	57
7	Business Case	58
7.1	Cost and Profit Structure	59
7.2	Financing	59
7.3	Sales Forecast	60
7.4	Target vehicle Manufacturers	61
7.5	Market Analysis	62
7.6	Competitor Analysis	62
8	Project Schedule	64
9	Risk Assessment	64
10	Code of Practice	65
11	Discussion	67
12	Conclusion	68
References		69
Appendices		74

List of Tables

1	User Required Specification	10
2	Variables For Stability Control Algorithm	30
3	Torque output mechanism design criteria	42
4	VFD Circuit Components	45
5	Thermal Conductivity	48
6	Die Casting Vs. CNC	54
7	Sales and Financial Forecasts	61
8	Risk Analysis	65
9	Code of Practice	66

List of Figures

1	Standard Mechanical Differential	9
2	TorqueDrive Product	11
3	Product Streams	12
4	Flow Process	13
5	Generalised CAN Bus	14
6	Standard CAN Frame [3]	14
7	The isometric view of the final PCB design	15
8	The top view of the final PCB design with certain components highlighted	16
9	Bottom View Of The Final PCB Design	18
10	Single Supply Load Cell Amplifier	19
11	Common and Differential Mode Filter	21
12	The schematics of the decoupling circuit for the microcontroller [4]	22
13	Control Algorithm Flow Process	23
14	Control Algorithm Modules	24
15	2 Degree of Freedom Bicycle Model	25
16	Non-linearity of lateral force with sideslip angle	28
17	Sliding Mode Control Schematic	29
18	Sliding Mode Control Simulation Results	30
19	Vehicle Braking Logic Diagram	33
20	Torque-Speed Characteristics	33
21	Regenerative Braking - Battery SOC	34
22	Final location for ECU casing (highlighted in blue)	35
23	Longitudinal View of CAD ECU Casing Prototype.	36
24	ECU Casing Vibrational Stress	37

25	ECU Casing Vibrational Stress Displacement	37
26	ECU Casing Impact Stress	38
27	ECU Casing Impact Stress Displacement	39
28	ECU Casing Vibrational Stress Fatigue	39
29	Metric Grade 10.9 bolts	41
30	Fixing Method for the ECU	41
31	VFD Circuit	43
32	VFD PWM Signal Generator Circuit	43
33	PWM Duty Cycle	44
34	Signal Minimisation Circuit	44
35	VFD Housing	45
36	VFD Casing Vibrational Stress Analysis Displacement	46
37	Fin Structure	47
38	PCB Cooling Fins Inside VFD Casing	47
39	Heat Transfer Model	48
40	CFD For Airflow In Cooling System	49
41	Fin Wall Temperature	50
42	Shedding Force On Singular Aluminium Fin	51
43	FEA On Singular Fin	52
44	Cables and receptacle housing connecting to the ECU	53
45	Final Location of the ECU and VFDs within the reference vehicle	57
46	BOM Breakdown For ECU, 4 VFD Units and Wiring	59
47	Product Sales Forecasts	60
48	Revenue, Gross Profit and Net Profit Forecasts	61
49	Rivian R1T Differential System.	63
50	Gantt Chart	64

Nomenclature

EV - Electric vehicle	SCM - Stability Control Module
ICE - Internal Combustion Engine	DoF - Degree of Freedom
SUV - Sport Utility vehicle	δ - Delta, radians
IP - Intellectual Property	β - Beta, radians
ECU - Electronic Control Unit	γ - Gamma, rad/s
VFD - Variable Frequency Drive	PID Controller - Proportional, Integral and Differential Controller
PCB - Printed Circuit Board	λ - Scaling Coefficient for the error,e
RFI - Radio Frequency Interference	e - Error between desired yaw rate and measure yaw rate
RTI - Referred-to-input	σ - Magnitude of the disturbance to the control algorithm
ABS - Anti-lock Brake System	EBD - Electronic Braking Distribution
FoS - Factor of Safety	SOG - State Of Charge
CNC - Computer Numerical Control	P - Number of poles in an induction motor
SMC - Sliding Mode Control	CAD - Computer Aided Design
PWM - Pulse Width Modulation	MPa - Mega Pascals
kWh - Kilowatt hours	AA7075 - Aluminium Alloy 7075
m - metres	g - grams
mm - millimetres	SAE - Society of Automotive Engineers
cm - centimetres	ASTM - American Society for Testing and Materials
μm - micrometres	AC - Alternating Current
kph - Kilometres per hour	3D - Three Dimensional
mph - Miles per hour	CFD - Computational Fluid Dynamics
v - Volts	A - Amps
CAN - Control Area Network	K - Kelvin
FD - Flexible Data	δx - Layer Thickness
EIC - External Interrupt Controller	k - Thermal Conductivity
IC - Integrated Circuit	q - Heat Transfer per unit area
LIN - Local Interconnect Network	N - Newtons
G - Gain	FEA - Finite Element Analysis
Ω - Ohms	HVIL - High Value InterLock
DC - Direct Current	W - Watts
Hz - Hertz	PCBA - Printed Circuit Board Assembly
LDO - Linear low DropOut	CO2 - Carbon Dioxide
ESD - ElectroStatic Discharge	
EMI - ElectroMagnetic Interference	
ETM - Embedded Trace Macrocells	
DVSM - Desired Vehicle State Model	

tCO ₂ e/t - Expected tonnes of Carbon Dioxide per tonne of material	σ_β - Disturbance to sideslip angle, rad
R&D - Research and Development	σ_λ - Disturbance to yaw, rad s ⁻¹
BoM - Bill of Materials	rpm - Revolutions per minute
£ - Great British Pounds	n_s - Motor stator speed, rpm
CAGR - Compounded Annual Growth Rate	f_s - Supply frequency, Hz
CPU - Central Processing Unit	\dot{x} - First derivative of x
VOCs - Volatile Organic Compounds	M_Z - External yaw moment
CoG - Centre of Gravity	β_{des} - Desired steering angle
L_f - Length from front wheel to CoG, m	γ_{des} - Desired yaw rate
L_r - Length from rear wheel to CoG, m	V - Vehicle velocity
m - Vehicle Mass, kg	ADC - Analogue to Digital converter
c_f - Front wheel cornering stiffness, N rad ⁻¹	r - Driver Control Dynamics
C_r - Rear wheel cornering stiffness, N rad ⁻¹	s - Sliding Surface
I_Z - Moment of Inertia, m ⁴	x_{des} - Desired Vehicle Dynamics
ISO - International Organisation for Standardisation	u - Reaching Law
AUTOSAR - AUTomotive Open System ARchitecture	

1 Introduction

The global Electric vehicle (EV) market is forecast at a 22% compounded annual growth rate until 2030. With legislation banning the sales of new internal combustion engine (ICE) cars after 2030 in the UK (and many other countries following suit), vehicle manufacturers are investing record amounts of capital into new EV technology to improve on existing functional systems. In particular, the increasing demand for efficiency and range within the EV market creates an opportunity to improve existing systems. The mechanical differential functions to deliver different torque values to individual wheels for improved turning stability and traction. However, the heavy and inefficient mechanical differential requires an alternative solution to reduce any power losses and increase range. Figure 1 shows an example mechanical differential. This report presents

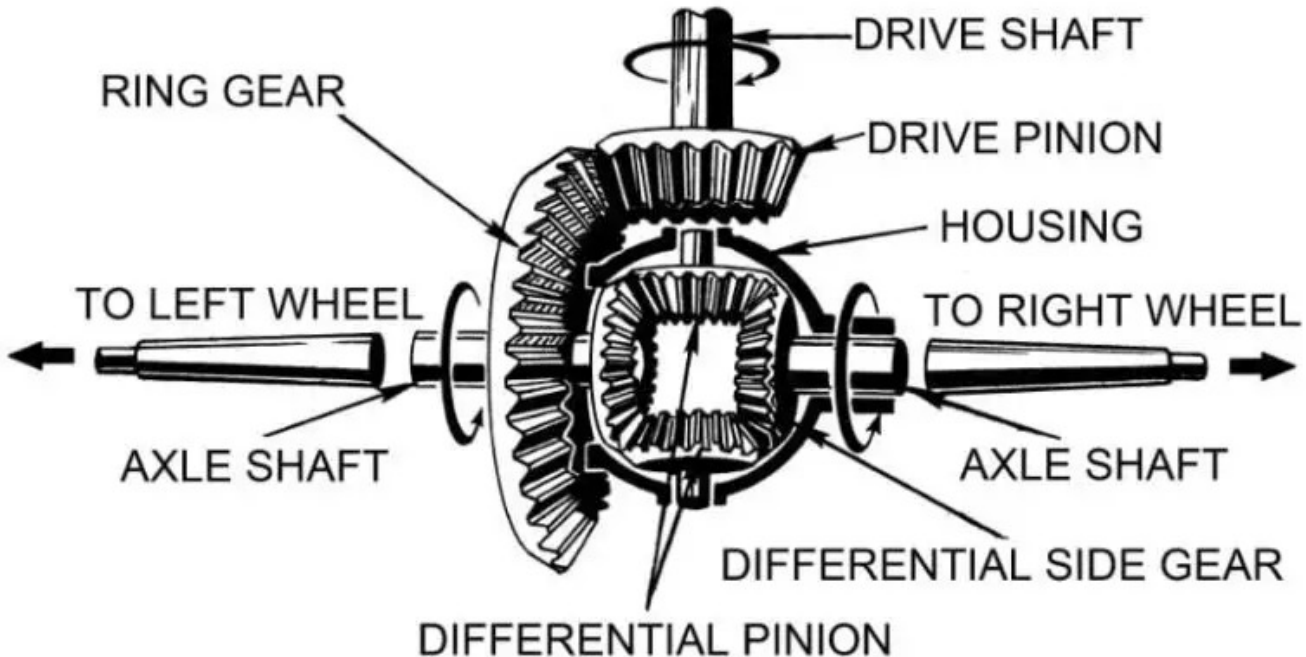


Figure 1: Standard Mechanical Differential [1]

an efficient electronic differential system which simulates and improves on the functionality of a mechanical differential. Specifics regarding the desired characteristics for the replacement system can be seen in Table 1. Further, the report outlines TorqueDrive's credible business strategy for selling its electronic differential within the EV market. The product outlined in this report is designed for a four-motor electric sport utility vehicle (SUV), with each motor responsible for the independent control of one wheel. The electric SUV is chosen as the vehicle market is forecast to have a 25.5% compound annual growth rate up until 2030 [2]. A four-motor system also provides opportunity for a better control and performance design of the electronic differential, allowing torque control both longitudinally and laterally.

User Condition/Benefit	Project Specific	Description
1. Safety	1.1. Matches safety regulations 1.2. Allows interrupts from other safety systems within vehicle 1.3. Fail safe mode in event of an accident 1.4. Must not put vehicle into unstable vehicle dynamics	Regulations such as 'ISO26262' ABS system can override torque control system within 0.1 seconds System removes torque control from 4 motors after interrupt noting crash Control system preventing understeer/oversteer developments below 55mph
2. Reliability	2.1. Mechanical housing capable of withstanding significant impacts 2.2. Water and dust resistance 2.3. Automotive grade electronic components	ECU and VFD housing capable of withstanding a 37.2823mph (60kph) crash Achieving IP57 standard Most components meet AEC-Q100 standard
3. Functionality	3.1. Regenerative braking system capable of bringing vehicle to near stop 3.2. Torque control across all motors and improved efficiency from mechanical differential 3.3. Tangible weight reduction and efficiency benefits over a standard mechanical differential.	Braking distance of 14.5 m from 30 mph to a stop Efficiency improved by 30% Weigh less than 10% of a standard electronic differential.
4. Sustainability	4.1. Place large emphasis on sustainability when making material choices 4.2. Consider end of life for the product	EEA guidelines suggest that automotive companies should aim for >40% of waste to be recyclable. Ease of deconstruction at end of life, requiring no specialised heavy machinery
5. Adaptability	5.1. Aim for the system to be easily interchangeable between vehicle types 5.2. Ensure the system can be easily adapted to any new rules and regulations that come into force 5.3. Software Architecture 5.4. Custom circuit design	2- and 4-wheel drive capability across range of vehicle types e.g. SUV, New Security compliance regulations (2023) Use AUTOSAR to make software more future-proof Meet manufacturer specific requirements
6. Ease of integration/use	6.1. Communication with vehicle subsystems 6.2. No reconfiguration required by vehicle manufacturer	SAE J1939 CAN communication standard Plug and play
7. Cost	7.1. Minimise labour service required for component manufacture 7.2. Consider scalable manufacture process in design	Use standard manufacturing processes such as CNC. Use standard parts where possible and minimise cost when designing custom parts.

Table 1: User Required Specification

The integration of the electronic differential into the vehicle is a significant design challenge, and to keep customer options as open as possible, flexibility in the implementation to a range of vehicles is maximised and considered during solution development. Therefore, TorqueDrive is not limited to the SUV market and can follow emerging trends and technologies accordingly. Also, as the EV industry evolves, creating a future proof product will require careful consideration of regulations from the governing bodies such as the International Organisation for Standardisation (ISO).

2 Product Decomposition

Designing the software, sold as Intellectual Property (IP), to achieve the functionality of an electronic differential was considered, where the control software would be flashed onto a microcontroller. However, this design solution was disregarded due to the lack of added value. This stems from the IP's reliance on another company's hardware rather than the vehicle manufacturers directly, reducing the size of the target market. For these reasons, TorqueDrive will sell the hardware unit with the software included directly to vehicle manufacturers, and all the necessary wiring.

The main components of TorqueDrive's electronic differential are an Electronic Control Unit (ECU) and a Variable Frequency Drive (VFD) unit per motor as shown in Figure 2.

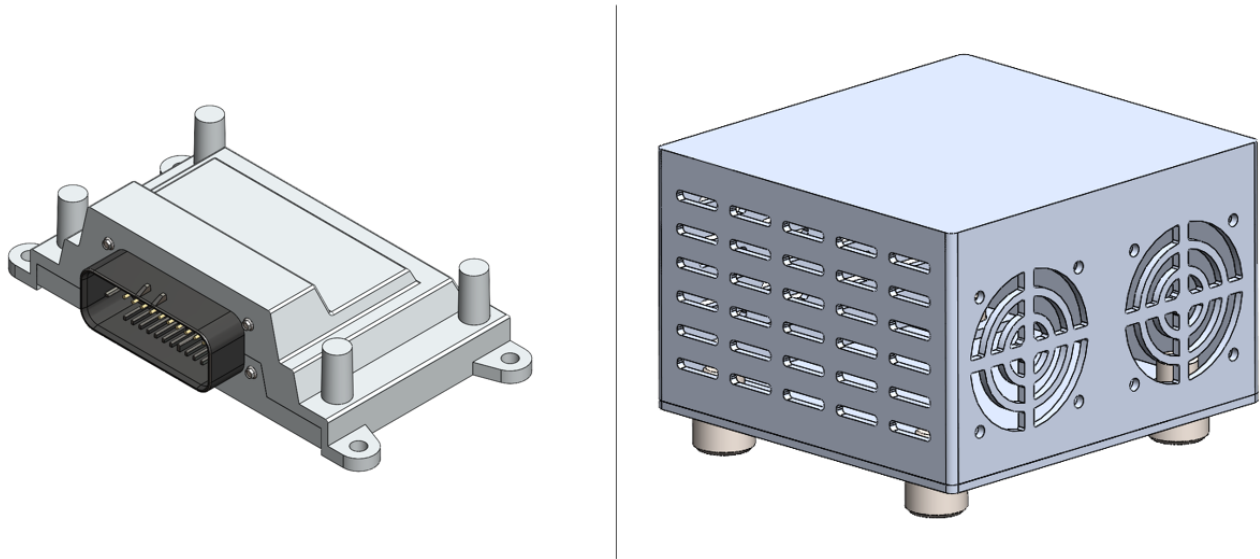


Figure 2: TorqueDrive's Product, ECU unit (left) and VFD unit per motor (right)

This ECU acts to intelligently relate the system inputs to the outputs, providing calculations to determine the torque distribution necessary. TorqueDrive's ECU will be integrated into an existing network of ECUs within the vehicle. Selling a separate ECU allows for easier maintenance

and upgrades, as the ECU is self-contained. Furthermore, there is no requirement for vehicle manufacturers to alter any existing subsystems. The addition of the ECU to the vehicle will have minimal interference, leaving other subsystems unchanged.

VFDs were chosen as the means of converting the theoretical torque outputs generated by the ECU to an actual change in torque on the individual motors. An in-house VFD was designed as no 800V systems are currently available on the market. However, 800V EVs are anticipated to be the future technology due to reduced power loss associated with higher voltage systems. This also has the added benefits of being cheaper than purchasing VFDs on the market and with consideration to the design criteria in mind.

3 Technical Summary

In order to design a functional electronic differential, the Porsche Macan SUV has been chosen as a reference vehicle due to its recent electric vehicle conversion. The internal layout and dimensions have been used to prove the product integrates well with minimal disturbance into the vehicle. However, TorqueDrive's electronic differential has a flexible design that can be adapted for any EV and is not limited only to the Porsche Macan SUV.

The necessary streams of the ECU and VFD units that have been considered to make a functional electronic differential are shown in Figure 3. Highlighted in blue are streams that have been designed and outlined in this report. Highlighted in orange are the parts of the solution which utilise pre-existing technology.

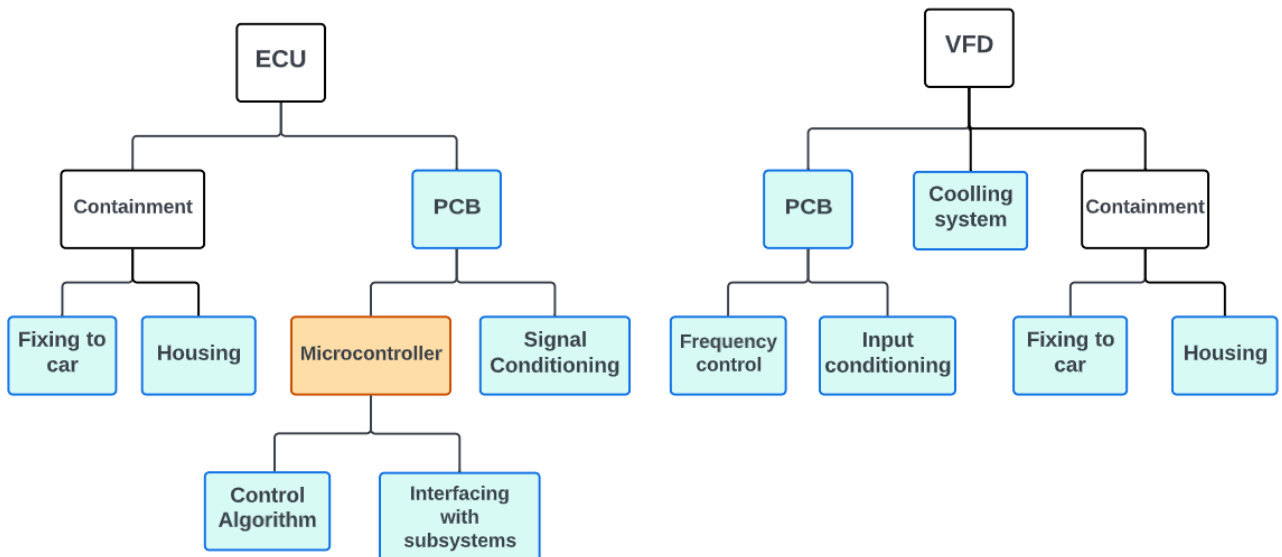


Figure 3: Product Streams

The flow process between the electrical systems is shown in Figure 4. Values for the vehicle dynamics and current state are measured from pre-existing sensors, which are connected to the ECU through a utilised communication network. Input manipulation and signal conditioning provides reliable sensor signals to the microcontroller, all of which is embedded within the ECU's electronics. The control algorithm will then perform necessary calculations, based on sensor values, to produce the desired torque distribution, which will be communicated to the VFDs. The VFDs then control motor speed to produce the desired torque.

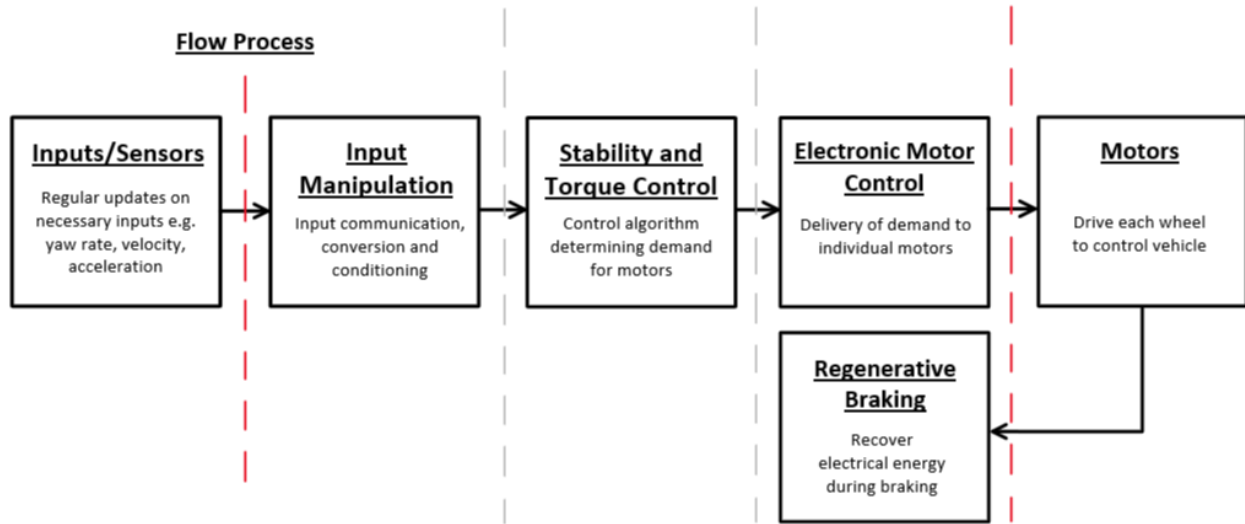


Figure 4: Flow Process

3.1 Integration into vehicle

3.1.1 Communication

Nathaniel Owen, Henry Wong

To evaluate the current vehicle state, data must be obtained using existing sensors, which interface with the torque distribution ECU. Therefore, designing an adaptable system is crucial. Sensors can have varying output types; they can use analogue signals, digital signals, or be transmitted using the CAN bus.

A Controller Area Network (CAN) bus is a bidirectional serial communication protocol that allows communication between devices without the need of a host computer. This is the standard system used throughout the automotive industry as point-to-point wiring can be replaced by one serial bus connecting all ECUs.

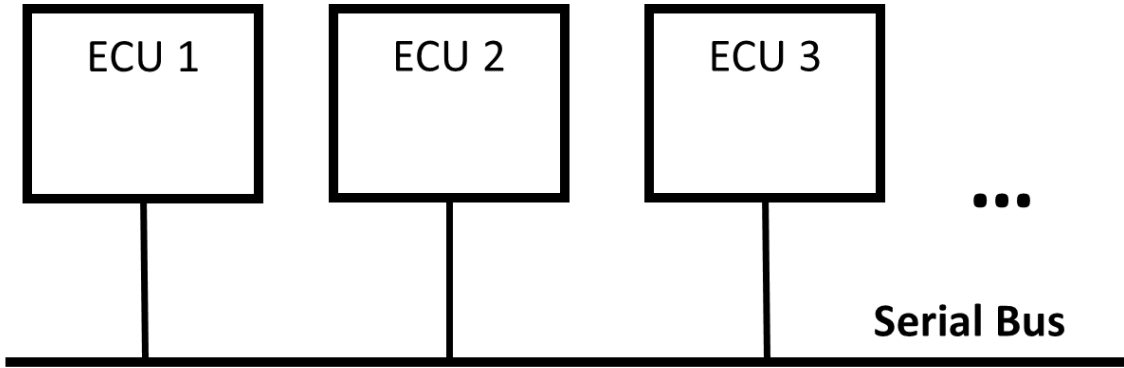


Figure 5: Generalised CAN Bus

Messages on the bus are called CAN frames, as shown in figure 6. The 11 bit identifier represents the priority of the messages. A CAN flexible data (FD) frame has a data section of 64 bytes instead of 8 bytes as in a standard CAN frame, allowing for faster communication.

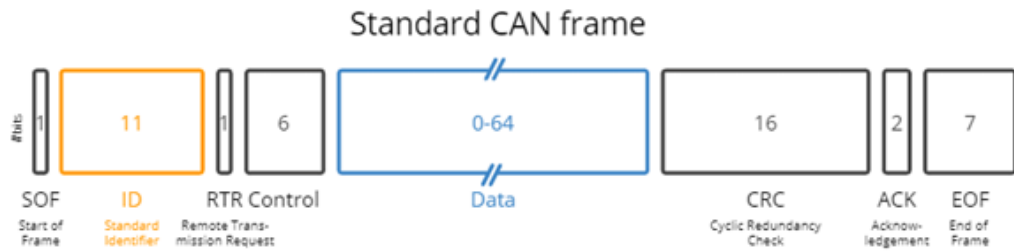


Figure 6: Standard CAN Frame [3]

3.1.2 Interrupt System

Nathaniel Owen

Whilst the differential system will control the torque of the wheels continuously under normal driving conditions, most modern vehicles use an anti-lock brake system (ABS) in the interest of driver safety. The ABS prevents the wheels from locking up during braking, allowing the driver to maintain control of the vehicle. The system achieves this by modulating the brake pressure on each wheel, preventing skidding, and improving stopping distance.

As this feature only engages in typically dangerous circumstances, it is crucial that the differential system does not affect the function of the ABS and hands over control of the vehicle immediately. To achieve this, the micro-controller will make use of the External Interrupt Controller (EIC). This handover will be immediate and smooth as the differential will be monitoring the slip of each wheel and thus be able to predict excess skidding and therefore be expecting the ABS to engage.

3.2 Electronic Control Unit

Nathaniel Owen, Henry Wong

The Printed Circuit Board (PCB) connects all the electronic components and circuits to ensure they function as a unit. Communications between the microcontroller, integrated circuits (IC) and other electronic components take place within the PCB. The final PCB design is shown in Figure 7.



Figure 7: The isometric view of the final PCB design

Choosing suitable electronic components and designing a custom PCB adds value to TorqueDrive's electronic differential as customers' specific requirements can be achieved. This makes the product adaptable to different vehicles. Further, custom designing of the PCB reduces costs significantly as it will be produced directly from factories, and allows full control of the electronics making troubleshooting, debugging, maintenance and upgrades more convenient. This is essential during the development phase and ensures that TorqueDrive's ECU will not become outdated.

3.2.1 Microcontroller

Henry Wong

The microcontroller acts as the brain of all the electronics. Whilst receiving input data, it computes, according to firmware algorithms, the torque and speed output values for each motor. These outputs will then be converted into the correct digital format so that they can be sent to the motors for execution.

An ideal microcontroller will provide sufficient performance without excessive costs. Highlighted in red in Figure 8, the final microcontroller selected for the ECU is the ATSAME54P20A-VAO, a microcontroller designed by Microchip Technology Inc., specifically for automotive motor control applications. This microcontroller meets the desired specifications for this project and allows some additional leeway for future upgrades.

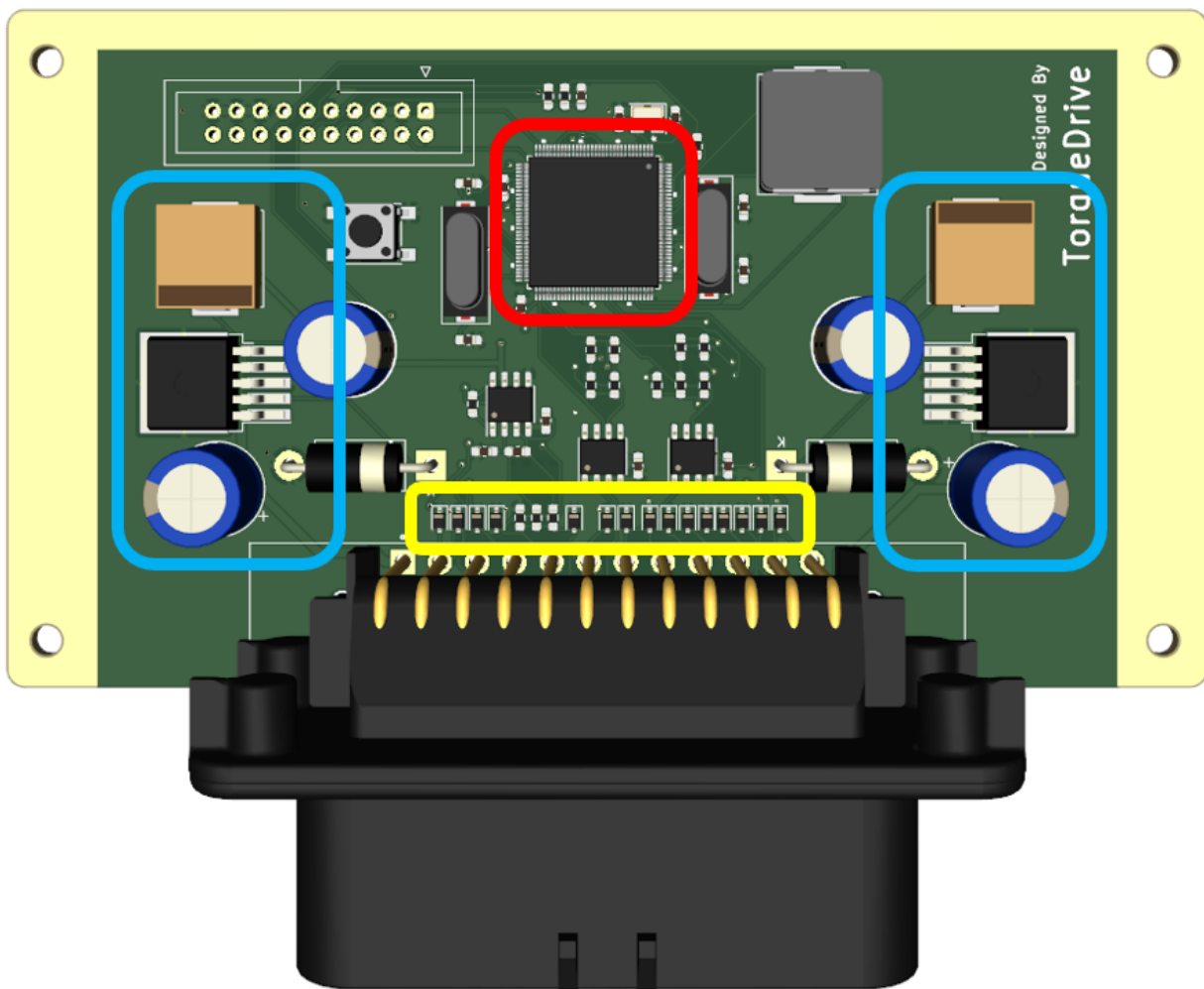


Figure 8: The top view of the final PCB design with certain components highlighted

The VAO version of the ATSAME54P20A has been chosen as it represents automotive standard products, which offers better material selection, "Zero Defect" quality control and safer tests provided by Microchip Technology Inc. The VAO version also meets safety standards such as ISO 26262 and AEC-Q100.

The ATSAME54P20A-VAO features the Arm® Cortex®-M4F CPU architecture [4] which is a highly efficient and low-power embedded processor offering high performance motor control. Processing at 40 MHz, the microcontroller computes with a latency of 12 ms which is faster than the desired specification point .

The chosen microcontroller has a relatively large memory architecture compared to alternatives currently on the market, with 1 MB on-chip EEPROM flash memory and 256 KB on-chip SRAM allowing for more than sufficient memory space for the firmware and future upgrades.

The microcontroller has 144 pins and 32 ADC channels. Therefore, it can accommodate all the necessary sensors inputs as well as outputs to the motors. The microcontroller also supports CAN and Local Interconnect Network (LIN) communication protocols which are widely used by vehicle manufacturers as the interface between different ECUs. With two on-chip CAN FD controllers, it can communicate with high and low speed CAN networks which have become more popular in the automotive industry.

Finally, the ATSAME54P20A-VAO supports AUTOSAR (AUTomotive Open System ARchitecture), which is a software architecture that is recognised within the automotive industry which will make the PCB more standardised, scalable and safer.

3.2.2 AUTOSAR Software Architecture

Henry Wong

To make maintenance and updates easier to implement in the future, a software architecture is required. A simple software architecture divides the development of software into two layers, basic software layer (BSW) and application layer. Using a well-designed software architecture, should future upgrades require changes in hardware, only the basic software layer would need reconfiguration. The software in the application layer can remain unchanged and the microcontroller will still function in the same behaviour, making the software easier to manage in the future.

Automotive Open System Architecture (AUTOSAR) is a standardised software architecture developed by partnership of automotive interested parties, such as vehicle manufacturers, semiconductor and software companies. Various large vehicle manufacturers such as Ford Motor Company, Mercedes-Benz, Volkswagen, etc, use AUTOSAR as it is very appealing. Its advantages include the scalability to different vehicle and platform variants, transferability of software and maintainability during the product lifecycle [5].

3.2.3 Connector

Henry Wong

To allow communications between the microcontroller and external devices, the AMPSEAL series connector has been selected. Manufactured by TE Connectivity with 35 pins, it accommodates all the necessary input and output pins required for external communication. It is designed specifically for automotive application with an interlocking mechanism to ensure that the connection is secure. It also features sufficient dust and water resistance that will be needed (specification 2.2).

3.2.4 CAN Transceiver

Henry Wong

Two CAN transceivers need to be connected between the microcontroller and the CAN bus. When receiving a message from the serial bus, the data stream will first be converted to a readable level. The CAN controller then stores the converted serial bits from the bus until a complete message is received, which can then be fetched by the microcontroller for processing. When transmitting messages, the CPU sends the message to the CAN controller, which then transmits the bits serially onto the bus via the CAN transceiver when the bus is free.

Shown in Figure 9, highlighted in pink, two ATA6561 CAN transceivers are selected as it is an automotive grade high speed CAN transceiver suggested by Microchip Technology Inc [6]. to be used with the ATSAME54P20A-VAO microcontroller.

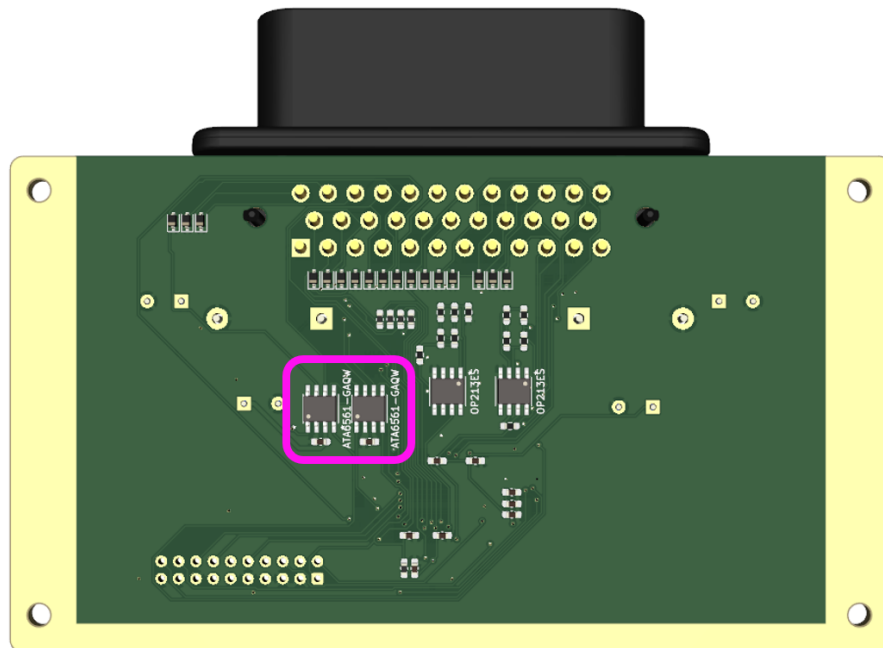


Figure 9: The Bottom View Of The Final PCB Design With CAN Transceiver (pink)

3.2.5 Signal Conditioning

Nathaniel Owen

Signal conditioning is a critical aspect of electronic circuits, as it plays a vital role in ensuring that signals are accurately measured and processed [7]. In essence, it refers to the manipulation of an input signal in such a way that it can be accurately measured, transmitted, or used for further processing. This can involve a variety of techniques including amplification, filtering, and modulation.

The signal conditioning is important because electronic circuits are often subject to various forms of noise and interference which can distort the input signal and make it difficult to accurately measure or process. In a vehicle this can arise from radio frequency interference (RFI), vibration and heavy current. To achieve the necessary conditioning, a single-supply load cell amplifier and a common and differential mode filter have been designed for signals that range from 0 to 5V and minimise power consumption.

1. Single supply load cell amplifier:

The single-supply amplifier simplifies the circuit design by eliminating the need for a negative power supply voltage [8]. It also operates on the same voltage as the ECU supply and most sensors and thus no additional components are required to manipulate the supply voltage to an appropriate level.

Figure 10 shows a generalised circuit diagram using the typical values for an input signal at 5V:

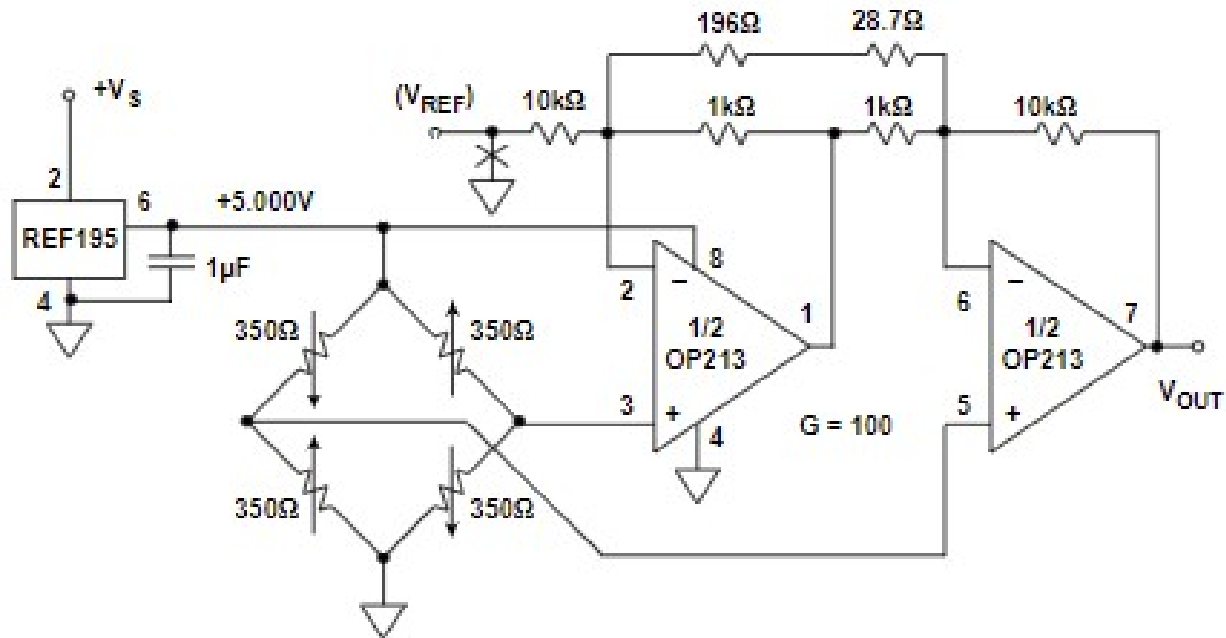


Figure 10: Single Supply Load Cell Amplifier

The excitation voltage to the bridge must be precise and stable to avoid introducing an error in the measurement. In this circuit, a precision REF195 5V reference is used as the bridge drive. This component can supply more than 30mA to a load and thus can drive the 350Ω bridge without requiring a buffer. The OP213 is configured as a dual in-amp with a gain of 100. The resistor network sets the gain according to the equation 1:

$$G = 1 + \frac{10k\Omega}{1k\Omega} + \frac{20k\Omega}{196\Omega + 28.7\Omega} = 100 \quad (1)$$

For optimum common-mode rejection, the resistor ratios must be precise. High tolerance resistors ($\pm 0.5\%$ or better) have been used. For a zero-volt bridge output signal, the amplifier will swing to within 2.5mV of 0V. This is the minimum output limit of the OP213. Due to the single supply design, the amplifier cannot sense signals which have negative polarity but this is no concern to the integration as the sensor signals will be positive. The design uses a minimum number of critical resistors and amplifiers, making the entire implementation accurate, space efficient, and cost effective.

2. Common and Differential Mode Filter:

A common-mode amplifier amplifies the voltage of a signal that is common to the two input terminals [9]. The common-mode voltage is present on both input terminals of an amplifier. The purpose of a common-mode amplifier is to amplify this while rejecting any differential-mode voltage.

A combined common and differential mode filter circuit combines both common-mode and differential-mode filtering into a single circuit. The function of this type of circuit is to suppress both common-mode and differential-mode noise or interference in an electrical signal, while allowing the desired signal to pass through. By using this circuit, it is possible to improve the accuracy and reliability of electronic circuits and systems that are subject to both types of interference.

In addition to filtering the inputs and the power pins, amplifier outputs need to be protected from radio frequency interference (RFI), especially if they must drive long lengths of cable. RFI on the output can couple into the amplifier where it is rectified and appears again on the output as a DC offset shift.

Figure 11 shows a generalised schematic for this circuit:

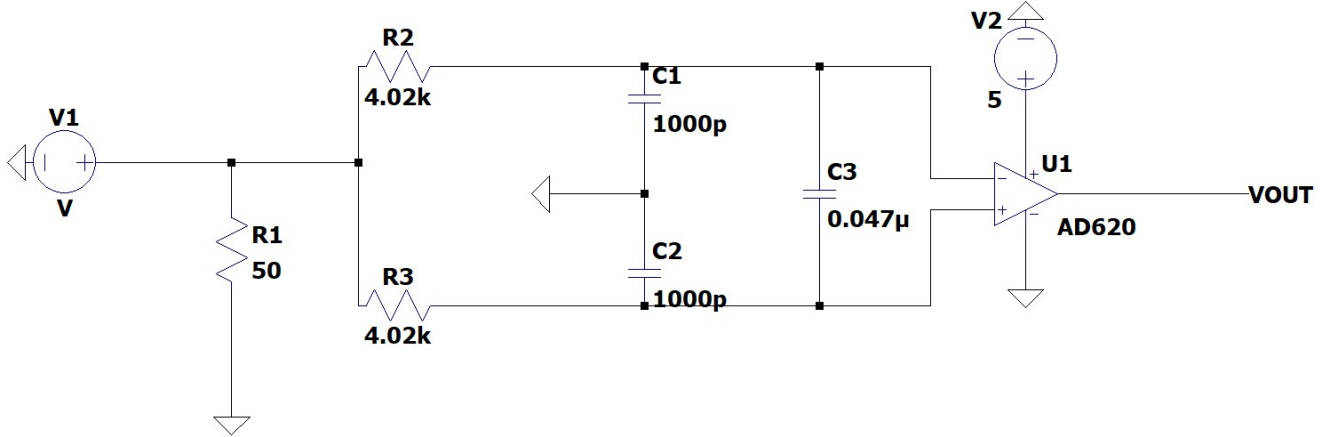


Figure 11: Common and Differential Mode Filter

The common-mode rejection is tested by applying a 1V common-mode signal to the input resistors and the AD620 gain was 1000. The referred-to-input (RTI) offset voltage of the in-amp is measured as the frequency of the sine wave source and varies from DC to 20MHz. This frequency is far beyond the typical frequency of any analogue circuit to ensure precision. The maximum RTI offset voltage shift was $1.5\mu\text{V}$ and the filter bandwidth was approximately 400Hz.

3.2.6 Voltage Regulating Circuits

Henry Wong

To ensure that all electronic components operate as desired, the 12V vehicle battery needs to be voltage regulated to the correct operating levels for the PCB. For instance, the two CAN transceivers and most signal conditioning circuits operate at 5V while the rest of the PCB operates at 3.3V. This means two voltage step-down regulators are required, one regulator for 5V and the other one for 3.3V. LM2596s-5 and the LM2596s-3.3 switching buck regulators are chosen over linear low-dropout (LDO) regulators. This is because switching buck regulators have much higher efficiency and much lower heat dissipation compared to LDO regulators. The circuits are designed according to the LM2596s datasheet [10] with decoupling capacitors and inductors to increase performance. Due to the large inductors used, the voltage regulating circuits are placed away from all the signal conditioning and microcontrollers, highlighted in blue in Figure 8, to minimise the magnetic interference near delicate signal circuits.

3.2.7 Protection Circuits

Henry Wong

To safe-guard components, the finalised PCB also includes decoupling capacitive circuits, electrostatic discharge (ESD) protection circuits and electromagnetic interference (EMI) protection circuits.

Shown in Figure 12, the most important decoupling capacitive circuit is designed for the microcontroller according to the ATSAME5P20A-VAO datasheet [4] to filter out any voltage spikes thus increasing performance. The capacitors' values are chosen carefully with reference to the datasheet so that it performs filtering as desired while not introducing any timing delay issues for the microcontroller.

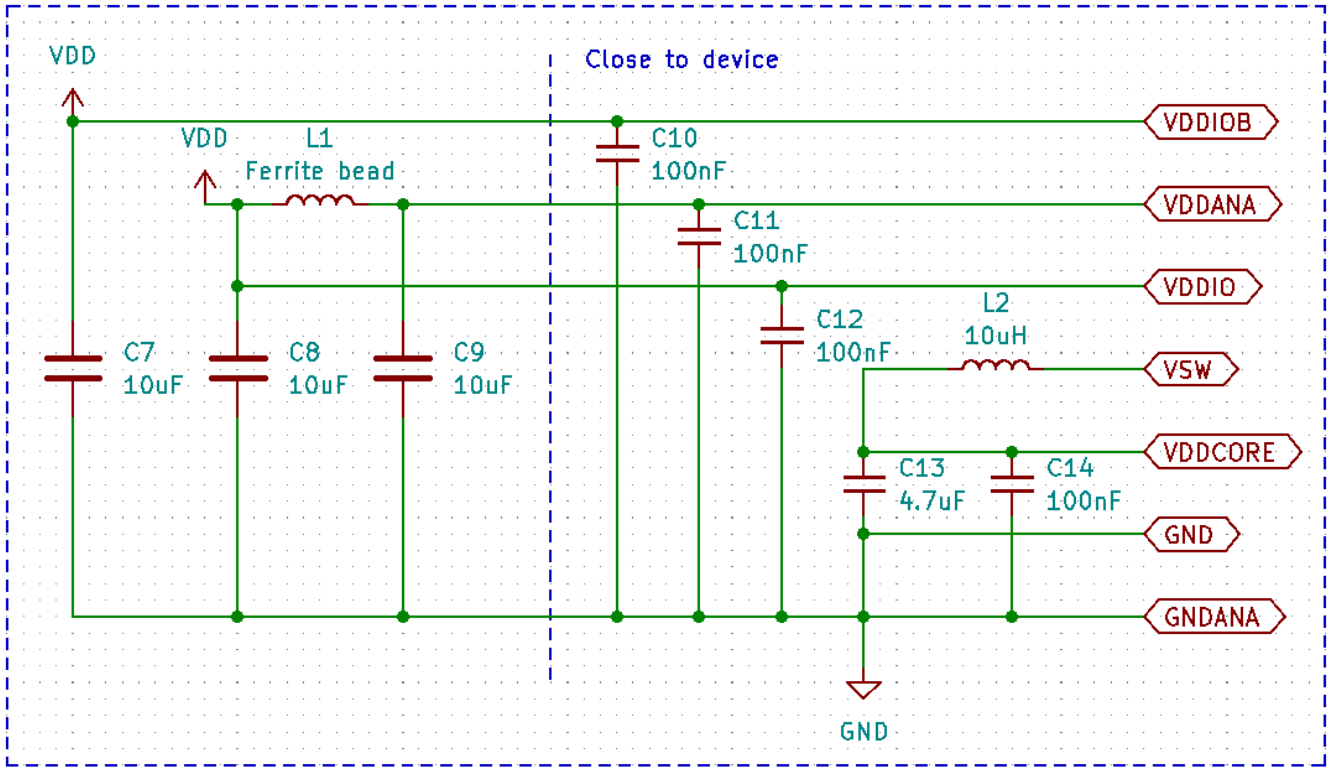


Figure 12: The schematics of the decoupling circuit for the microcontroller [4]

For ESD protection, every pin of the connector is grounded with surge diodes shown in Figure 8, highlighted in yellow. Any electrostatic discharge introduced from the external environment is immediately grounded, protecting all electronic components on the PCB.

For EMI protection, the PCB features ground copper fills around the circuit creating a Faraday Cage [11] which helps protect all signal circuits at the centre of the PCB. Further, the top layer tracks are wired perpendicular to the bottom layer tracks to avoid coupling effects induced.

3.2.8 Thermal and Mechanical Considerations

Henry Wong

The copper fill at the edge of the PCB is exposed so that when assembled with a metallic casing, heat can be transferred through the casing to the external environment to provide cooling. Teardrops are added to tracks from copper pads to increase the structural integrity of the board. Mitigating risks associated with vibration and flexing of the PCB, and drill breakouts [12]. Four M3 mounting holes are placed at the corners for mounting the PCB to the casing.

3.2.9 Future-Proofing

Henry Wong

An Embedded Trace Macrocells (ETM) debugging connect port is implemented to make debugging and troubleshooting more convenient. ETM is a real-time trace module providing instruction and data tracing of the CPU [13] which is crucial to both development phase and future updates.

The PCB also has unused space so that any future upgrades requiring additional electronic components can be added to the PCB without changing the casing for the PCB. Doing this makes the ECU more future-proof while the increase in the cost of the PCB is negligible.

3.3 Control Algorithm

Matthew Youngman, Sam Berry

The control algorithm is a critical part of the design that aims to manipulate the current vehicle dynamics to match the driver's desired vehicle characteristics while maintaining a stable system. It looks to translate the inputs from the sensor communication network to the output torques at each wheel of the vehicle, as shown in Figure 13. It also controls the differential type to simulate any mechanical or performance-based differential, such as limited slip, differential lock or torque vectoring.

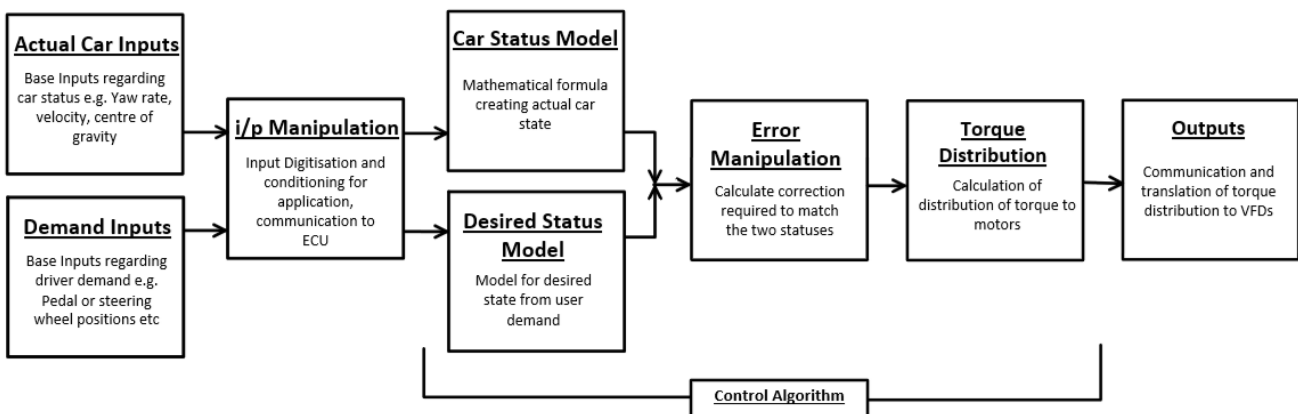


Figure 13: Control Algorithm Flow Process

The designed algorithm is written as software on the application layer and will be implemented on the microcontroller's persistent memory during production by flashing. Software based execution requires no additional physical components, reducing the carbon footprint and improving the scalability of the product. Also, it provides the means for regular system patches and improvements at no expense to the customer, as updates can be simply rewritten over the memory. As such, the design of the control algorithm looks to implement functionality over optimisation at this stage but has potential for enhancements.

3.3.1 Overarching Control Structure

Matthew Youngman

Figure 14 shows the structure for the control algorithm, where it is split into 3 modules. The desired vehicle state model (DVSM) takes inputs of the current dynamics, from state sensors, and driver inputs, such as the steering angle. It then translates these into a desired current state model for the vehicle, the characteristics of which progress through to the stability control module (SCM).

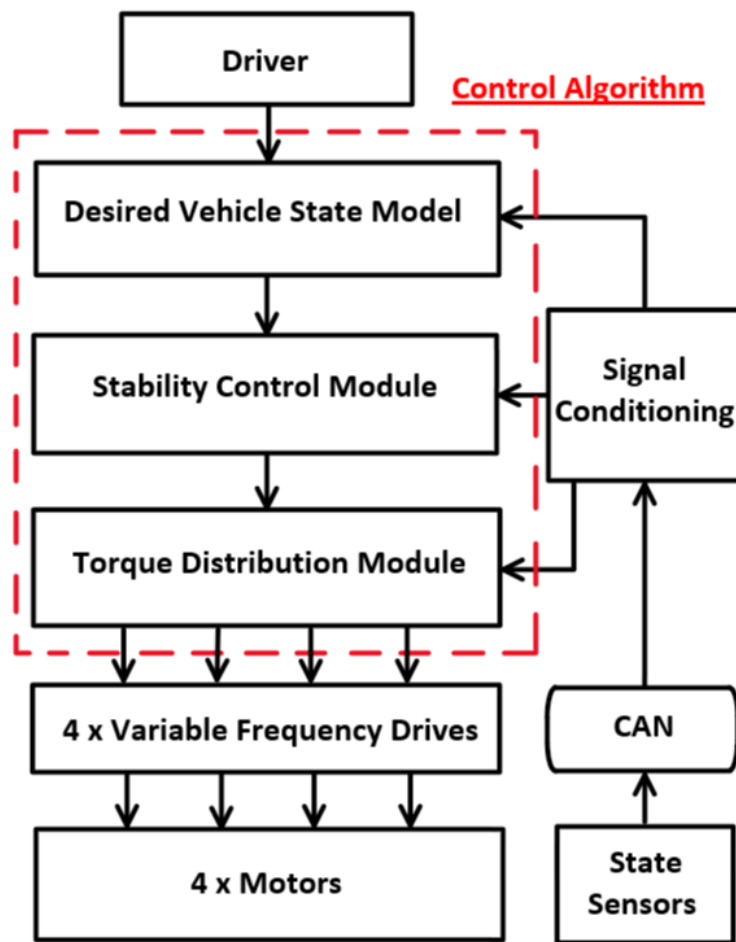


Figure 14: Control Algorithm Modules (red box) and Integration With Other Systems

The SCM uses engineered controllers to calculate a stable method of matching the current dynamics to the desired vehicle characteristics. This method is then implemented in the torque distribution module, where calculated changes to the variable frequency drives (VFDs) provide the required motor torques to correct the vehicles dynamics.

This method is chosen to ensure total control of the vehicle is given to the driver by comparison of the desired and actual dynamics, with the key idea being undetectable control from the driver. This structure is beneficial as it can integrate well with pre-existing systems in the vehicle. It can also be applied to a range of vehicle designs, irrespective of the motor type, vehicle characteristics or sensors.

3.3.2 Vehicle State Models

Matthew Youngman

For comparison between the desired state and actual vehicle dynamics, models for both systems need to be created within the software algorithm and acts before any torque distribution. Looking initially at the actual vehicle dynamics, a 2 Degree of Freedom (DoF) model [14] can be used to encapsulate necessary dynamics noticeable to the driver and is shown in Figure 15. This model ensures quick calculation of the control variables for reduced response time for stability control of the vehicle, as well as incorporating user inputs such as the driving angle, δ .

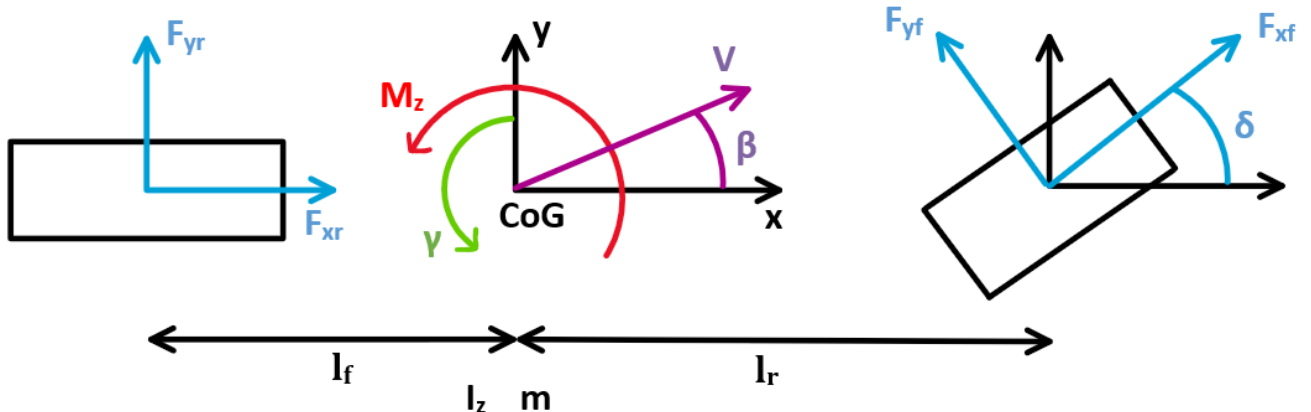


Figure 15: 2 Degree of Freedom Bicycle Model

The variables the algorithm looks to control are the sideslip angle, β , and the yaw rate, γ . The sideslip angle is the angle between the velocity vector, V , of the vehicle and its forward-facing direction, x , and the yaw rate is the rate of rotation around the centre of gravity (CoG). These variables are chosen to ensure stability in the vehicle, filling 1.4 in the specification, and are the fundamental inputs the user controls when turning. Hence, these values will be matched to the driver's desired values, described later.

Through the resolution of forces and assumptions including linearity of the system, included in Appendix E, (2) describes the state-space equation required for the control algorithm [15]:

$$\dot{x} = Ax + Bu + C\delta \quad (2)$$

where,

$$x = \begin{bmatrix} \beta \\ \gamma \end{bmatrix} \quad A = \begin{bmatrix} \frac{-2(c_f + c_r)}{mV} & \frac{-2(c_f l_f + c_r l_r)}{mV^2} - 1 \\ \frac{-2(c_f l_f - c_r l_r)}{I_z} & \frac{-2(c_f l_f^2 + c_r l_r^2)}{I_z V} \end{bmatrix}$$

$$u = \begin{bmatrix} 0 \\ \Delta M_z \end{bmatrix} \quad B = \begin{bmatrix} 0 \\ I_z \end{bmatrix}$$

$$C = \begin{bmatrix} \frac{2c_f}{mV} \\ \frac{2c_f l_f}{I_z} \end{bmatrix}$$

Constants for the vehicle characteristics such as the mass, m, the moment of inertia, I_z , and the front and rear wheel cornering stiffnesses, c_f and c_r respectively, would need calibration upon integration into the vehicle. Sensors provide the centre of gravity location, required for its distance from the front wheel, l_f , and rear wheel, l_r . Velocity, V, is provided from the GPS system.

The control of β and γ is achieved by changing only the external yaw moment, M_z , within the control variable, u. This ensures undetectable effects from the driver, where another method of changing the wheel angles can cause sudden noticeable steering hence is undesired [16]. The external yaw moment is varied using the torque distribution across the wheels, and its value is passed to the torque distribution module before actuation using the VFDs, see Figure 14.

The desired vehicle dynamics, r , controlled by the driver contains β_{des} and γ_{des} , representing the desired sideslip angle and yaw rate respectively. β_{des} is selected to be zero to ensure vehicle stability, while γ_{des} follows the input from the steering wheel angle using (3) [15]:

$$r = D\delta \quad (3)$$

where,

$$r = \begin{bmatrix} 0 \\ I_z \end{bmatrix} \quad D = \begin{bmatrix} 0 \\ \frac{V}{l_f + l_r + \frac{mV^2(c_rl_r - c_f l_f)}{2c_f c_r(l_f + l_r)}} \end{bmatrix}$$

These equations are written in software and implemented as the description of the vehicle for comparison and control of its dynamics.

3.3.3 Stability Control Module

Matthew Youngman

Integration of the vehicle state models with a control system required analysis of assumptions made. The linearisation of the system will, in practice, create issues for stability. This is due to non-linear characteristics in real applications, such as the forces caused at larger sideslip angles, shown in Figure 16, or cornering stiffness values. Also, large disturbances that occur due of the vehicle's environment, such as wind or bumps in the road, mean a very robust stability control system is required.

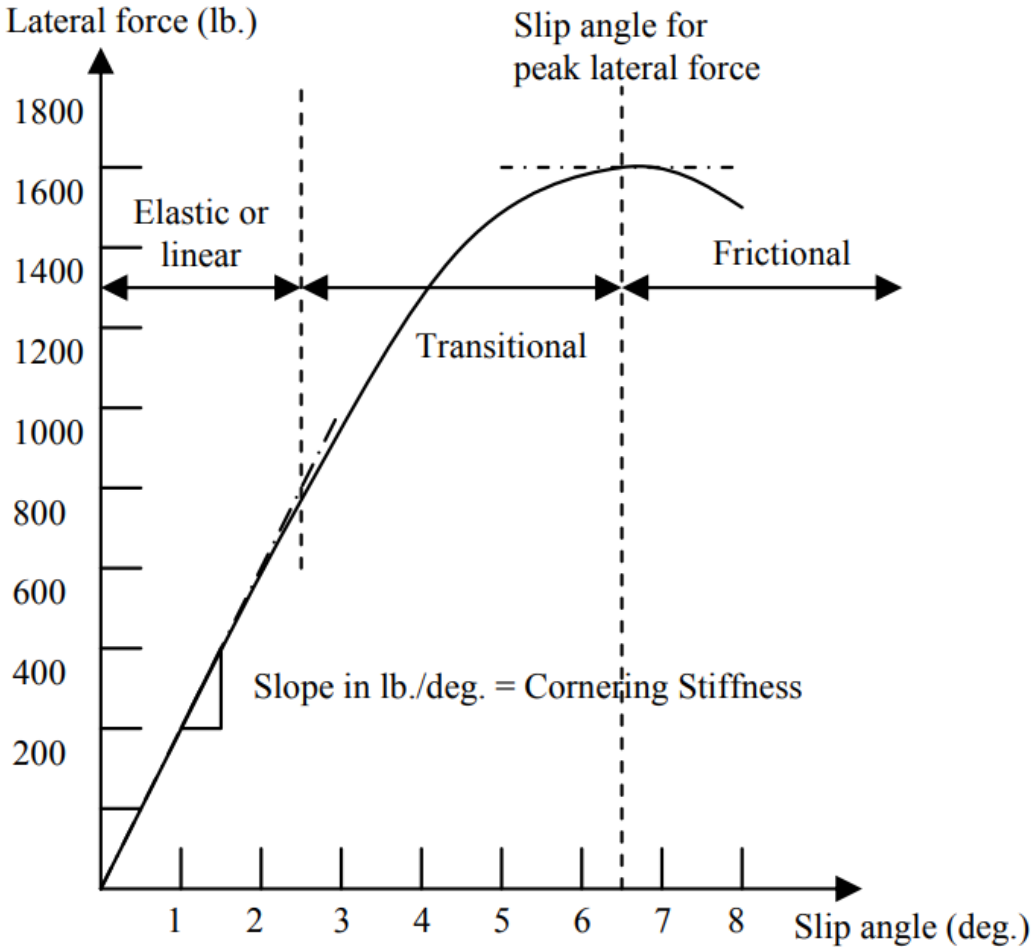


Figure 16: Non-linearity of Lateral Force With Sideslip Angle [17]

As a result, the commonly used proportional, integral, and differential (PID) controller [18], which relies on a linear, low disturbance plant, would not perform well. Instead, the method of sliding mode control (SMC) is implemented [19], often used in electromechanical systems due to its robustness and reliability. This method acts like a variable control structure, Figure 17, where the design of a reaching law always forces the system towards its desired characteristics. These characteristics are defined along a sliding surface, which is where the system wishes to function, following x and \dot{x} .

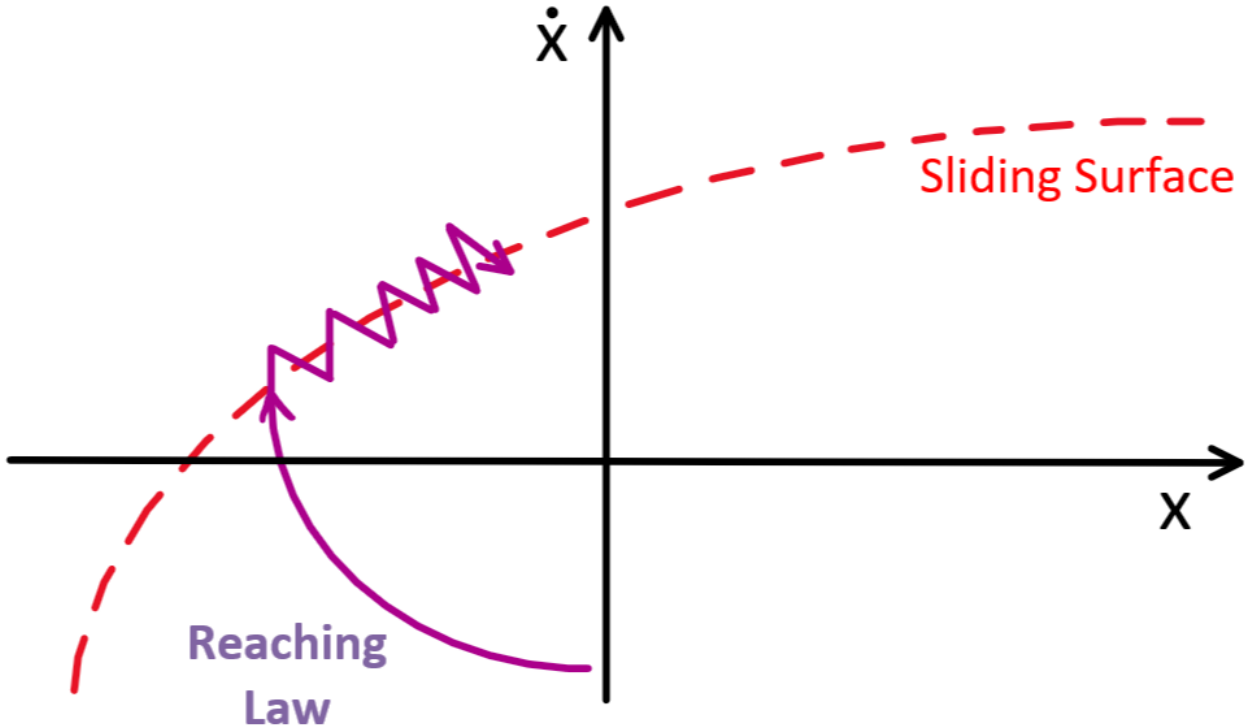


Figure 17: Sliding Mode Control Schematic

Definition of a sliding surface using the comparison of desired and actual vehicle dynamics creates (4), which follows a guiding principle for SMC where $s = 0$ is the desired sliding characteristic.

$$s = \lambda(x - x_{des}) = \lambda e \quad (4)$$

Here, λ is the scaling coefficient for the error, e , that defines the rate at which the system moves towards the sliding surface. Following this, a reaching law (5) can be designed to control (2) from the vehicle dynamics by acting as the feedback variable, u , driving the dynamics towards the desired values, the derivation of which is in Appendix F.

$$u = B^{-1}(-Ax - C\delta + \dot{x}_{des} - \lambda^{-1}\sigma \operatorname{sign}(s)) = \begin{bmatrix} 0 \\ \Delta M_z \end{bmatrix} \quad (5)$$

where,

$$\operatorname{sign}(s) = \begin{cases} 1, & \text{if } s > 0 \\ -1, & \text{if } s < 0 \end{cases} \quad (6)$$

The magnitude of the disturbance, σ , is cancelled in (5) following use of the polarity change of the sliding surface in (6). This makes the system robust if the maximum size of any disturbance is known.

Simulation of the stability control algorithm is implemented in Matlab, with the parameters shown in Table 2. The simulation recreates a lane change at 55mph.

Term	Symbol	Value/Expression	Units
Initial sideslip angle	β	-0.1	[rad]
Initial yaw rate	γ	-0.25	[rads^{-1}]
Velocity	V	24.6	[ms^{-1}]
Steering angle	δ	$0.1\sin(t)$	[rad]
Length from front wheel to CoG	L_f	1.4035	[m]
Length from rear wheel to CoG	L_r	1.4035	[m]
Front wheel cornering stiffness	c_f	6000	[Nrad^{-1}]
Rear wheel cornering stiffness	c_r	5000	[Nrad^{-1}]
Mass	m	2510	[kg]
Moment of Inertia	I_Z	5.4	[m^4]
Disturbance to sideslip angle	σ_β	$0.2\sin(1.5t)$	[rad]
Disturbance to yaw	σ_γ	$0.3\sin(2t)$	[rads^{-1}]

Table 2: Variables For Stability Control Algorithm

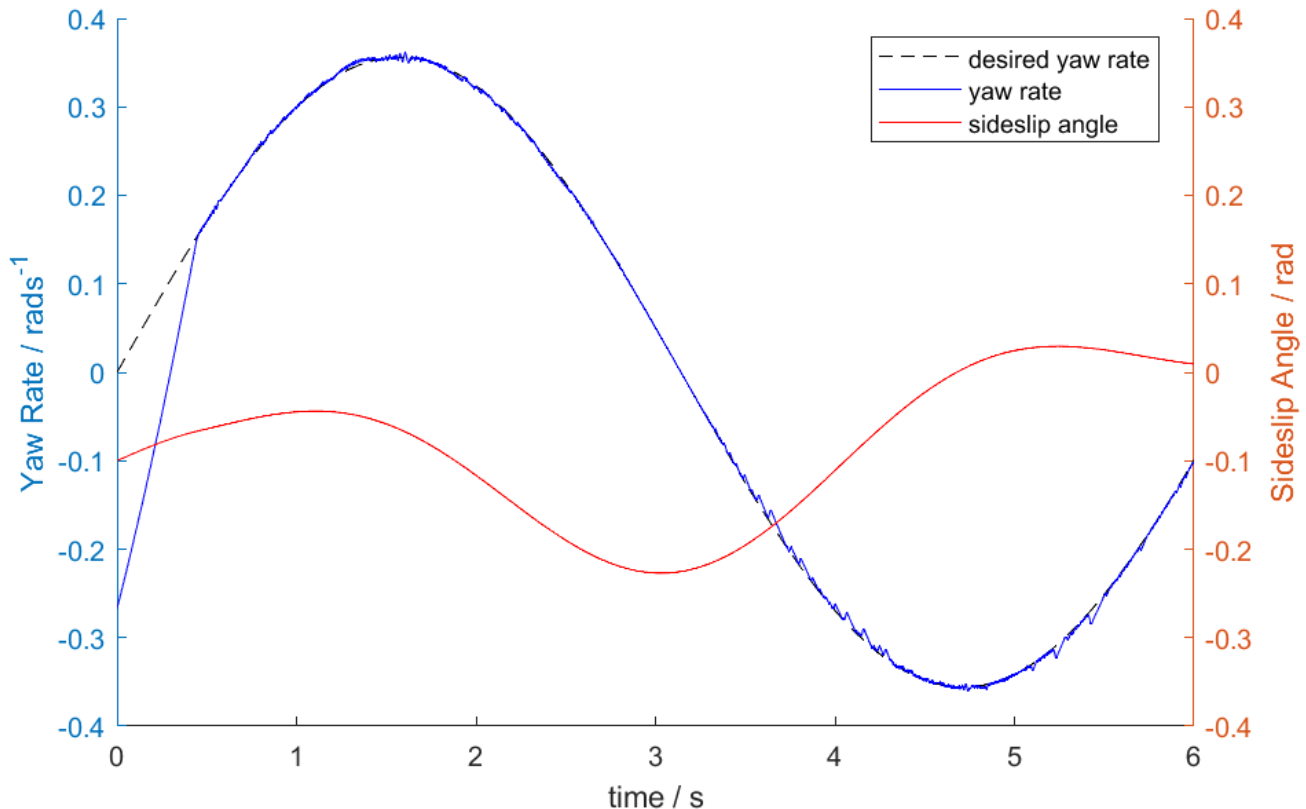


Figure 18: Sliding Mode Control Simulation Results

Figure 18 shows the results of the control algorithm. The desired yaw rate follows (3) to ensure behaviour of the dynamics matches the driver's commands. The yaw rate is tracked to its desired value rapidly, with correct alignment after 0.45s, ensuring complete control of the system despite a large disturbance profile being present. Also, the sideslip angle is small, despite not reaching it's optimum value due to continued turning characteristics (2), helping to eliminate understeer and oversteer characteristics. Finally, the effect of chattering, where the controlled variables experience high frequency oscillations around the desired value, has been minimised to prevent losses in the motors.

3.3.4 Torque Distribution Module

Matthew Youngman

The reaching law, u , is found from the stability control module through application of SMC to the vehicle dynamics. It is then passed through to the torque distribution, where its equivalent value of the yaw moment can be used to distribute corresponding torques across the wheels.

With a four motor vehicle with independent wheel control, a proportional control law can be used in combination with torque vectoring. Torque vectoring is the process of electronically managing the torques to each wheel independently, and has the potential to optimise driving performance. Following values from Table 2, torque vectoring can be implemented using (7) (8) [20], where k is the proportional gain.

$$T_f = k \times l_r \times \Delta M_z \quad (7)$$

$$T_r = -k \times l_r \times \Delta M_z \quad (8)$$

This will supply functional torque distribution to the front and rear wheels, l_f and l_r respectively, however the optimisation of this process requires large amounts of prototype testing to ensure correct implementation. This is not possible before product manufacture, however methods of software enhancements through updates to the application layer can enable this at later stages in design.

Simulation of a mechanical differential can thus be achieved by also changing the torque distribution algorithm, e.g. (7), to a relevant desired differential type such as limited slip or differential lock. Also, due to the architecture of the control algorithm, additional driver experience options for changing the differential type could be implemented after integration into the car.

3.3.5 Regenerative Braking

Sam Berry

During a conventional vehicle's braking cycle, the kinetic energy is lost to the environment in the form of heat dissipation at the friction brake pads. TorqueDrive's electronic differential will utilise regenerative braking to recover this wasted energy. The lost kinetic energy will drive the electric motor as a generator and recharge the vehicle battery. Depending on the driving cycle, regenerative braking can save from 8% to as much as 25% of the total energy used by the vehicle [21].

TorqueDrive's electronic differential will manage both driving and braking control. This adds value to the product as currently most regenerative braking control systems are sold separately to electronic differentials in the EV market. Offering an all-in-one package eliminates the need to integrate different products to work together via communication protocols.

Electronic Braking Distribution (EBD) will be used to distribute the required braking torque to each wheel. The ECU will calculate the position of the vehicle's centre of gravity using the wheel load sensor inputs. From here the ECU will distribute increased braking torque to those wheels under an increased load. This is achieved by sending the appropriate PWM signal to the individual motor variable frequency drives (VFD). Some examples of uneven loading between wheels include deceleration, cornering, and uneven cargo loading. Distributing increased braking torque to wheels under more load helps avoid tyre slip due to varying levels of traction and reduces the braking distance, helping to reduce brake pad wear. Currently brake pad wear emissions account for 20% of PM 2.5 roadside emissions [22], which are known adverse health effects. The EBD system will act as a pre Anti-Lock Braking system (ABS). The EBD will aim to avoid any tyre slip, however, once slip is detected the ABS system will take priority and create an interrupt to override the EBD system. The EBD will regain control of braking once the vehicle has regained tyre traction.

A serial braking system concept will be implemented to integrate regenerative and friction braking. Regenerative braking will be used whenever possible and the friction brakes will only be used when regenerative braking cannot deliver the required braking torque. In this case both braking methods will be used in tandem. Figure 19 shows a schematic of the serial braking control system. Note, no regenerative braking will occur when the state of charge (SOC) of the battery is above 80%. This is to prevent regenerative current damaging the battery components. Also, no regenerative braking will occur at speeds below 6 mph, as the motor rpm is so low that regenerative braking becomes inefficient. In these situations where the regenerative braking will not be used, the friction brakes will step in to deliver the required braking torque.

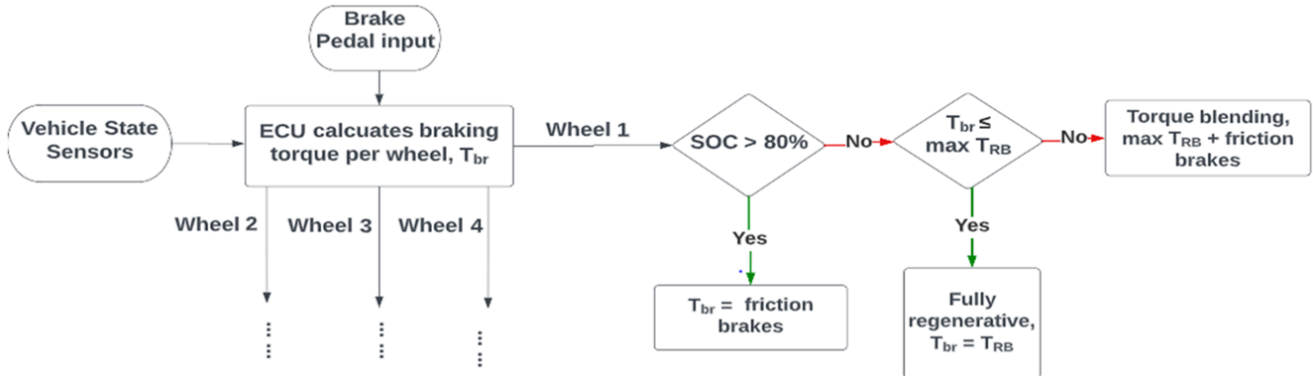


Figure 19: Vehicle Braking Logic Diagram

Figure 20 shows a characteristic induction motor Torque Speed plot (blue). Using a PWM signal, the ECU can control the position of the blue line. The induction motor will operate at the point where the blue line and the tyre speed (red line) intersect. The induction motor runs in the generating phase and produces a negative counter torque. By continuously moving the blue line, the motors can deliver the required braking torque as the vehicle decelerates. Equation 9 shows how the PWM signal sent by the ECU can control the positioning of the torque-speed characteristic for each motor individually.

$$n_s = \frac{120f_s}{P} \quad (9)$$

The VFD continuously changes the stator frequency, altering the value of the motor stator speed (n_s) and moving the characteristic line. Note, P refers to the number of poles in the induction motor.

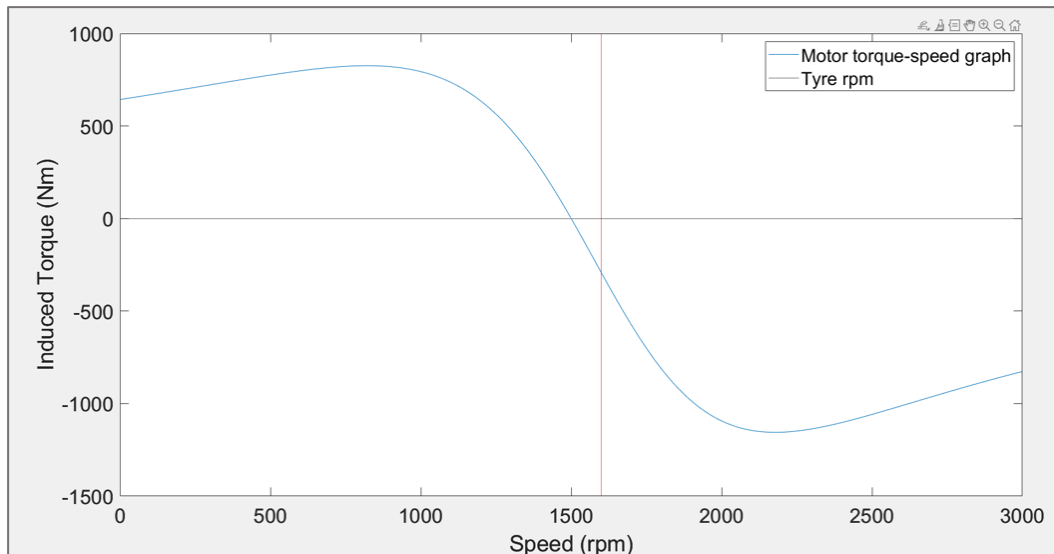


Figure 20: Induction Motor Torque-Speed Characteristic (blue) and Wheel Speed (red)

3.3.6 Adjustable Regenerative braking - No Pedal Depression

Sam Berry

The system offers the user an adjustable regenerative braking scale for when neither the gas nor brake pedal are depressed. This adds value to the product by tailoring the braking experience to the user's choice. The user can choose from a scale 1-4 at the user interface, where 1 feels like a conventional vehicle with no regenerative braking and 4 feels very aggressive allowing for 'one pedal driving'. In other words, the driver can bring the vehicle to a near stop without depressing the brake pedal. A problem encountered when designing this system was that the driver may be expecting regenerative braking but due to circumstances such as the battery SOC being over 80%, no regenerative braking will be delivered. This could be a huge safety concern if the driver becomes reliant on the regenerative braking when no pedals are depressed. To solve this problem, regenerative braking will take place so the motors produce the required counter torque. However, the regenerative current will not be fed to the vehicle battery, but instead be grounded.

Simulations of braking cycles were run in MATLAB to test the adjustable regenerative braking system. The simulations are run assuming dry road conditions (friction coefficient = 0.8) and using the specifications of the reference vehicle. Figure 21 shows the increasing state of charge (SOC) of the battery during different levels of regenerative braking. The simulation models deceleration from 30mph to 6mph, as below 6mph no regenerative braking occurs due to its high inefficiency. The point of plateau shows when regenerative braking disengages as the car has decelerated below 6mph. Evidently higher levels of regenerative braking increase the SOC of the battery more per braking cycle.

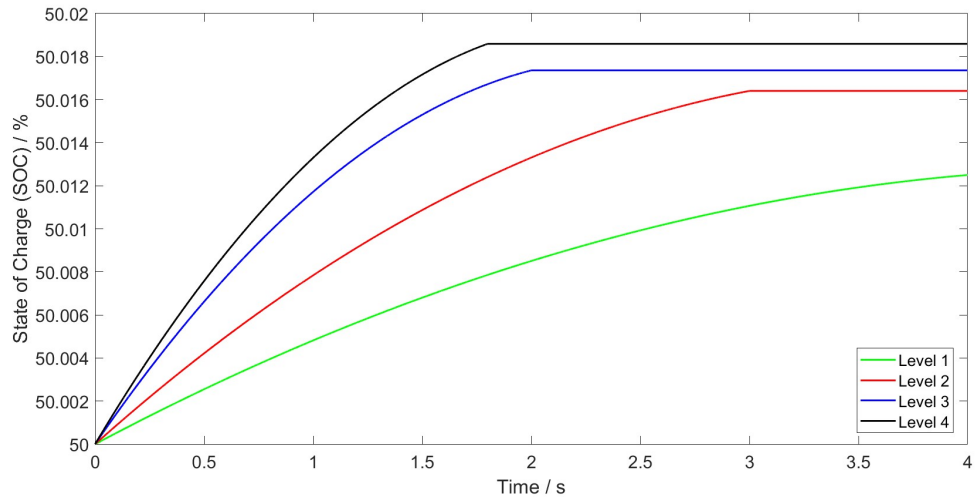


Figure 21: Regenerative Braking state of charge recovery For Varying Regenerative Braking Intensities

3.4 Housing, Fixing and Casing of the Electronic Control Unit

3.4.1 Location

Finlay Sanderson

From industry research [23], the majority of current large vehicle manufacturers store their most important ECUs in either the bonnet or the glove box. Currently, there are no regulations or standards that govern the location of ECUs within the vehicle, so the decision on where the ECU was stored was solely based on optimising performance. Considering the following multiple factors, it was decided that the glove box was the most suitable location to store the ECU used, with the final location shown in Figure 22:

- Proximity to the majority of the systems and sensors used by the system, to minimise latency.
- Lower and reduced temperature variation, as the glove box is further from the engine, thereby reducing the chance of heat damage to the PCB.
- Smaller and less frequent vibrations, due to the glove box being supported by the suspension, again to reduce risk of damage to the PCB.

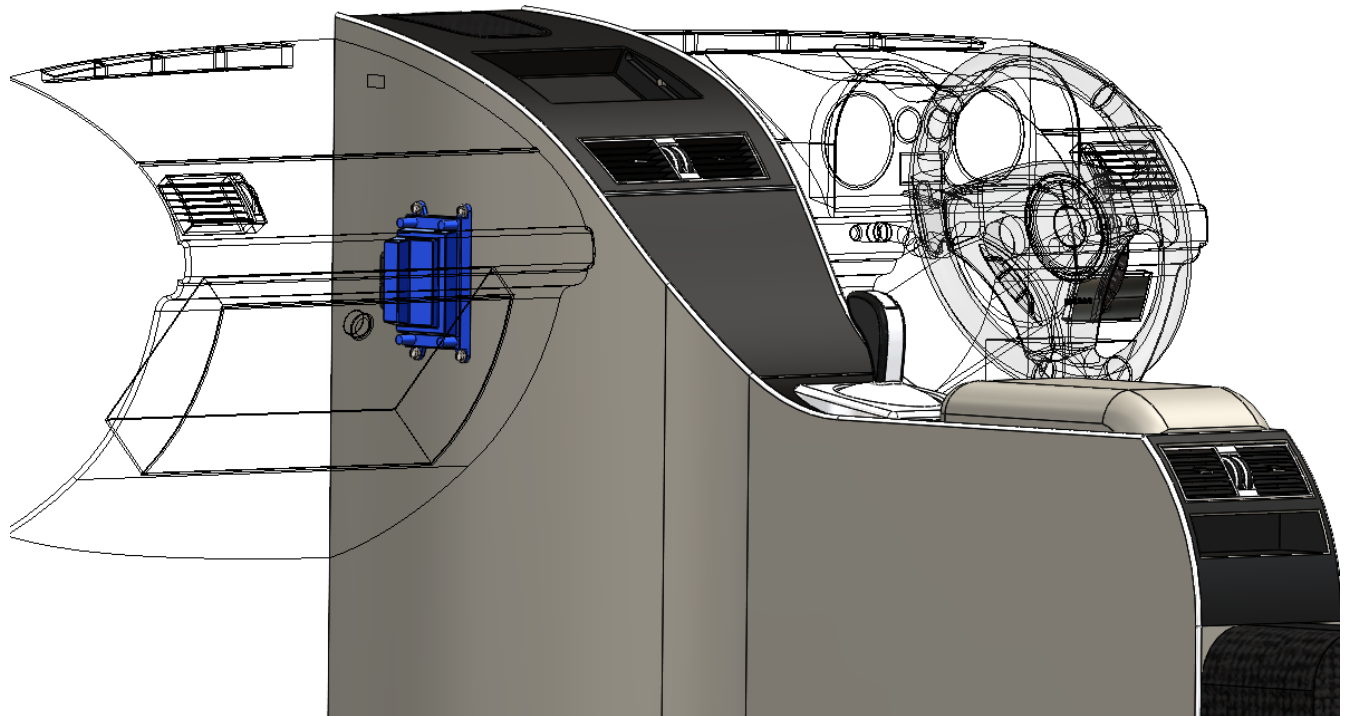


Figure 22: Final location for ECU casing (highlighted in blue)

3.4.2 Stress Analysis

Finlay Sanderson

Once the location for the ECU had been chosen, a Computer Aided Design (CAD) model of the casing prototype was produced, shown in Figure 23. This model was then used in Solidworks Simulation to analyse the stresses that the casing would experience during normal driving. This was done using random vibrational analysis in Solidworks, with the external load on the casing being the base excitation it would experience when travelling at 30mph over bumps. Random vibrational analysis was selected as the most appropriate form of stress analysis, as it best simulates the shocks and stresses that the casing would experience as the vehicle navigates speed bumps and other undulations in the road surface. 30mph was chosen as the speed, as this is the maximum speed limit on UK roads where there is the potential for speed bumps [24].

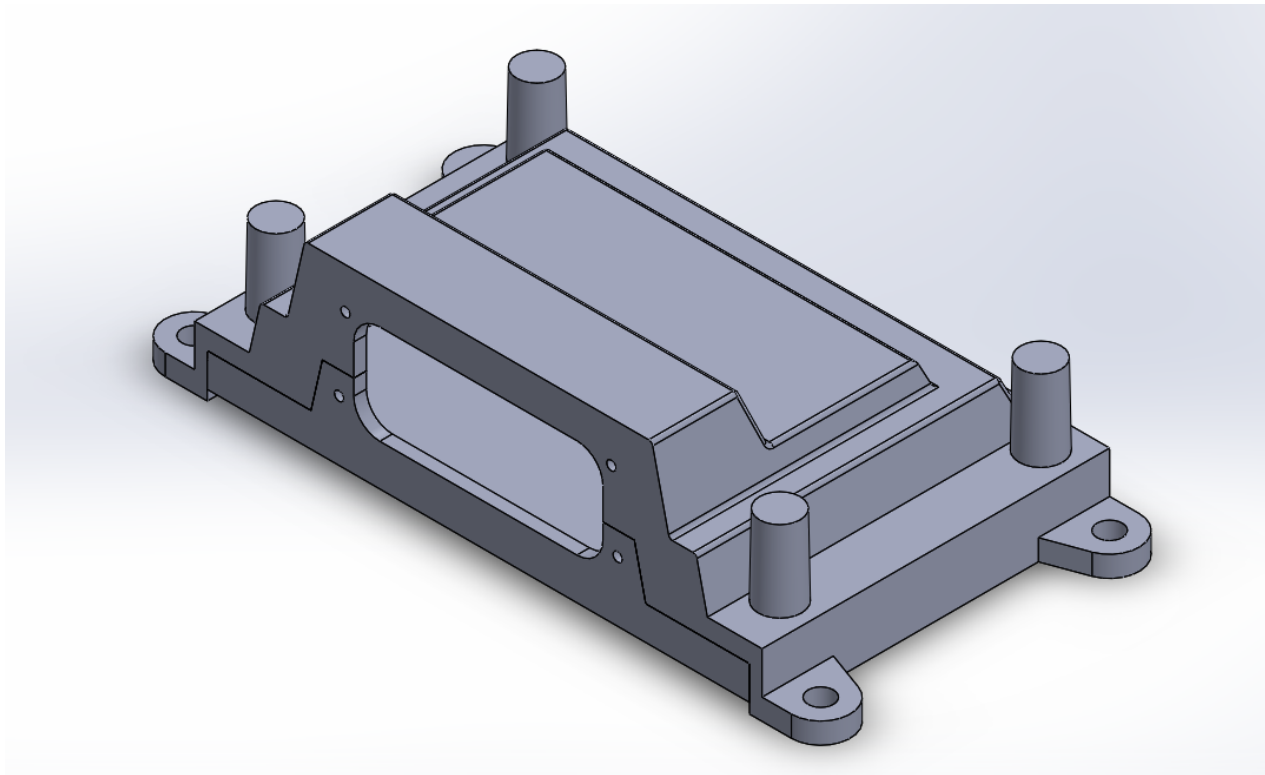


Figure 23: Longitudinal View of CAD ECU Casing Prototype.

From this initial stress analysis, it became clear that the maximum vibrational stress the casing would experience was 20.35 MPa. A factor of safety (FoS) of 3 was then applied to this stress, which is the standard FoS used in the automotive industry [25], leading to the material for the casing having a yield strength higher than 61.05 MPa. Although Figure 24 seems to show some deformation of the casing under vibrational stress, Figure 25 shows the actual displacement of the casing, with a maximum displacement of around $10\mu\text{m}$, which is negligible when compared with the 2mm case thickness.

Model name: ECU1.0_Assem (1)
Study name: Vibrational Stress(-Default-)
Plot type: RMS Value of nodal stress Stress1
Deformation scale: 15,947.9

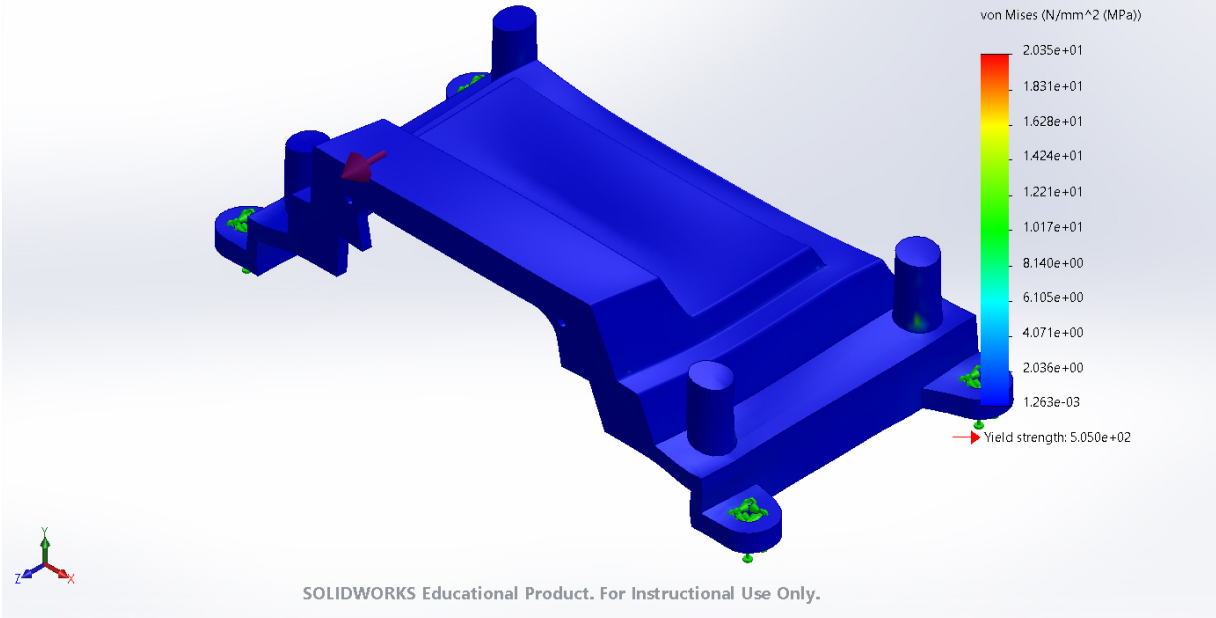


Figure 24: ECU Casing Vibrational Stress

Model name: ECU1.0_Assem (1)
Study name: Vibrational Stress(-Default-)
Plot type: RMS Value of displacement Displacement1
Deformation scale: 15,947.9

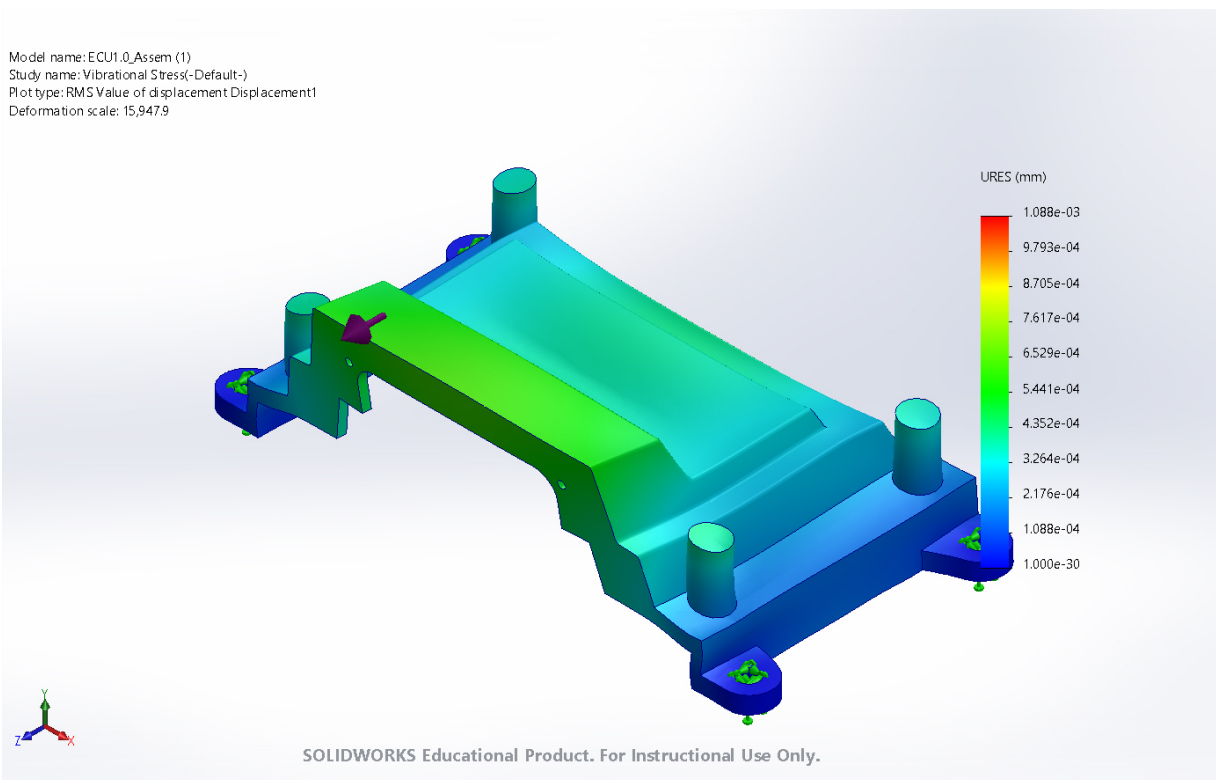


Figure 25: ECU Casing Vibrational Stress Displacement

In addition to the stress analysis, a crash simulation was carried out, shown in figure 26, with the stress experienced equal to the stress a passenger would experience in a 37.28mph (60kph) crash, which is the speed the automotive industry expects a vehicle's crash structure to begin to show signs of damage [26] and hence will be what the maximum allowable stress for the ECU casing is based on. From the simulation, a maximum impact stress of 164.6 MPa was calculated and using an FoS of 3, the maximum allowable stress was calculated as 493.8 MPa. Similarly to the vibrational displacement, the impact stress shown in Figure 26 again appears to show some deformity in the casing as a result of the impact. However, Figure 27 shows the displacement of the case, with the maximum displacement the casing would experience being 100 μ m, which is again very small when compared to the overall size of the casing. On top of the vibrational stress analysis and crash simulation, the fatigue stress on the casing was also analysed. A period of 7 years was analysed, which is the expected product life length in the automotive industry [27], with Figure 28 showing the results of the fatigue analysis. From Figure 28, it is clear to see that the ECU casing will not fail due to fatigue, as the percentage of damage throughout the casing is minimal, and the expected life exceeds 7 years.

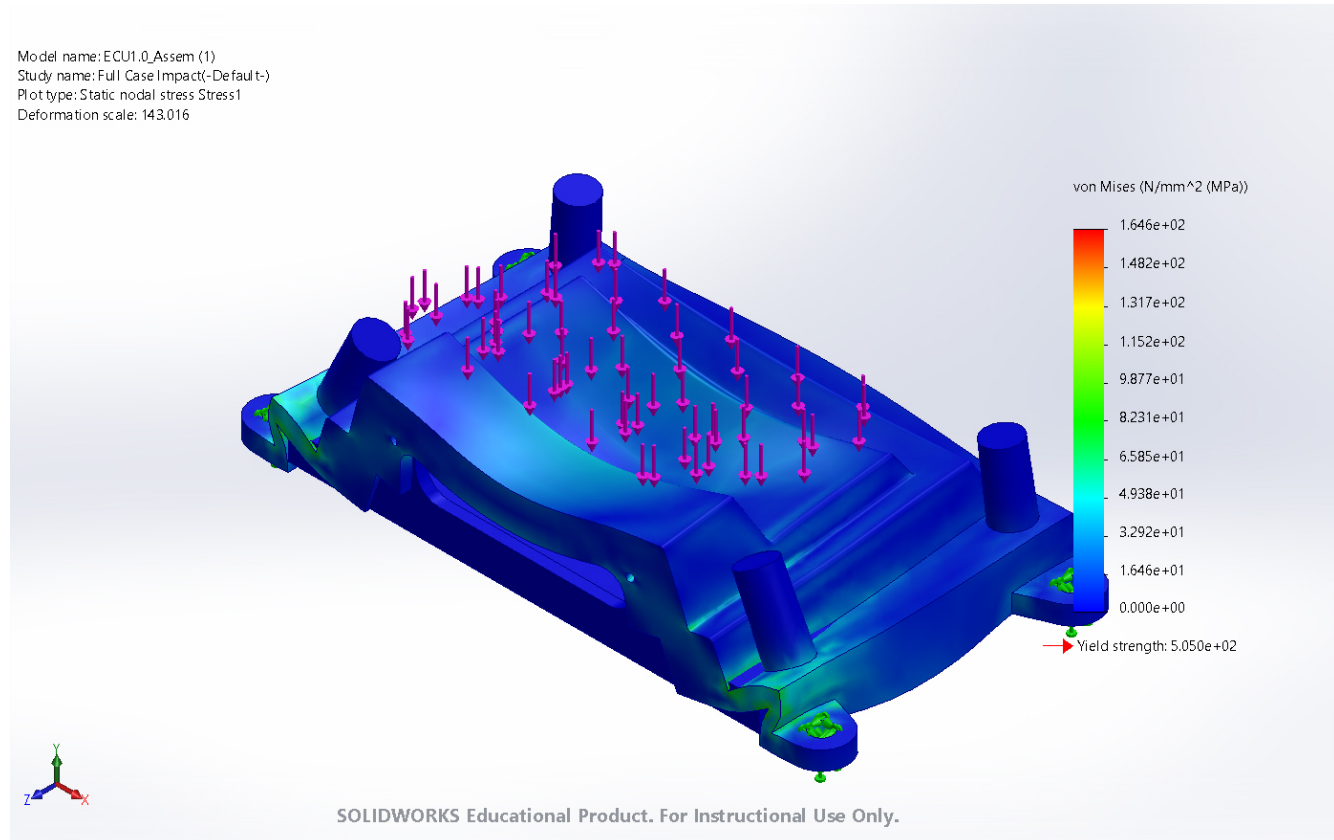


Figure 26: ECU Casing Impact Stress

Model name: ECU1.0_Assem (1)
Study name: Full Case Impact(-Default-)
Plot type: Static displacement/Displacement1
Deformation scale: 143.016

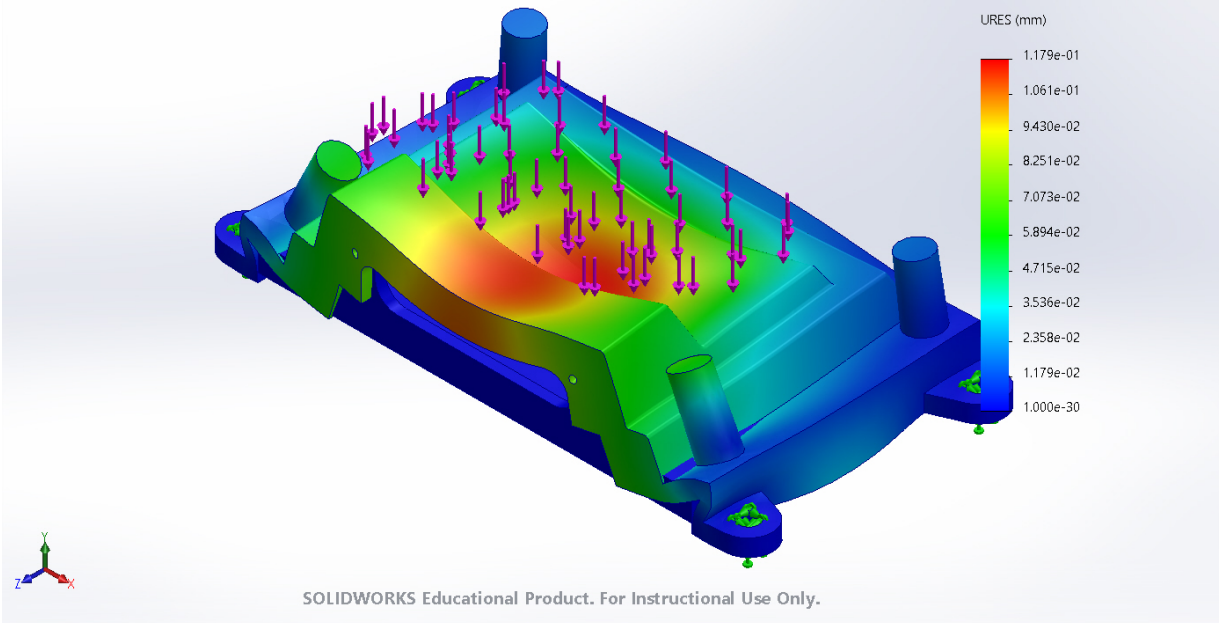


Figure 27: ECU Casing Impact Stress Displacement

Model name: ECU1.0_Assem (1)
Study name: Fatigue(-Default-)
Plot type: Fatigue(Damage) Results1

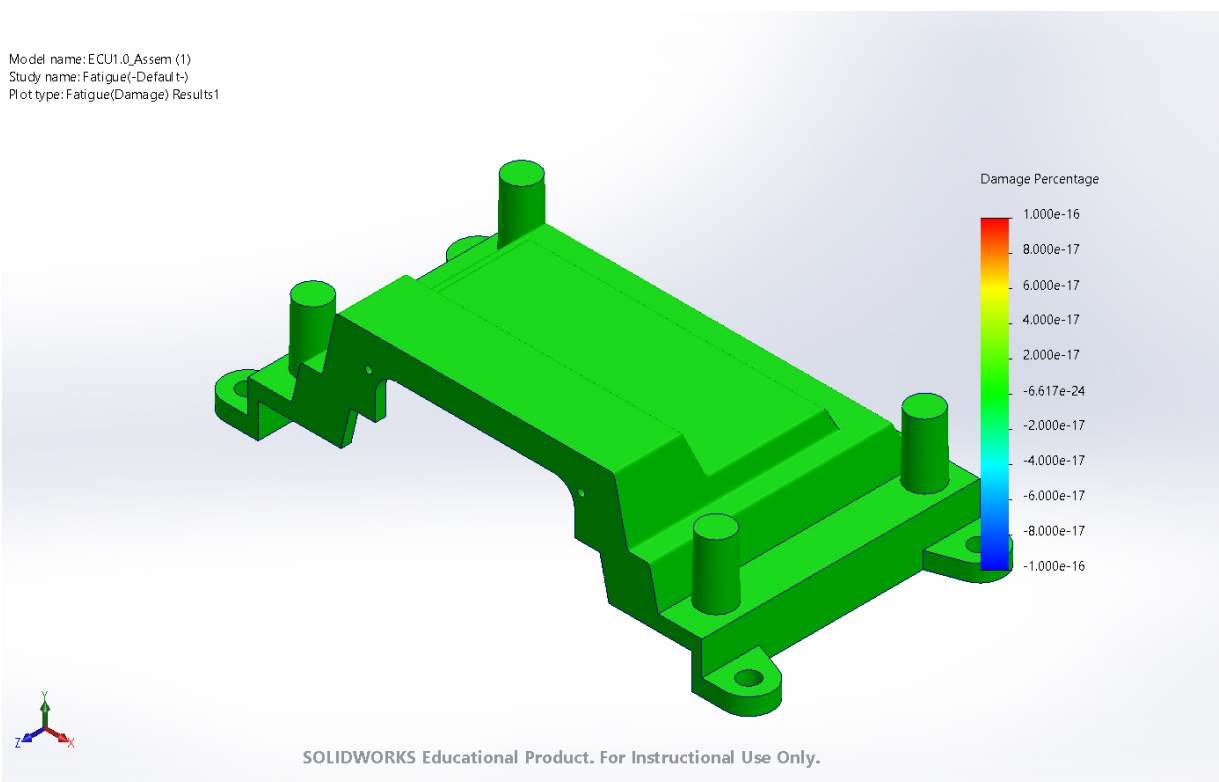


Figure 28: ECU Casing Vibrational Stress Fatigue

3.4.3 Material Choice

Finlay Sanderson

As one of the main benefits of an electronic differential over its mechanical counterpart is the weight reduction, one of the main aims when choosing the material for the casing was to ensure that it was as light as possible, whilst still offering a high enough yield stress to exceed the maximum stress. Another factor when considering the material for the casing was its sustainability, with section 5 detailing this analysis. Based on these design criteria, the best choice for the casing material was aluminium 7075 (AA7075), with thickness of at least 2mm throughout. Firstly, AA7075 has a density of $2.81\text{g}/\text{cm}^3$, which matches up well with other potential choices such as mild steel ($7.85\text{g}/\text{cm}^3$), and stainless steel ($8.03\text{g}/\text{cm}^3$). AA7075 also has a yield strength of 503MPa (reference), which exceeds the maximum stress on our casing, fulfilling the criteria set out in table 1, as it has a FoS of 3.06. However, aluminium tends to be slightly more expensive than other options such as stainless steel, but this slightly increased expenditure can be justified due to aluminium's decreased density and sustainability benefits. Using aluminium as the choice of material gives the ECU casing a mass of around 115g.

3.4.4 Fixing

Finlay Sanderson

Currently in industry, many vehicle manufacturers leave their ECUs unsecured and loose. However, due to the importance of this ECU to the function of the differential system and the vehicle, it will be secured to the wall of the glove box due to the following reasons:

- Fixing the casing to the wall allows comprehensive stress analysis, detailed in section 3.4.2 , which allows complete safety validation of the materials used to construct the casing.
- Fixing the casing improves passenger safety in the event of a crash, preventing ejection of a loose ECU from the glove box. The ECU will be fixed to either the left or right side of the glove box, so that even if the bolts holding the ECU in place fail due to an extreme load, the ECU would not could not injure the passenger upon ejection.
- Reduces risk of wires detaching from the ECU, as the ECU is locked firmly in place, minimising the movement of the system.
- Reduces chance of minor damage to the casing , as the casing is locked in place, and will not collide with other items in the vehicle.

Multiple methods of securing the ECU to the wall of the glove box were considered, such as welding, or use of an adhesive. The method selected was bolting the ECU to the wall of the glove box. This is because bolting offers the most well-rounded solution, as the correct selection of bolts ensures that they will be able to withstand the maximum stresses on the casing, whilst allowing for easy maintenance as the bolts can be removed by a professional. Metric grade 10.9 bolts were chosen, shown in figure 29, commonly known as ‘car bolts’ [28], as they are the most widely used bolts in the automotive industry. They have a yield strength of 940MPa and tensile strength of 1040MPa, which means they conform to ASTM A324 grade BD and SAE J429 grade 8 [29]. The yield strength of these bolts far outweighs the maximum stress detailed in section 3.4.2, which demonstrates that these bolts would not fail or deform due to the loads experienced by the casing and are therefore suitable for use in this system. The final fixing solution is shown in Figure 30.



Figure 29: Metric Grade 10.9 bolts, similar to the ones TorqueDrive will use.

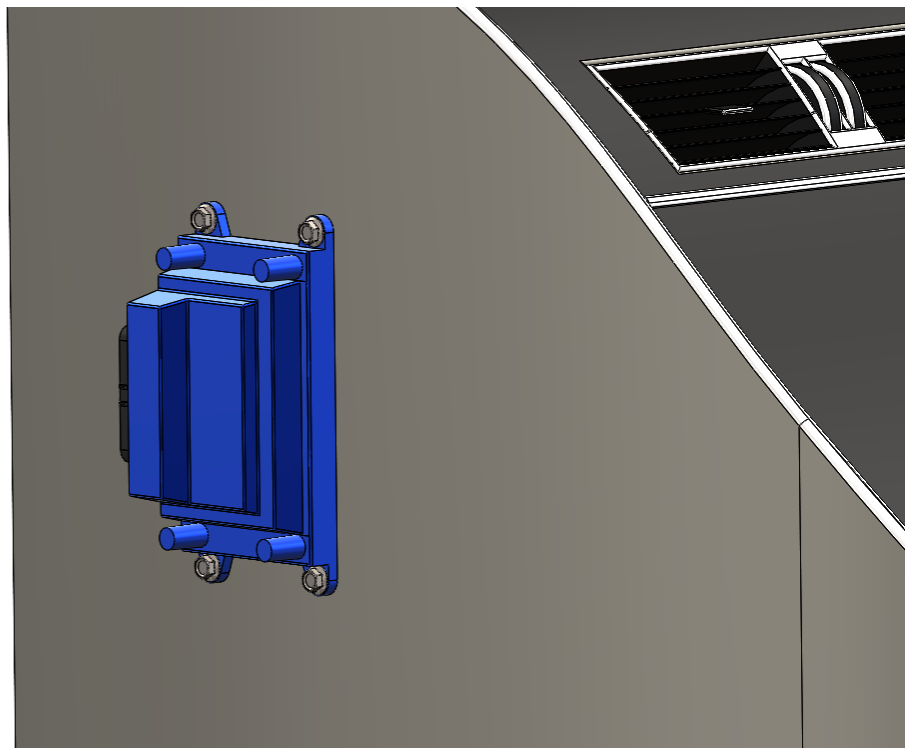


Figure 30: Fixing Method for the ECU

3.5 Variable Frequency Drive

Christian Garry

The ECU generates the required torque adjustments to maintain stability and peak traction based on sensor input with algorithms. The next stage is to translate this code output into a physical change in torque applied by the motors.

A VFD has been identified as the best option for this product. A VFD is an electronic device that controls the speed of an alternating current (AC) motor by changing the frequency of the power supplied to it. It works by converting the incoming AC voltage into direct current (DC), and then using pulse width modulation (PWM) techniques to convert the DC voltage back into AC with the desired frequency.

An in-house VFD circuit was designed allowing the use of the first 800-volt model. This is also cheaper [30] than simply purchasing an existing one had there been a suitable VFD. A custom VFD also allows it to be specialised to fulfill the design criteria described in Table 3. The use of VFD modules also provides the best flexibility as it allows the product to be easily integrated into any vehicle as no proprietary motor controllers need to be considered. However, if a vehicle manufacturer desires, the ECU can be altered to interface with existing motor controllers in the vehicle.

Criteria	Value
Voltage	800
Input Conditioning	Create PWM signals
Pin Minimisation	Decrease the number of ECU pins required
Cost Delta	Multiple Thousands of Pounds Cheaper

Table 3: Torque output mechanism design criteria

3.5.1 Variable Frequency Drive Circuit

Christian Garry

The VFD takes a three-phase [31] AC input from the vehicle's main inverter, there are then three sets of power electronics that each control one phase of the AC voltage. [32] Each consisting of a diode rectifier [33], a DC bus capacitor [34], and an inverter [35].

The diode rectifier converts the incoming AC voltage into DC, which is stored in the DC bus capacitor. This DC voltage is converted back to AC by alternating the state of the two transistors. When the output voltage should be positive the transistor that is connected to the positive DC bus is switched on, and when the output voltage should be negative the positive DC bus transistor is switched off and the negative DC bus transistor is switched on [36].

In order for the output voltage to be a sine wave the duty cycle of the PWM signal is varied sinusoidally producing a sinusoidal voltage output. The frequency of this PWM signal is altered by the ECU to change the frequency of the VFD output voltage.

The completed VFD circuit is shown in Figure 31.

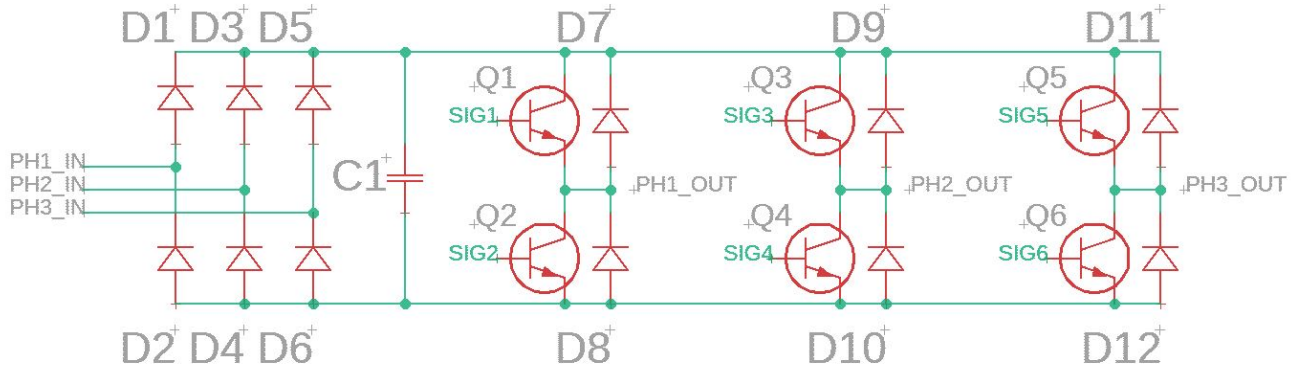


Figure 31: VFD Circuit

3.5.2 Control Signal Generation

Christian Garry

To control the transistors in the VFD circuit, 6 control signals are required. These are connected to the gates of the transistors and control when each transistor is outputting. These are PWM signals which have a sinusoidal duty cycle. To create this sinusoidal duty cycle a triangular wave (carrier wave) is compared to a sine wave [37] using an op-amp [38]. When the amplitude of the sine wave is greater than the amplitude of the carrier wave, the output of the op-amp is 3.3V, otherwise, the output is 0V. The circuit shown in Figure 32 creates the sinusoidal duty cycle shown in Figure 33.

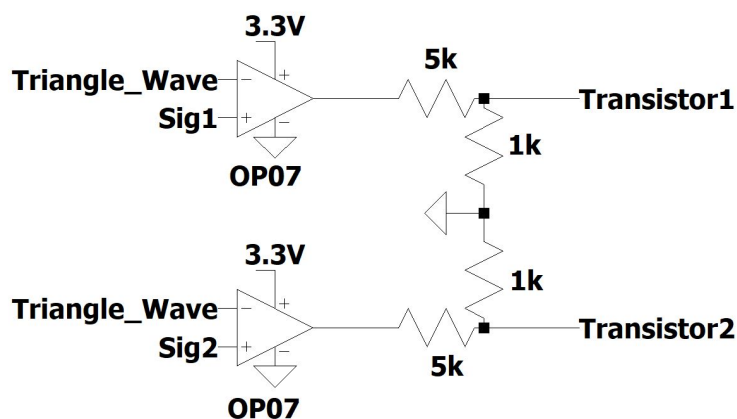


Figure 32: VFD PWM Signal Generator Circuit

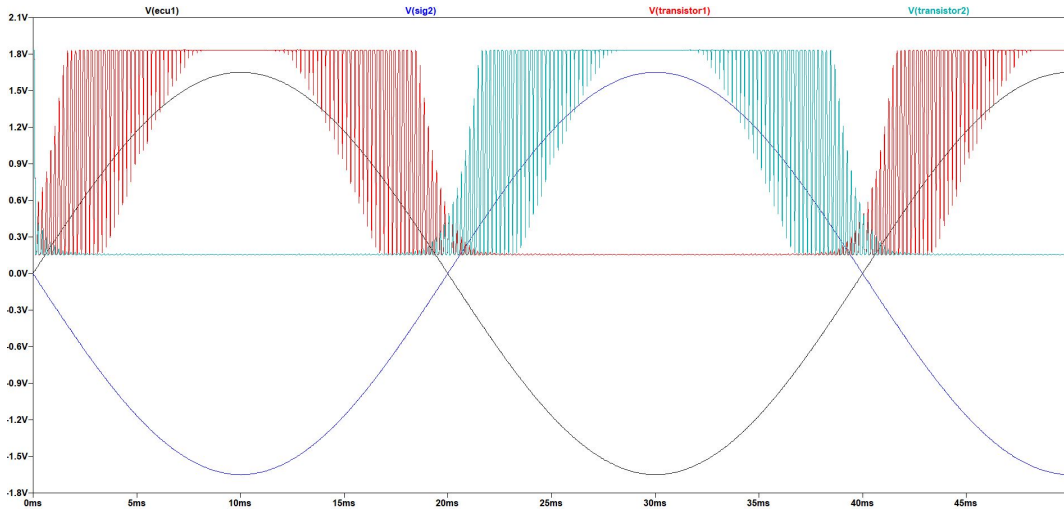


Figure 33: PWM Duty Cycle

3.5.3 Electronic Control Unit Signal Minimisation Circuit

Christian Garry

Pins on a microcontroller can be at a premium. This system of control for the VFD circuit would require 28 pins. Therefore, any optimisation made to reduce the number of pins required is desired. Since half the sine waves are simply the inverse of the other half, an inverting amplifier with unity gain can be used to produce all 6 sine waves from 3 ECU signals. The triangular waves are the same for all VFDs and as such can be combined saving a further 3 pins. This has the added benefit of ensuring that all VFD modules have the exact same carrier wave for the duty cycle increasing the accuracy of the torque differential between wheels. These optimisations reduce the required pins on the microcontroller down to only 13, saving 15 pins for other uses. The circuit for one phase is shown in Figure 34.

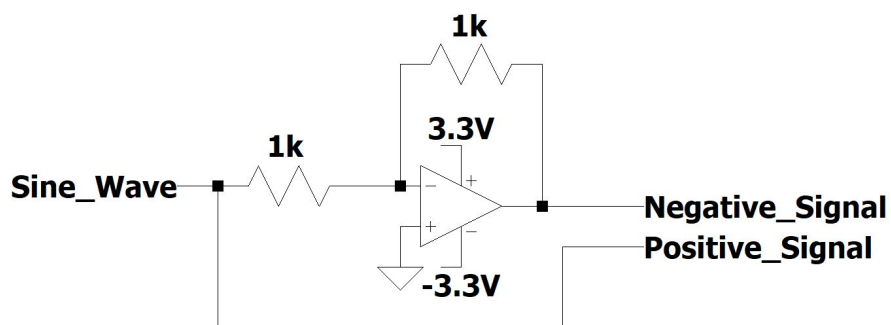


Figure 34: Signal Minimisation Circuit

3.5.4 Printed Circuit Board

Christian Garry

All the components utilised in the PCB [39] were chosen based on their rated specifications, price, and suitability as detailed in Table 4.

Component	Voltage Rating (V)	Current Rating (A)	Price (£)
Op-Amp	5.5	10mA	0.5
1k Resistor [40]	400	10	0.007
5k Resistor [41]	200	7	0.116
Diode	1000	3	0.137
Transistor	800	1.5	0.081
Capacitor	1000	2	2.00

Table 4: VFD Circuit Components

3.6 Housing, fixing and casing of the Variable Frequency Drives

Nathaniel Owen, Finlay Sanderson

The housing for the VFDs has been constructed using the same aluminium 7075 as for the ECU casing. The design includes a heat sink and a fan which are necessary to cool the diodes in the PCB. A 3D model can be seen in figures x and y, and the relevant drawings are in Appendix A. The design consists of a base, which the PCB will be fixed to with thermal adhesive, and a case containing the fan and the cooling system, which will be bolted to the base.

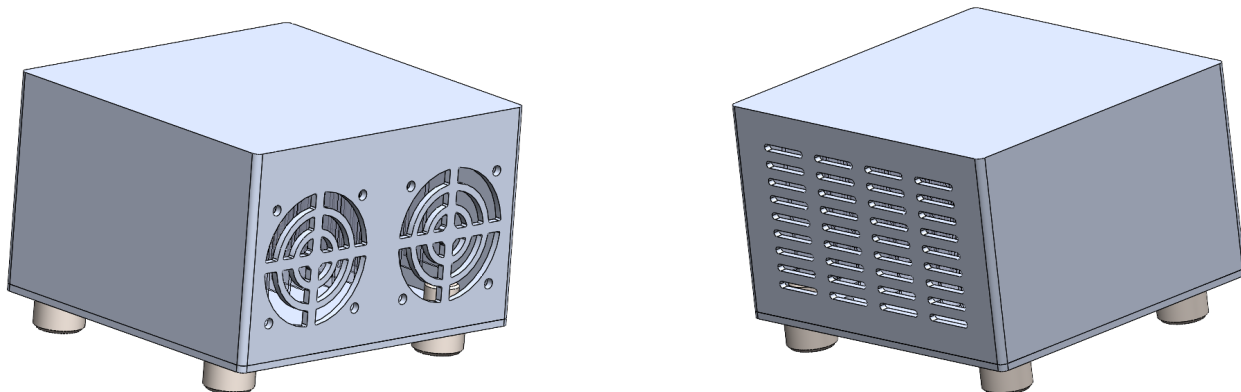


Figure 35: VFD Housing

The case has been designed to minimise material use and withstand the necessary vibrational stresses. This is shown in figure 36 as the maximum stresses in the case are roughly 1000 times smaller than the material yield strength. Optimising the material quantity not only reduces the cost but also decreases the waste and energy required for manufacturing.

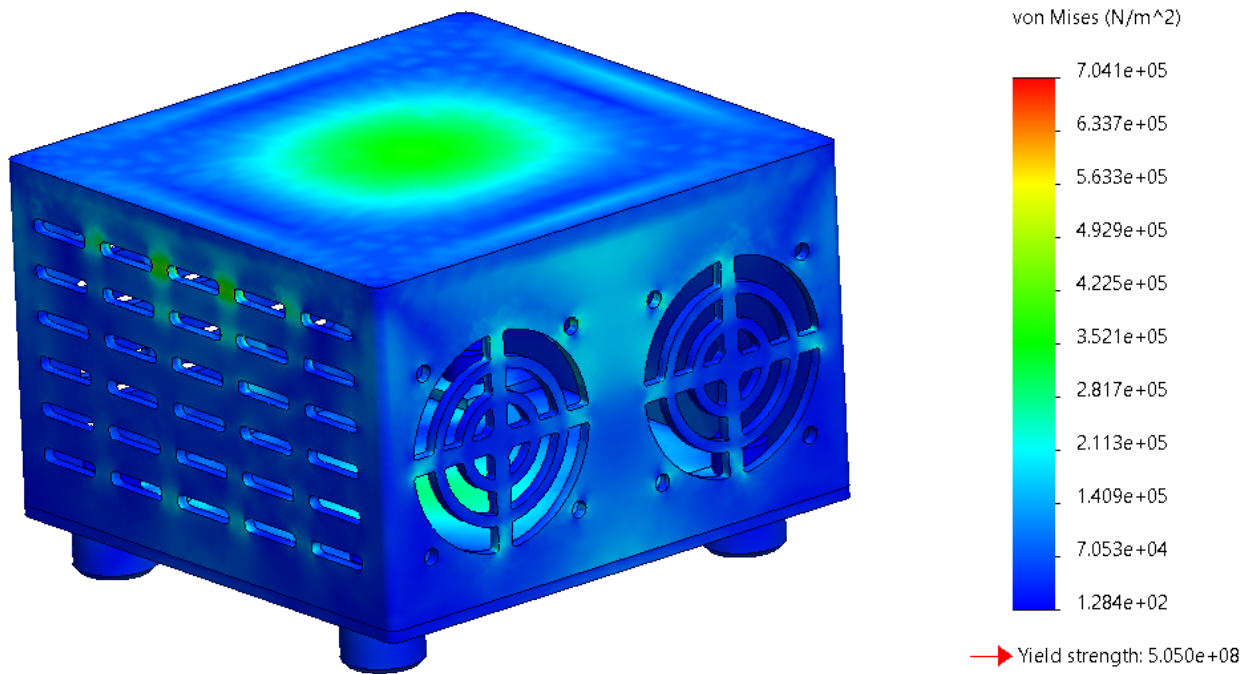


Figure 36: VFD Casing Vibrational Stress Analysis Displacement

3.6.1 Variable Frequency Drive Cooling

Sam Berry

The PCB electronics within the Variable Frequency Drive (VFD) unit under high load can lead to large amounts of heat production. Without a controlled cooling system these high temperatures risk permanently damaging the integrity of the other PCB components. The cooling system must be able to maintain a safe operating temperature below 370K for the PCB components [42]. In order to dissipate the heat, two fan units will draw airflow into the VFD casing and run the flow over a series of aluminium 1060 alloy fins as shown in figure 37. The fins maximise the surface area for heat exchange with moving air. Aluminium 1060 alloy has been chosen due to its high thermal conductivity and low density.

Figure 37 also shows the PCB board (in green) fixed to the aluminium base (1060 alloy) using AS1803 Silicone thermal adhesive. The ebm-papst 400 F Series Axial Fans are used and are able to push air at an axial velocity of 5 ms^{-1} [43]. Figure 38 shows the PCB and aluminium cooling fins within the VFD casing.

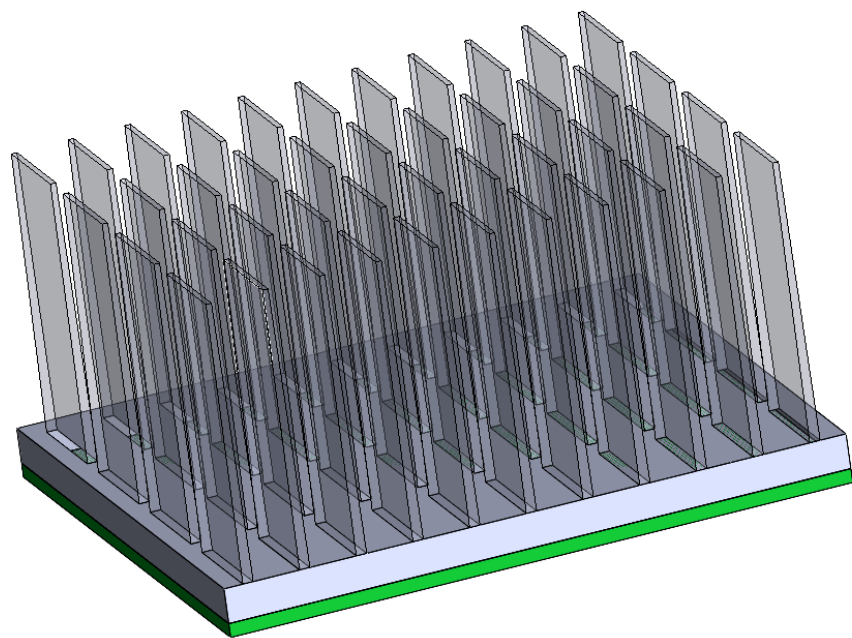


Figure 37: Aluminium 1060 Fin Structure Attached To PCB (green)

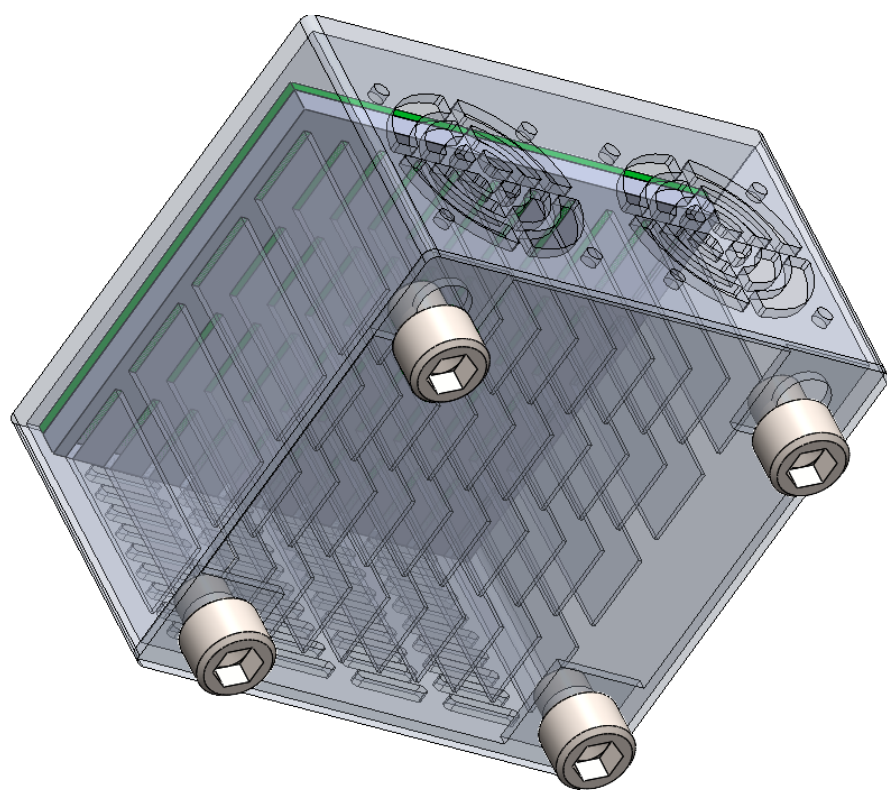


Figure 38: PCB Cooling Fins Inside VFD Casing

A combination of theory and Computational Fluid Dynamics (CFD) has been used to test the cooling system under the highest anticipated heat flux produced from the PCB components. 800W was used as a worst-case scenario where the diodes and transistors are 100% inefficient (800V, 1A).

A constant heat flux is assumed to pass through the PCB board, thermal adhesive, and aluminium unit. Since the PCB's cross-sectional area is $0.0072m^2$ the delivered heat flux from the PCB components to the aluminium fins is taken as 11.758 kW/m^2 . The analysis neglects any heat transfer from the sides of the material layers because the depth is very small compared to the cross-sectional area. Further, all the analysis neglects any heat dissipation between the PCB components and the VFD casing because the heat transfer rate is substantially less than that of the flowing air over the aluminium fins. Both assumptions lead to a worst-case scenario as the PCB will in reality cool faster than expected as some heat is dissipated from the surface of the PCB board and from the sides of the material layers. Figure 39 shows the model used for heat transfer between the PCB board and base of the aluminium fins. Table 5 evaluates the thermal conductivity and depth for the mediums in Figure 39.

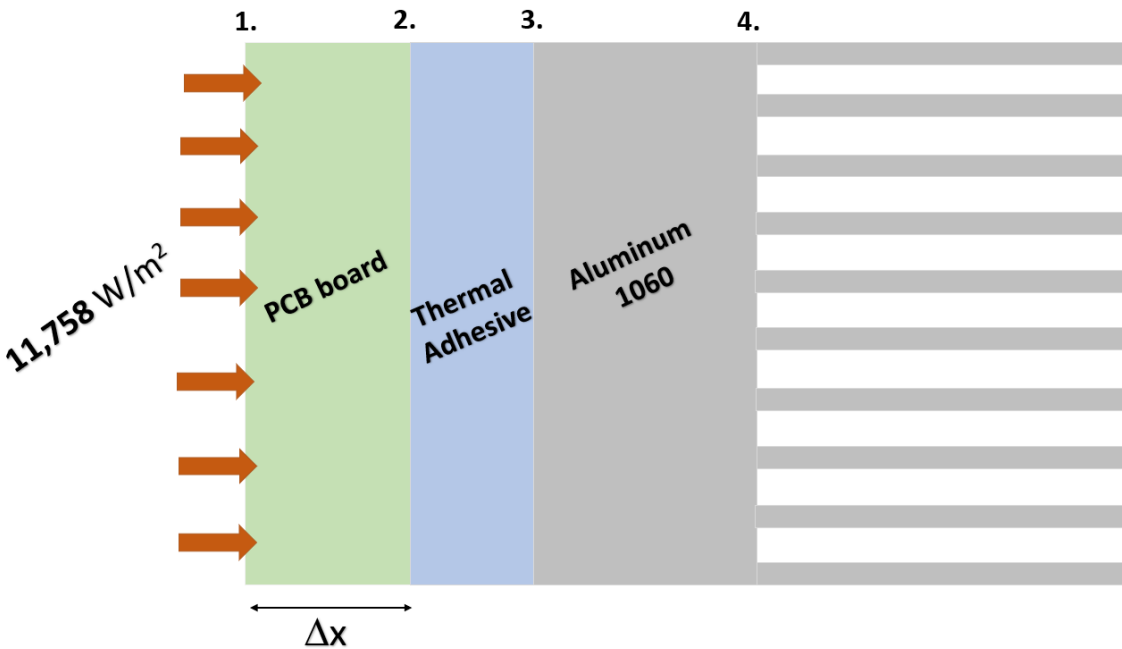


Figure 39: Heat Transfer Model From PCB To Aluminium Fins

Medium	Thermal Conductivity, k (W/mK)	Depth Δx
PCB (1-2)	1.6	1
Thermal Adhesive (2-3)	1	0.1
Aluminium 1060 (3-4)	170	10

Table 5: Thermal Conductivity and Medium Depth In Heat Transfer Model

Using CFD software in Solidworks, an external fluid flow simulation is run in real-time to monitor the aluminium fin temperature. The simulation runs at the maximum anticipated heat flux and the fans' maximum rpm as shown in Figure 40. Figure 41 shows the monitored surface temperature at the base of the fins over 5 seconds. Once the flow has developed the wall temperature is maintained at 360K. Then, implementing heat transfer theory, equation 10 is used to trace back and calculate the temperature at the PCB components.

$$q = \frac{T_1 - T_4}{\frac{\Delta x_{12}}{k_{12}} + \frac{\Delta x_{23}}{k_{23}} + \frac{\Delta x_{34}}{k_{34}}} \quad (10)$$

The layer thicknesses (δx) and thermal conductivities (k) are defined in Table 5. The temperature at the PCB components is calculated as 369K when under the highest anticipated load. Therefore, the fan cooling system is capable of maintaining a temperature at which the PCB electronics are not damaged when under the highest anticipated load.

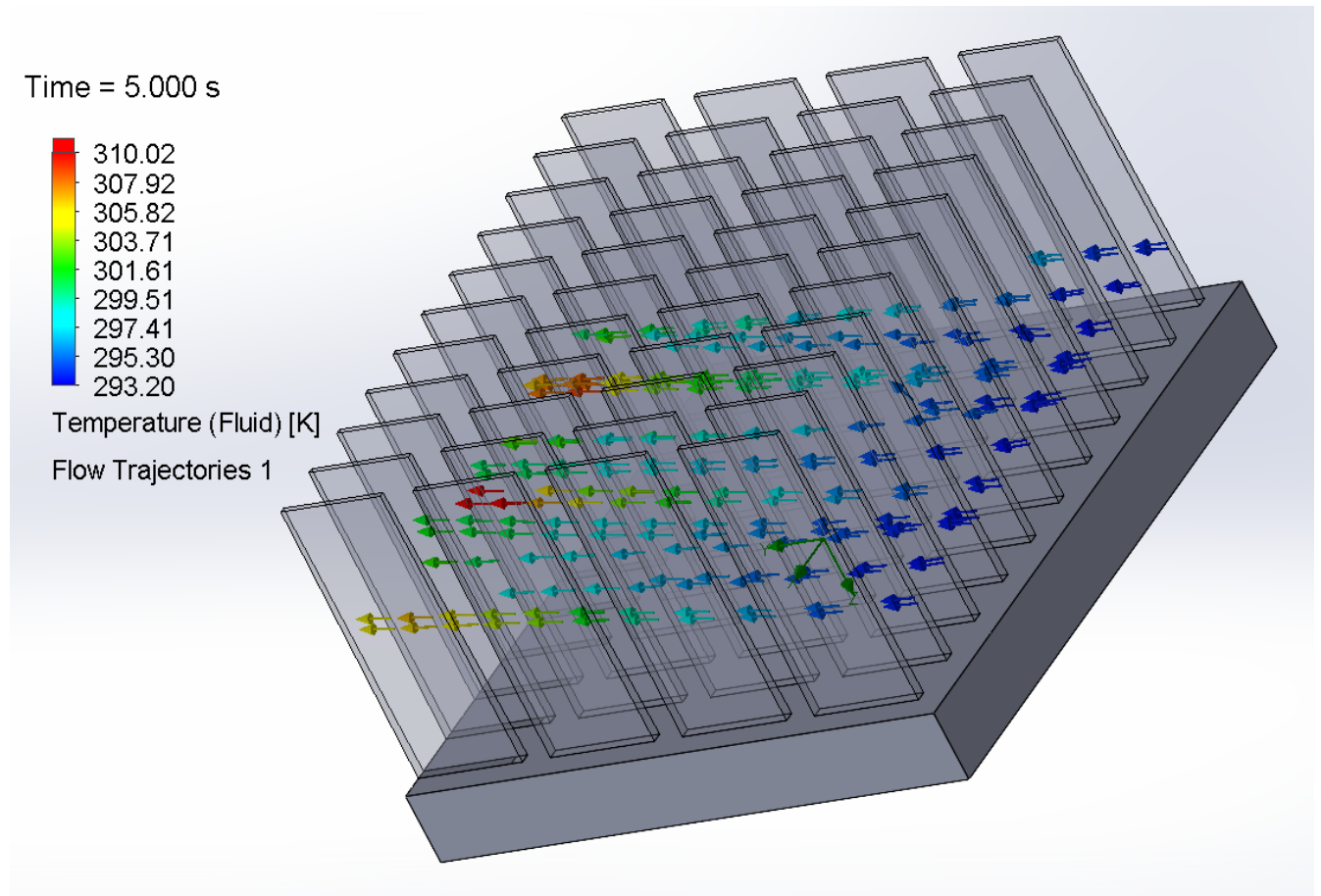


Figure 40: CFD For Airflow In Cooling System

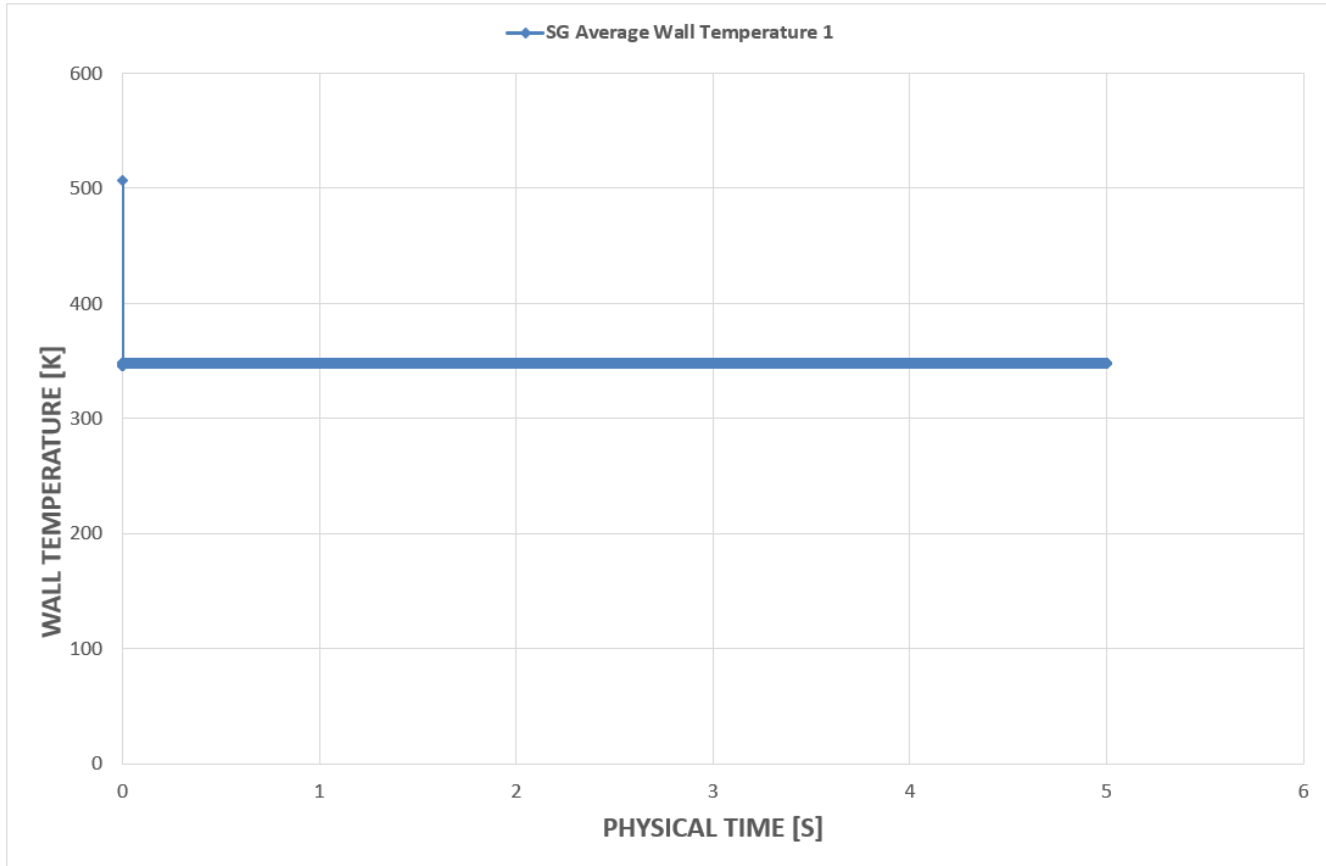


Figure 41: Aluminium Fin Wall Temperature In Real-time

3.6.2 Sheding force analysis

Sam Berry

A key mechanical design consideration with flow past structures are vortex shedding forces. Vortex shedding occurs when the flow past a bluff body creates forces on the structure in the direction perpendicular to the flow direction [44]. Since the aluminium fins have a base 10 times longer than they are wide, any normal forces along the width of the fin may cause high stresses at the fin base. Further, if these stresses go beyond the yield stress the fin structure may detach and break. The flow simulation monitored these perpendicular forces along the width of each fin. The monitored results can be seen in figure 42 over 5 seconds, when the axial fans run at maximum rpm. Although the force settles at 0.01N and this seems to be negligible, further stress analysis should be run considering the fins are extremely thin (2mm).

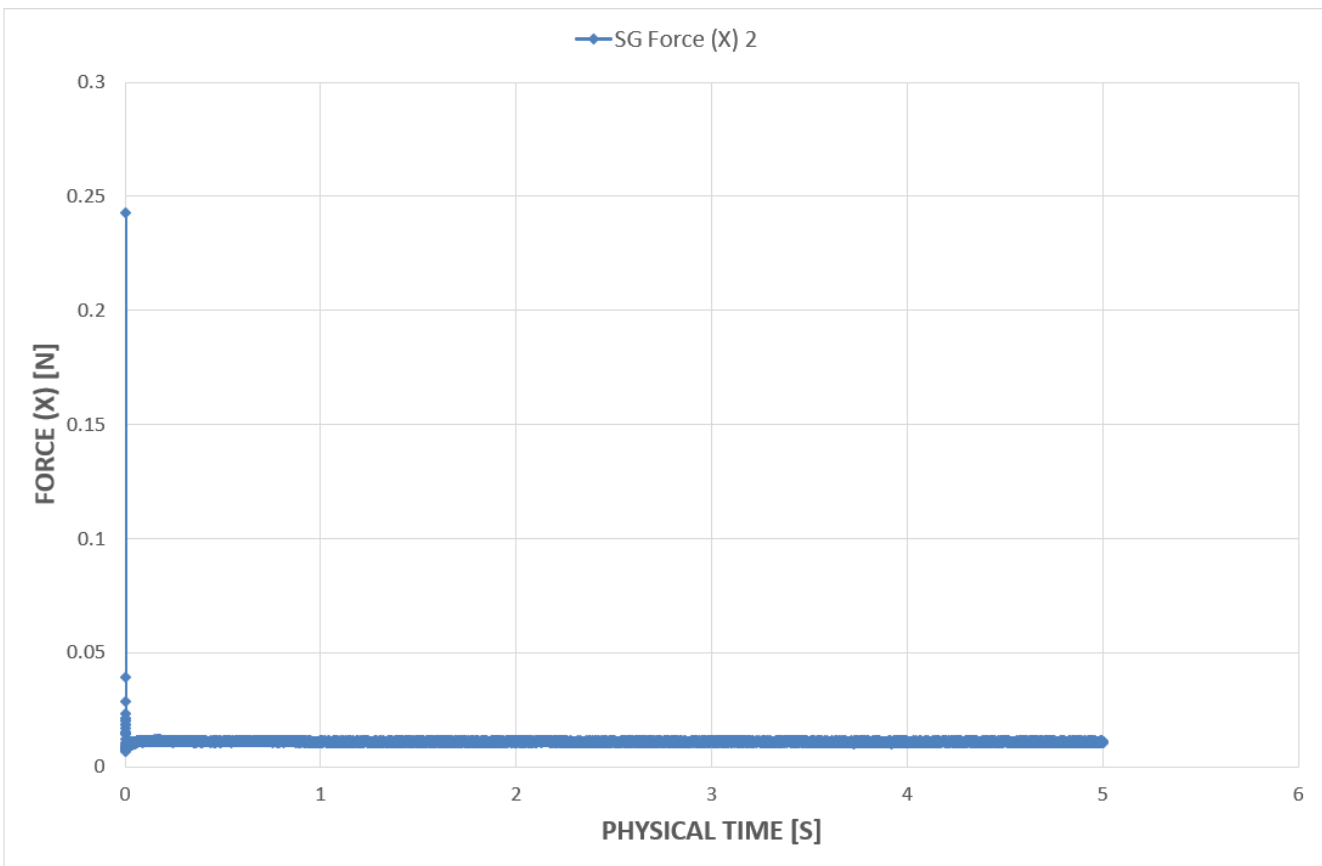


Figure 42: Shedding Force On Singular Aluminium Fin

Stress analysis is run in Solidworks using the predicted force along the width of the fin. Figure 43 shows the Finite Element Analysis (FEA) over a singular fin. The maximum stresses at the base of the fin are 1.74 MN/m^2 . The yield strength of Aluminium 1060 alloy is 27.6 MN/m^2 meaning that when the fans are running at maximum speed, the stresses in the fins have a FoS of 15.

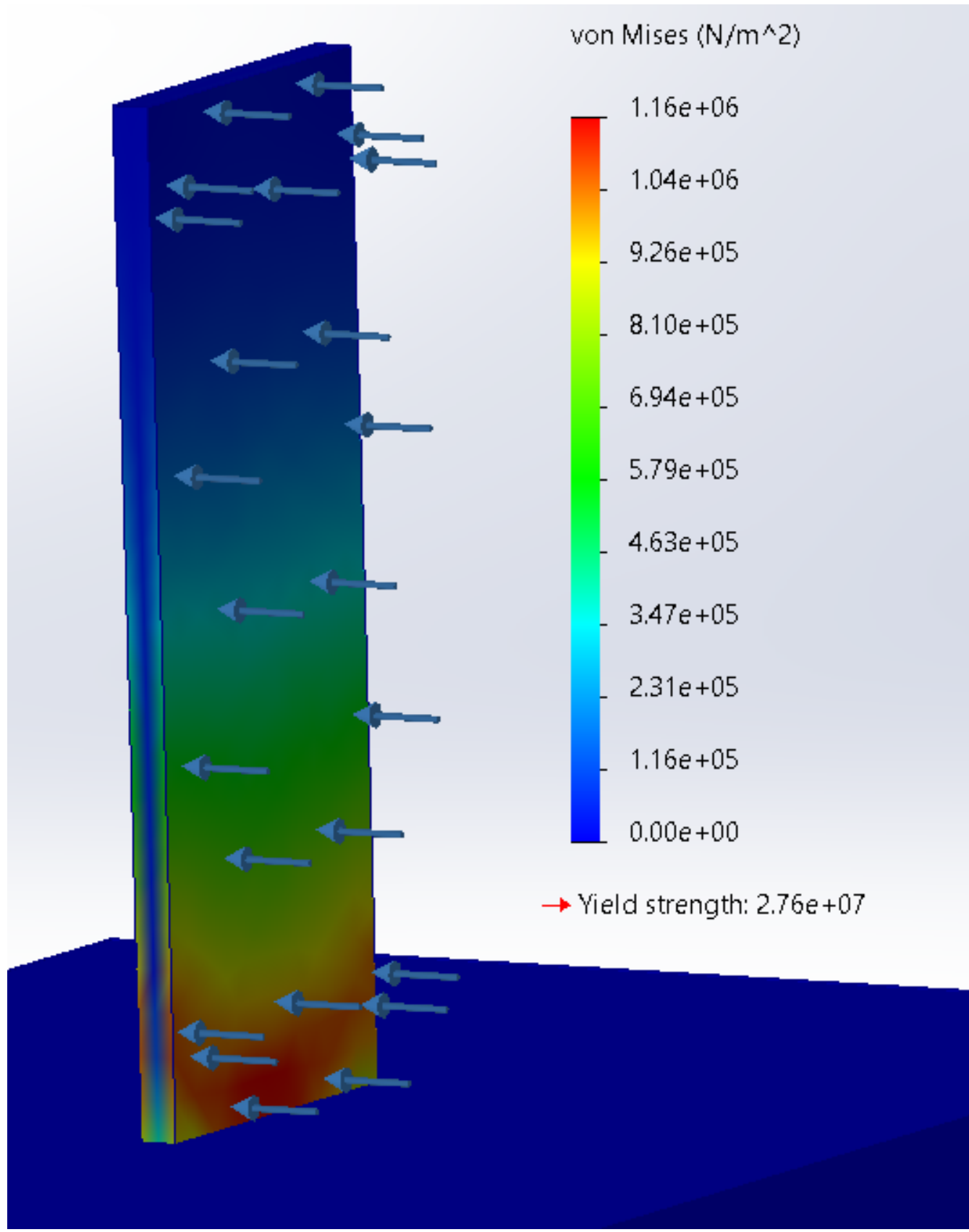


Figure 43: Finite Element Analysis On singular Aluminium Fin With Applied Shedding Force

3.7 Connections

Nathaniel Owen, Christian Garry

The electronic components are wired to each other and the external systems in the vehicle using a variety of cables. Figure 44 shows the cables that will be connected to the ECU for external communications. The low voltage ($<5V$) signals will be transmitted through standard gauge signal wires. The exact size is dependant on the sensor but all are compatible with the pin connector for the ECU. Sensors are usually only connected to the ECU that processes the data. As the Torque Distribution ECU is high priority, all the necessary sensors will be connected directly and their signals will be broadcasted to the CAN bus from the transceiver.

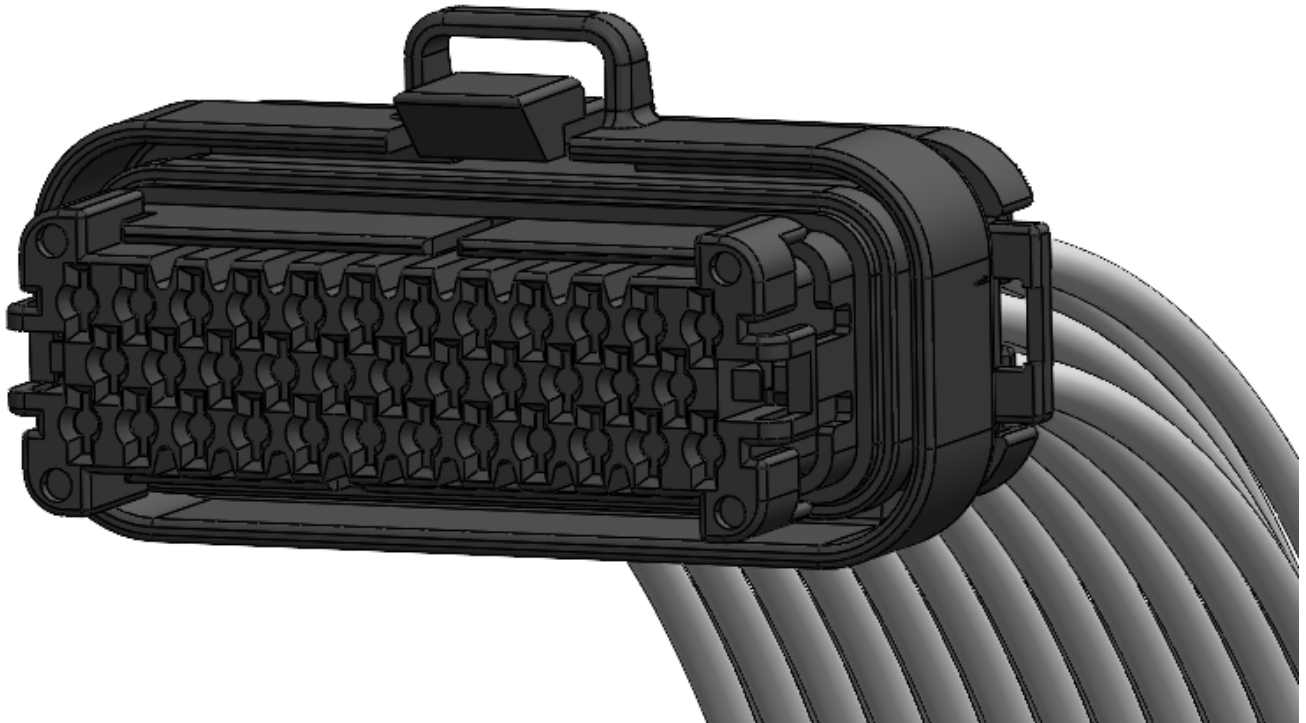


Figure 44: Cables and receptacle housing connecting to the ECU

For the high voltage circuits, high voltage interlock (HVIL) cables [45] are used, these are common within the electric vehicle industry. They have 3 connections for 3 phase power and also have a HVIL signal line, which all connect together and ensure that the connector is plugged in correctly. If any connector is incorrectly plugged, it will be noticed by the system and an appropriate warning will be displayed.

4 Design for Manufacture

Nathaniel Owen, Finlay Sanderson, Henry Wong

With initial plans for batch production to meet low demand in the first year of manufacture, sourcing methods for materials and labour should match this. The manufacturing and assembly of the product will be out-sourced to reduce initial costs, with the idea of moving more of these processes in-house with company growth. Production will be based in Asia since the current market share covers 56% of EVs and low labour costs will aid start-up. The product has been designed to minimise material usage and number of parts, resulting in 212 parts required for assembly. As a result, storage and waste management costs can be minimised.

The product will be shipped to the customer as a self contained product, which will be fitted at the appropriate point in the production line at the discretion of the car manufacturers. The VFDs will be installed with the motors, and be attached to the sub-frame which sits upon the chassis. The torque distribution ECU will be installed later in production, along with the other electronic control units in the vehicle. Finally the wiring will be completed in parallel with all wiring in the vehicle. This provides a feasible outline for the integration process.

4.1 Manufacture of Casing

Finlay Sanderson

With the location and material choice set for the ECU and VFD casing, the next step was to analyse the two main manufacturing methods, die casting and Computer Numerical Control (CNC). Die casting involves melting AA7075 and injecting it into a steel mould, whereas CNC automates the process by using a machine to sculpt the part. Table 6 evaluates the benefits and drawbacks of each manufacturing process.

Criteria	CNC	Die Casting
Volume	CNC removes tooling costs, and is the better choice for low volume production	Consistent quality at high quantity ensures suitability for mass production.
Speed	Faster for prototyping and smaller volume parts	Repeatable and extremely fast, making it more reliable for producing large quantities.
Precision	Great precision and tolerance, especially for highly customised small parts.	Precisely forms complicated geometrical shapes but can sometimes result in surface defects
Waste	Subtractive manufacturing method produces high material waste leave.	Additive manufacturing, producing little waste, and reducing costs.

Table 6: Die Casting Vs. CNC

From analysis of table 6, the most suitable manufacturing process for the ECU and VFD casings is die casting, due to high quality mass production potential. Furthermore, die casting is the quicker process, allowing for rapid scalable production of the casing which aligns with the business model moving forward. Die casting is also the clear choice when considering sustainability, as it produces significantly less waste, and does not require the implementation of a complex recycling system for reducing waste.

The aluminium die casting will be outsourced to a third party, with this costing taken into account in the labour costs. The resultant casing will be assembled in house by the TorqueDrive team, before being sent out for delivery to the customers. The PCB will be attached to the casing using AS1803 Silicon Thermal Adhesive, which has a thermal conductivity of 1.55W/mK, which aids in heat removal from the PCB to maintain optimum function of the PCB. The casing will be sealed using VT-131 Silicone Sealant, in order to protect the PCB from any water or dust damage, in line with point 2.2 in table 1.

4.2 Aluminium Fin Heat Sink

Finlay Sanderson

The cooling system for the VFDs will be manufactured from aluminium 1060 alloy using Computer Numerical Control (CNC) since it is an intricate part that requires precise manufacturing. The manufacturing process will be outsourced, whilst the assembly will be completed in-house. The fins will be fixed to the PCB and the case with AS 1803 Silicon Thermal adhesive.

4.3 PCB Manufacturing

Henry Wong, Nathaniel Owen

The PCBs are manufactured and the components are soldered on by a subcontracted Printed Circuit Board Assembly (PCBA) manufacturer. The firmware is then flashed onto the microcontrollers. Quality control and testing will be done by the same manufacturer. The PCBs will be produced using the chemical etching method. The PCBs are copper-filled, minimising chemical etching required, thus reducing production time and cost for the PCB. All surface mount devices will be machine-soldered, while through-hole components will be hand-soldered. The circuit boards are made using aluminium oxide ceramic which is 1.6mm thick. There are also four mounting holes which are 3mm diameter and the PCB will be mounted using M3 screws.

5 Design for Sustainability

Finlay Sanderson

Aluminium is widely regarded as the ‘most sustainable building material in the world’ [46], as recycling one tonne of aluminium saves nine tonnes of CO₂ emissions and 14,000kWh of electricity, whilst also saving 95% of the energy used in its production from raw materials [47]. ISO 14021 suggests that, in general, there are two types of materials from a sustainability perspective:

- Pre-consumer material - material diverted from the waste stream during a manufacturing process. As the manufacturing process creates a small amount of waste, a very small percentage of the aluminium used by TorqueDrive will be pre-consumer material.
- Post-consumer material - Waste material generated by a product at the end of its’ life. As the majority of the recyclable aluminium used by TorqueDrive will come at the end of its’ life, the majority of the aluminium waste will be post-consumer material.

The post-consumer material can be easily recyclable as long as a suitable recycling process is adhered to, with post-consumer aluminium having a carbon footprint of 0.5 tCO₂e/t [46]. This compares very well with other popular building materials such as steel, which has a carbon footprint of 1.4tCO₂e/t [48], which is almost 3 times higher than aluminium. Materials with a lower carbon footprint than aluminium are rare, with newly developed SmartPlys [49] and other wood-based materials offering a lower carbon footprint. However, these materials are several times more expensive than aluminium, and do not have the material properties to fulfill the technical requirements for the casing, so therefore cannot be used.

Pre-consumer aluminium is almost 100% recyclable [46], but as the amount of pre-consumer aluminium created by the manufacturing process will be down to the CNC of the heat-sink fins, which will be a very small amount, it is inconsequential when compared with the post-consumer aluminium. Therefore, with the correct recycling procedures in place, the majority of AA7075 used in the casing will be recyclable, which fulfills specification point 4.1 in table 1.

To avoid the use of energy intensive processes, thermal adhesives have been used to fix parts within the ECU and VFD casings. Welding was disregarded as a fixing method due to its unsustainable nature. In particular, arc welding contributes significantly to global warming, acidification and, eutrophication.

6 Final Product

TorqueDrive's final product, solving the problem laid out by the design brief and in section 1 is a torque vectoring electronic differential system, that allows for independent torque control at each wheel, with the ECU and 4 VFD locations shown in Figure 45. The creation of a system allowing independent control creates TorqueDrive's unique selling point, as the current market lacks a system that replicates a mechanical differential using independent torque control.

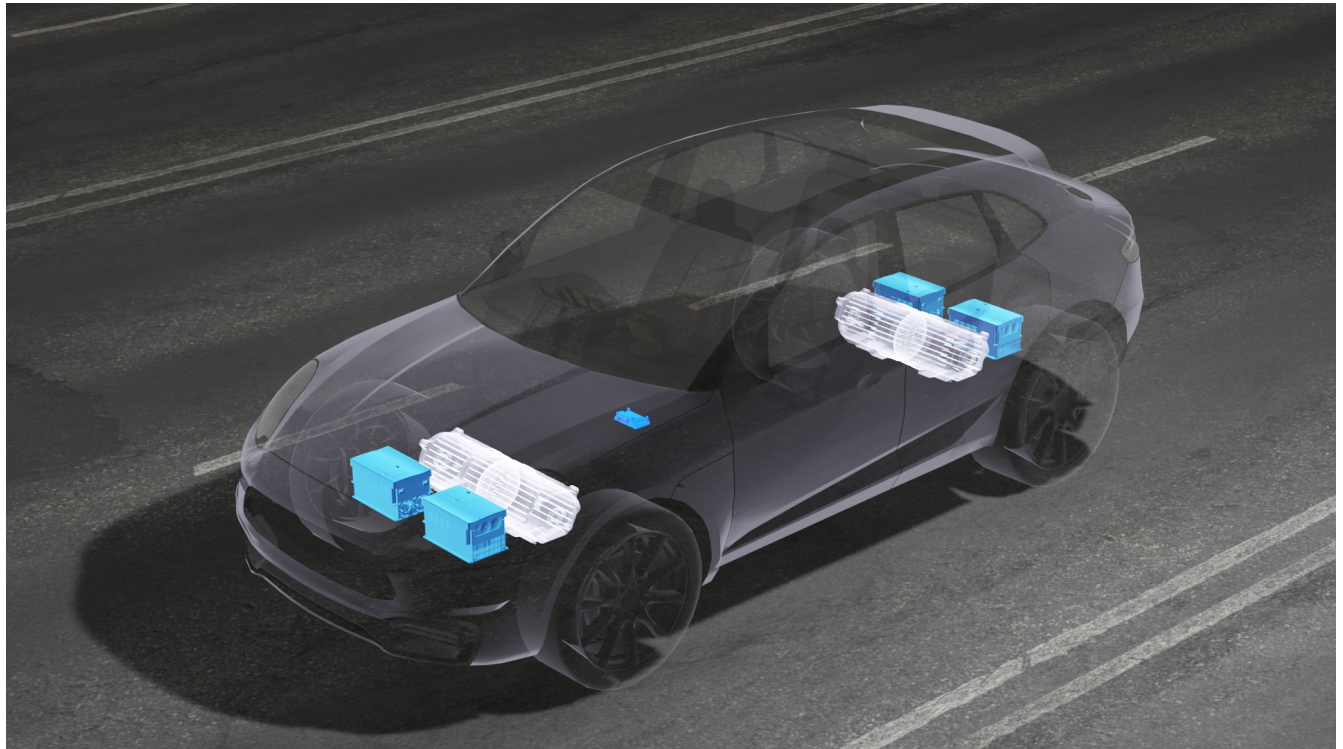


Figure 45: Final Location of the ECU and VFDs within the reference vehicle

The final system incorporates a model that deals with the cornering and acceleration of the vehicle. This consists of an ECU, complete with thoroughly analysed casing, which receives inputs from the vehicle's sensors such as steering angle, velocity and acceleration. A control algorithm, flashed onto the ECU during the manufacturing stage, then calculates a desired yaw moment based on the sensor inputs, and compares this against a measured yaw moment from the vehicles sensors, before minimising the error between the two using SMC. The minimisation of this error produces a torque output, which is the torque difference required to equate the measured yaw moment to the desired yaw moment. This desired torque is then passed to 4 VFDs, with each VFD controlling the torque to an individual wheel. Each VFD adjusts the torque delivered to each wheel depending on the output of the control algorithm, which would then stabilise the vehicle during cornering, successfully simulating the effects of a mechanical differential.

With TorqueDrive currently weighing 2.5kg, the system operates at roughly 4% of a standard mechanical differential's mass (60kg) [50]. This represents a 3% drop in the overall mass of the Macan (1845kg), with current estimates suggesting this could lead to a 4.2% increase in electric vehicle driving range [51], solely from using TorqueDrive over a standard mechanical differential. In a vehicle of smaller mass, the efficiency benefits would be even greater with the incorporation of TorqueDrive, as the reduction in weight would represent a greater percentage decrease, thereby leading to a higher driving range for the EV.

Alongside the cornering model, the TorqueDrive system operates a sophisticated Regenerative Braking model. The ECU uses electronic braking distribution to uniquely control the level of regenerative braking in individual motors. This helps the vehicle to reduce slip and the braking distance. When necessary the friction brakes work in tandem with the regenerative braking or in some situations will provide all the required braking torque. Further, when no pedals are depressed the user can adjust the regenerative braking on a 1-4 scale of varying strengths.

7 Business Case

Sam Berry, Finlay Sanderson

TorqueDrive is a start-up company and therefore, with no sales history, it is essential a comprehensive business strategy is put into place to gain interest from automobile companies. Almost all innovative ideas and products must first go through a company's R&D department. TorqueDrive will be pitched to these departments to win production contracts and create long-lasting relationships.

It is expected that the sales format will be a contract-based agreement where TorqueDrive will be hired to provide units for a particular vehicle in production over a set period of time. For example, TorqueDrive may win a contract to provide the differential units for a newly released vehicle over a period of 3 years. Although entry into new companies is very important, it is equally pertinent for TorqueDrive to remain competitive within the market. EV companies are always on the lookout for new technologies and therefore are reluctant to sign long-term contracts that may restrict their future growth. When these contracts expire TorqueDrive must be in a position to reconvince a company of the product's potential. To remain competitive TorqueDrive must itself invest in R&D to follow technological trends and ensure contracts are extended.

Applying for patents is another procedure TorqueDrive can utilise to remain competitive in contract deals. Ensuring the company remains unique and ahead of the market is worth any small patent overheads for successful contracts.

7.1 Cost and Profit Structure

Sam Berry

TorqueDrives's electronic differential's full Bill of Materials (BOM) is shown in Appendix A. Per electronic differential the direct material costs total £1,154. This includes the components of the ECU unit, 4 VFD units and wiring. Figure 46 displays a breakdown of the major components for the ECU, VFDs and wiring. The total direct labour costs of £95 are estimated for each product sold, bringing the total direct cost per differential to £1249. The direct labour costs are estimated by taking a soldering hourly cost and assuming each unit takes 1 hour to assemble.

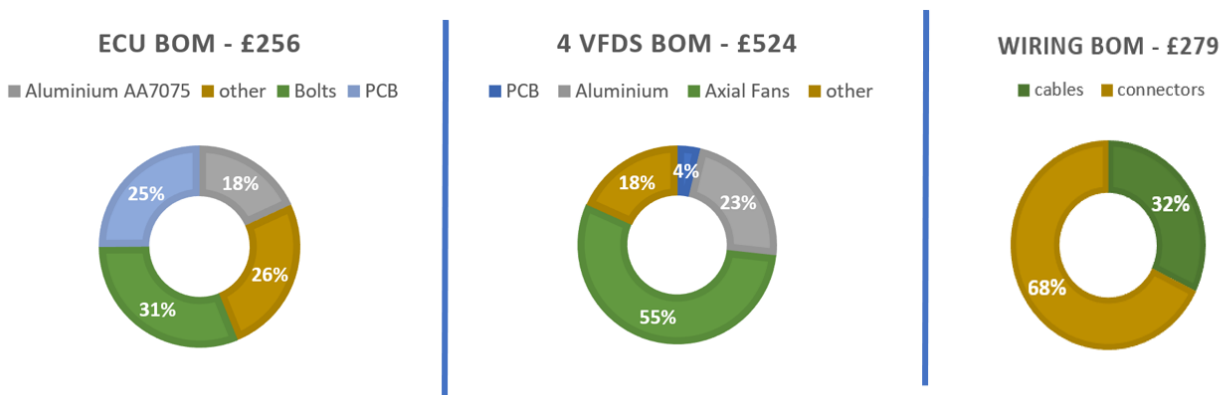


Figure 46: BOM Breakdown For ECU, 4 VFD Units and Wiring

The units are sold at £2,700 generating a gross margin of 57.3%, which is widely considered to be a healthy gross margin for any start-up company. The first-year overheads are predicted to be £553,000. This incorporates indirect costs to the business such as salaries for 6 engineers, storage costs, and rent for a small-sized mechanic workshop. These overheads are forecast to increase each year. For the profit forecasts, it is assumed overheads will scale up in line with the rate of revenue increase.

7.2 Financing

Sam Berry

Overheads for at least the first year must be financed using raised capital. Further, enough capital must be raised to cover underperforming sales figures in the initial years. There are two main options for TorqueDrive's financing. Firstly, raising capital in the form of equity from venture capital firms, who in return take some equity share of the company. Alternatively, capital can be raised in the form of debt from corporate banks, who in return take no equity but interest and principal payments. For TorqueDrive, debt financing is chosen as the most suitable option as venture capital requires large portions of equity to be given away, whereas debt financing loses 0% of the company's equity.

The 2023 outlook for Venture debt looks promising despite hiking interest rates. Global private equity and venture debt investments in electric vehicles and components stood at \$9.45 billion through the first 10 months of 2022 according to S&P Global Market Intelligence data.

TorqueDrive will take on £1 million of debt finance, at a predicted 12% interest for the profit forecast. Further, for the projected finances it is assumed the debt will be repaid over a 3 year period in equal principal amounts.

7.3 Sales Forecast

Sam Berry

Figure 47 shows TorqueDrive's sales predictions for the first 3 years. Only the first three years are forecast as the inaccuracies in forecasts past year 3 are too large. Based on the predicted sales, Figure 48 shows the forecast finances for TorqueDrive over the next 3 years. The corresponding data is displayed in Table 7 including the post-debt profit. This is the net profit minus any principal debt payments. The forecasts have been generated in this way to stay in line with accountancy methodology. Debt principal payments are not on the profit loss account but instead classed as a liability on the company's balance sheet. A corporation tax rate of 25% has been used (beginning April 2023, UK).

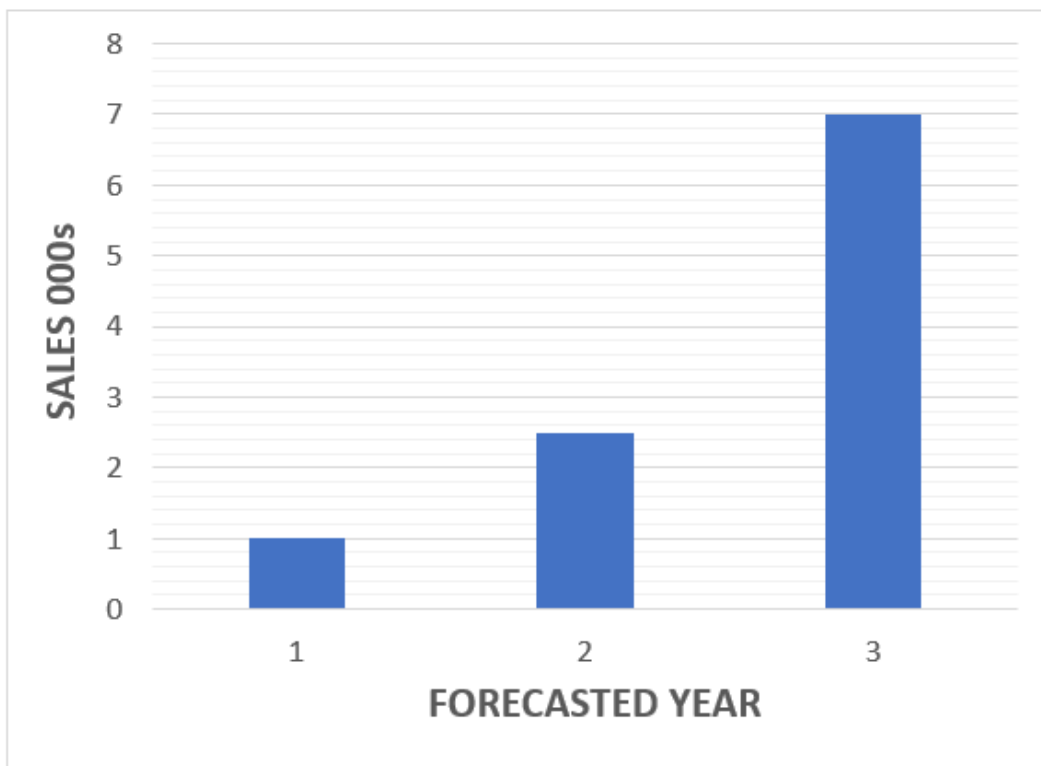


Figure 47: Product Sales Forecasts

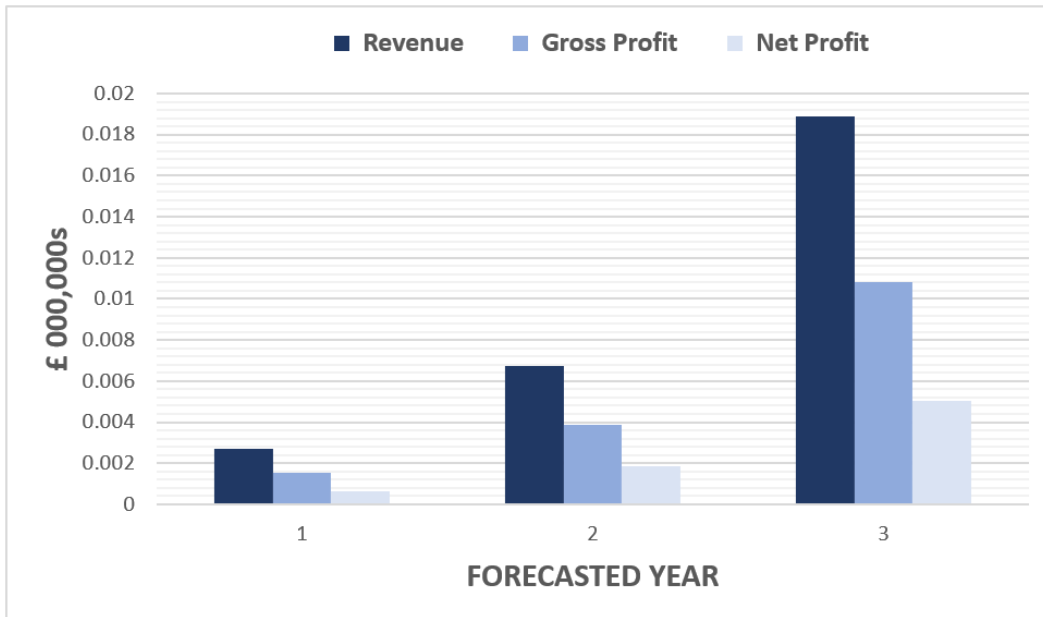


Figure 48: Revenue, Gross Profit and Net Profit Forecasts

Year	Sales	Revenue (£000s)	Gross Profit (£000s)	Net Profit (£000s)	Post Debt Profit (£000s)
1	1000	2700.00	1545.63	645.47	321.14
2	2500	6750.00	3864.08	1870.56	1537.22
3	7000	18900.00	10819.41	5024.56	4691.22

Table 7: Sales and Financial Forecasts

7.4 Target vehicle Manufacturers

Sam Berry

In order to break into the market, TorqueDrive will initially prioritise selling to newer emerging electric vehicle companies. Although many large automobile corporations will also be targeted in the initial start-up, the majority of funding will be aimed at newer companies with high growth rates. The two main companies TorqueDrive will aim to break into are Polestar and Lucid Motors. Polestar sold approximately 21,000 vehicles in Q4 of 2022 and their 2023 sales target is 80,000. Lucid Motors has also displayed rapid growth over the last couple of years having sold 15 times as many vehicles in Q4 of 2022 than the entire of 2021. This strategy will help TorqueDrive build up a strong reputation within the EV market. When TorqueDrive decides to direct more capital to enter larger vehicle companies it will have gained the necessary credibility.

7.5 Market Analysis

Sam Berry

The global Electric vehicle (EV) market is forecast at 22% compounded annual growth rate (CAGR) until 2030. Legislation banning the sales of new internal combustion engine (ICE) vehicles is to be introduced in 2030 for the UK (and many other countries following suit). Vehicle manufacturers are beginning to invest their capital into new EV technology and infrastructure. It is predicted that 2026 will be the turning point: when vehicle companies will begin to fully phase out ICE vehicles. Therefore, entry into the market now provides an opportunity to gain credibility before EV sales ramp up in 2026. The global Electric SUV market is expected to reach \$320 Bn by 2030 and shows the fastest growth rate in sales among the electric vehicle class according to Acumen research and Consulting data.

7.6 Competitor Analysis

Finlay Sanderson

From research of both the EV and electronic differential market, there is only one direct competitor to TorqueDrive, which is the differential system used on the Rivian R1T, shown in figure 49. The differential system used on the Rivian offers independent torque control of each wheel using a 4-motor system, with Rivian referring to this as 'Quad-Motor drive' [52]. Quad-Motor drive offers very similar performance characteristics to TorqueDrive when it comes to cornering stability and acceleration. However, the Rivian differential still incorporates many of the heavy, inefficient parts from a standard mechanical differential such as the gearbox and clutch [53], meaning current estimates suggest the Rivian differential has a similar mass to a standard mechanical differential, and therefore offers limited efficiency and weight reduction benefits over. This is where the TorqueDrive system stands apart from its' direct competition, as the differential system offers comparable performance to the Rivian, whilst offering an increased driving range due to the increased efficiency of TorqueDrive.

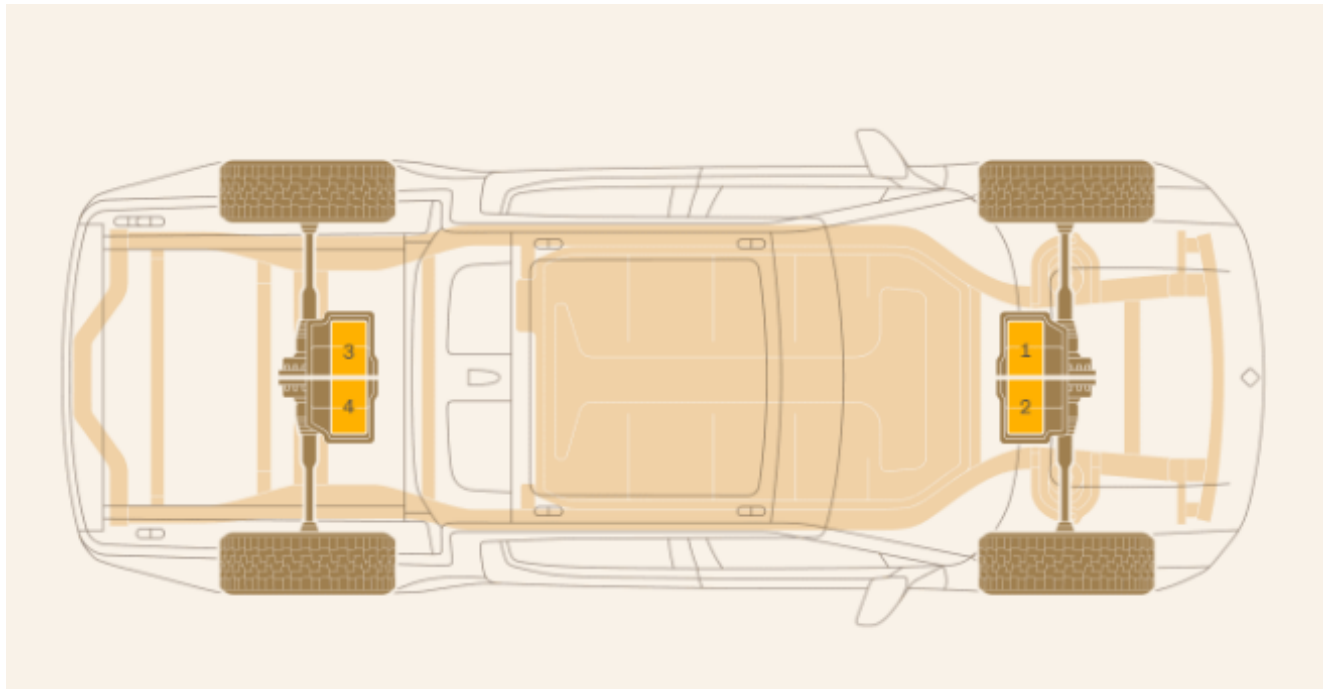


Figure 49: Rivian R1T Differential System.

8 Project Schedule

Matthew Youngman

The Gantt chart shown in Figure 50 describes the workload split throughout the product and business development. It is broken down into headings to focus team-members on specific goals, and the flow process has been followed throughout. Weekly splits between headings presented at meetings has also aid labour division, with hourly quotas required to be met by individuals.

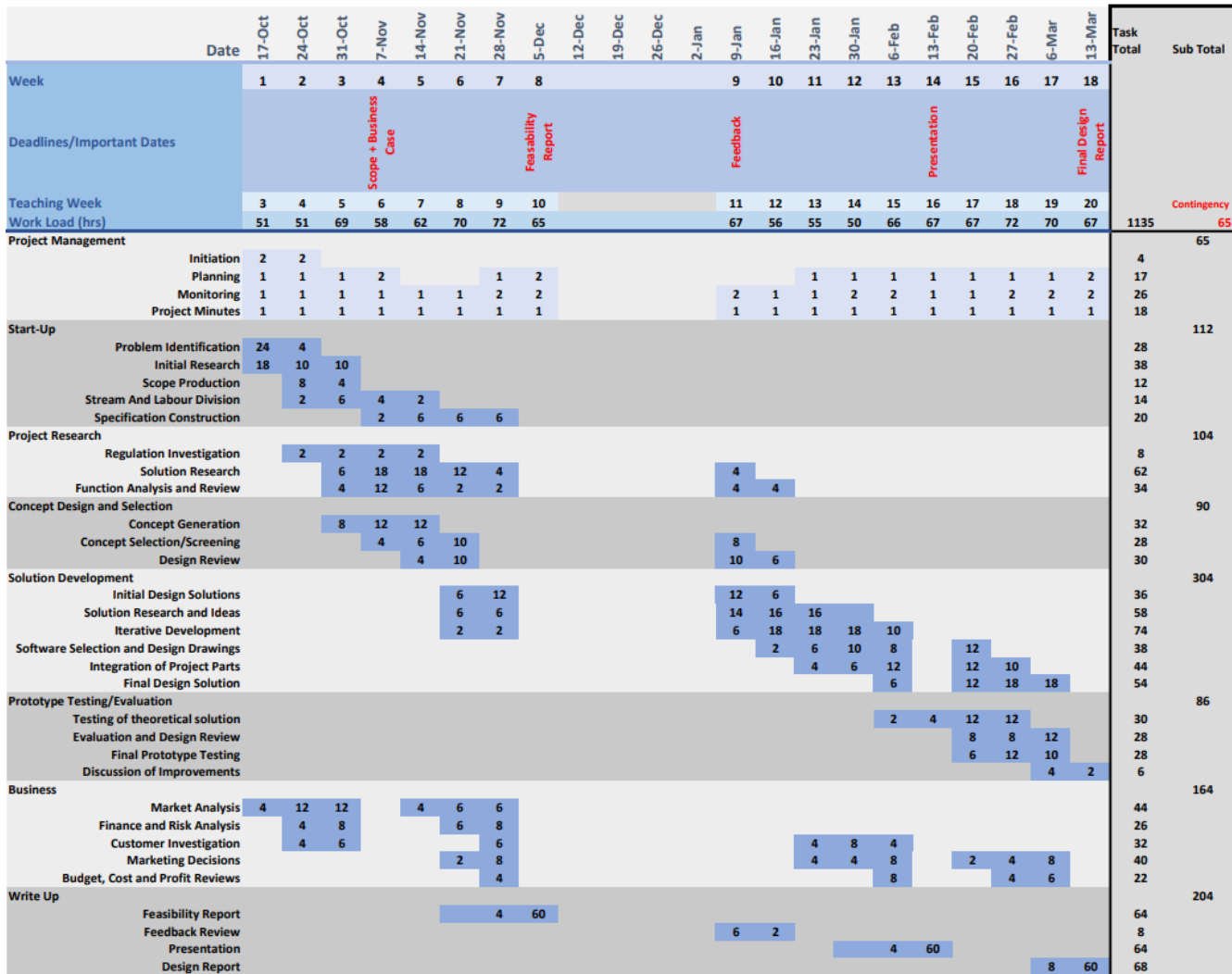


Figure 50: Gantt Chart

9 Risk Assessment

Table 8 demonstrates a comprehensive risk assessment for TorqueDrive. It evaluates technical risks such as updates to the regulations governing the industry, as well as commercial risks such as the emergence of new competitors as a result of the growing market. Table 8 also details mitigation strategies, in order to minimise each individual risk.

Risk	Mitigation
New fuel source emerges onto the market, such as hydrogen	<ul style="list-style-type: none"> • Ensure that the system acts independently of the fuel source, so that it can be easily adapted to any new fuel source.
Newly emerging market, therefore potential for lots of new companies	<ul style="list-style-type: none"> • The majority of the market is expected to shift towards electronic differentials in 2026, so the aim is to get ahead of the market and have the system ready ahead of the competition.
Updates to the standard and regulations that govern the system.	<ul style="list-style-type: none"> • Maintain a close relationship with customers, so that the system can be easily updated to conform to any updates to changes and regulations. • Ensure system itself can be easily updated, most likely through a software update, and act quickly on updates to regulations.
vehicle manufacturers decide to develop their own system, instead of purchasing TorqueDrive.	<ul style="list-style-type: none"> • Large manufacturers will increase demand ahead of 2026 focus switch. • Pre-developed system can target changing market to get ahead in the new market.
PCB is damaged or disrupted by impact	<ul style="list-style-type: none"> • Casing is designed to withstand maximum stress based on comprehensive stress analysis.

Table 8: Risk Analysis

10 Code of Practice

A detailed Code of Practice is required to help employees understand what standards are expected of them. Further, it guides leadership teams on how to enhance performance and enforce disciplinary action. The Code of Practice helps demonstrate to clients that TorqueDrive follow ethical principals and procedures. Table 9 shows the Code of Practice TorqueDrive will follow.

Requirements	Description
Installation into vehicle	<ul style="list-style-type: none"> System should be implemented into the vehicle by a trained professional, to ensure system is safely installed into the vehicle.
Strict testing and safety features	<ul style="list-style-type: none"> Ensure thorough safety testing is carried out on the system. Recommend monthly maintenance to manufacturers, to ensure safety of system.
User Override Function	<ul style="list-style-type: none"> System should have a working user override system, where the user can disable the torque vectoring differential.
Sensor Testing and Maintenance	<ul style="list-style-type: none"> Sensors are vital to the safe operation of this system, so regular checks should be undertaken to ensure they are functioning optimally. Any sensors not functioning would require immediate maintenance, as the system will not be able to operate without the sensors.
Competency of Engineers	<ul style="list-style-type: none"> Ensure each engineer operates in a field they are competent in, to guarantee quality of work produced.
Crash Testing	<ul style="list-style-type: none"> Current guidance expects vital systems to survive crashes up to 37.2823mph (60kph). carry out full crash simulation with our system incorporated into the vehicle at 37.2823mph (60kph) and ensure system functions as normal after impact.

Table 9: Code of Practice

11 Discussion

Use of TorqueDrive provides manufacturers with tangible weight reductions which offers significantly improved electric vehicle driving range, whilst the torque vectoring differential provides performance benefits such as increased traction and acceleration when cornering. Stability control methods and signal conditioning enhance the reliability and safety of the vehicle, with large disturbance rejection capabilities both electronically and mechanically. Design of VFDs operating on 800V systems and regenerative braking integration also provides customers with power loss reduction.

In comparison to rival competitors such as Rivian, TorqueDrive's improved user experience through extended driver options, such as regenerative braking on an adjustable scale and enhanced user options will appeal to vehicle manufacturers. Also, the flexibility of product integration into a multitude of vehicles, with potential for variation between 2 and 4 motors using the same core components adds potential for expansion into a wider market.

Developments in the control algorithm could improve performance, such as optimising the sliding mode control or improving the 2DoF model to a 7DoF model. This has been considered in the design, where updates can be flashed to the microcontroller. Further changes to the PCB microcontroller to use more advanced CPU architecture or communication protocols while operating at a faster clock rate could reduce latency beyond 12ms. Currently, the sealants and adhesives used to construct the casings release Volatile Organic Compounds (VOCs) during decomposition, which can be harmful on their own, or react with other gases to form other pollutants. As both are vital to the construction of the casing, and the subsequent protection of the PCB, the minimal amount of VOCs released during the deconstruction of the casing is unavoidable. Moving forward, sustainability improvements could be achieved through the development of a sealant or adhesive that performs functionally in the same way as the two currently in use, but that does not produce the same VOCs upon deconstruction.

12 Conclusion

This report details the successful design of an electronic differential capable of simulating the functionality of a mechanical differential, with a 95% weight reduction and a 92% latency improvement. The product will be fully integrated into the vehicle and is adaptable to different models and customer requirements.

An Electronic Control Unit (ECU) for torque distribution capable of stabilising non-linear vehicle dynamics within 0.45 seconds has been designed using sliding mode control. This algorithm is flashed onto the ATSAME54P20A-VAO microcontroller on the PCB to compute the torque values for each individual motor. Signal conditioning circuits have been carefully developed and RTI offset voltage has been minimised to $1.5\mu V$. Comprehensive stress testing for sufficient failure types has designed the casing for both the ECU and VFD, achieving a FoS of 3 throughout.

A Variable Frequency Drive (VFD) circuit has been successfully designed on a PCB board, capable of changing the motor stator frequency and output torque values. The PCB board is securely fixed to a designed VFD housing unit which itself will be mounted on the chassis of the vehicle. Further, a fan air cooling system has been designed within the VFD casing capable of maintaining a worst case PCB temperature 10K below the critical temperature.

Sustainability considerations for both the ECU and VFD led to aluminium casings, which is >95% recyclable. Outsourced die casting helps prevent waste, and ensures rapid manufacturing ready for mass production. Using thermal adhesives to fix parts of the casings together reduces the need for an energy intensive welding process.

A comprehensive business plan has been formed for the new company TorqueDrive to sell electronic differentials to the EV market. This includes a product gross margin of 57.3% and appropriate debt financing of £1 million to set up TorqueDrive. The sales strategy revolves around winning contracts with vehicle manufacturers for integration with vehicles in production, and managing to extend these contracts when completed.

References

- [1] Yousuf. *DIFFERENTIAL: 9 TYPES OF DIFFERENTIALS & HOW THEY WORK?* 2022. URL: https://www.theengineerspost.com/differential/?utm_content=cmp-true.
- [2] *Electric SUV market.* (Accessed on 03/16/2023). URL: <https://www.openpr.com/news/2824241/electric-suv-market-size-is-estimated-to-reach-usd-320-billion>.
- [3] *CAN Bus Explained - A Simple Intro [2023] – CSS Electronics.* (Accessed on 03/16/2023). URL: <https://www.csselectronics.com/pages/can-bus-simple-intro-tutorial>.
- [4] *SAM D5x/E5x Family Data Sheet.* (Accessed on 03/16/2023). URL: <https://ww1.microchip.com/downloads/aemDocuments/documents/MCU32/ProductDocuments/DataSheets/SAM-D5x-E5x-Family-Data-Sheet-DS60001507.pdf>.
- [5] *Home AUTOSAR.* (Accessed on 03/16/2023). URL: <https://www.autosar.org/>.
- [6] *ATA6560/1 High-Speed CAN Transceiver with Standby Mode CAN FD Ready Data Sheet.* (Accessed on 03/16/2023). URL: <https://ww1.microchip.com/downloads/aemDocuments/documents/OTH/ProductDocuments/DataSheets/20005991B.pdf>.
- [7] Walt Kester. *Practical Design Techniques for Sensor Signal Conditioning.* Analog Devices, 1999. ISBN: 0-916550-20-6.
- [8] Irwin A. Diaz-Diaz and Ilse Cervantes. “Design of a Flexible Analog Signal Conditioning Circuit for DSP-Based Systems”. In: *Procedia Technology* 7 (2013). 3rd Iberoamerican Conference on Electronics Engineering and Computer Science, CIECC 2013, pp. 231–237. ISSN: 2212-0173. DOI: <https://doi.org/10.1016/j.protcy.2013.04.029>. URL: <https://www.sciencedirect.com/science/article/pii/S2212017313000303>.
- [9] J.L. Schmalzel and D.A. Rauth. “Sensors and signal conditioning”. In: *IEEE Instrumentation & Measurement Magazine* 8.2 (2005), pp. 48–53. DOI: [10.1109/MIM.2005.1438844](https://doi.org/10.1109/MIM.2005.1438844).
- [10] *LM2596 SIMPLE SWITCHER® Power Converter 150-kHz 3-A Step-Down Voltage Regulator datasheet (Rev. F).* (Accessed on 03/16/2023). URL: https://www.ti.com/lit/ds/symlink/lm2596.pdf?ts=1678875750970%5C&ref_url=https%5C%253A%5C%252F%5C%252Fwww.ti.com%5C%252Fproduct%5C%252Fde-de%5C%252FLM2596.
- [11] *Beyond Design: Copper Pours in High-speed Design.* (Accessed on 03/16/2023). URL: <https://wwwpcb.ICONN007.com/index.php/article/132292/beyond-design-copper-pours-in-high-speed-design/132295/?skin=design>.
- [12] *Use PCB Teardrops to Increase Yield & Design Quality / Altium Designer.* (Accessed on 03/16/2023). URL: <https://resources.altium.com/p/how-to-increase-design-yield-quality-with-teardrops#why-use-pcb-teardrops>.

- [13] *Embedded Trace Macrocell Architecture Specification*. (Accessed on 03/16/2023). URL: <https://developer.arm.com/documentation/ihi0014/q/Introduction/About--Embedded-Trace-Macrocells>.
- [14] Ehsan Hashemi et al. “A comprehensive study on the stability analysis of vehicle dynamics with pure/combined-slip tyre models”. In: *Vehicle System Dynamics* 54.12 (2016), pp. 1736–1761. DOI: 10.1080/00423114.2016.1232417. URL: <https://doi.org/10.1080/00423114.2016.1232417>.
- [15] João Pedro Marques Antunes. “Torque Vectoring for a Formula Student Prototype”. Master’s thesis. City, Country: University Name, June 2017.
- [16] Yitong Song et al. “Direct-yaw-moment control of four-wheel-drive electrical vehicle based on lateral tyre-road forces and sideslip angle observer”. In: *IET Intelligent Transport Systems* 13.2 (2019), pp. 303–312. DOI: <https://doi.org/10.1049/iet-its.2018.5159>. eprint: <https://ietresearch.onlinelibrary.wiley.com/doi/pdf/10.1049/iet-its.2018.5159>. URL: <https://ietresearch.onlinelibrary.wiley.com/doi/abs/10.1049/iet-its.2018.5159>.
- [17] Shiang-Lung Koo, Han-Shue Tan, and Masayoshi Tomizuka. “Nonlinear Tire Lateral Force versus Slip Angle Curve Identification”. In: *SAE International Journal of Passenger Cars-Mechanical Systems* 4.1 (2011), pp. 299–308.
- [18] *The PID Controller & Theory Explained*. (Accessed on 03/16/2023). URL: <https://www.ni.com/en-gb/innovations/white-papers/06/pid-theory-explained.html>.
- [19] Sarah Spurgeon. “Sliding mode control: a tutorial”. In: *International Journal of Control* 82.2 (2009), pp. 222–250.
- [20] Rajesh Rajamani. *Vehicle Dynamics and Control*. Ed. by Frederick F. Ling. Mechanical Engineering Series. Springer, 2011.
- [21] BJ Varocky. *Benchmarking of regenerative braking for fully electric car*. Tech. rep. Unpublished report, 2011.
- [22] Wansu Song et al. “Effects of reinforcing fibers on airborne particle emissions from brake pads”. In: *Wear* 484-485 (2021), p. 203996. ISSN: 0043-1648. DOI: <https://doi.org/10.1016/j.wear.2021.203996>. URL: <https://www.sciencedirect.com/science/article/pii/S0043164821003847>.
- [23] James Allen. *What is an ECU (electronic control unit) in a car?* Feb. 2023. URL: <https://www.carwow.co.uk/guides/glossary/what-is-an-ecu-in-a-car%5C#:~:text=They%5C%20shouldn't%5C%20be%5C%20too,listed%5C%20in%5C%20your%5C%20owner's%5C%20manual..>

- [24] Louis Smith. *Understanding speed bump regulations in the UK*. Mar. 2022. URL: <https://streetsolutionsuk.co.uk/blogs/news/speed-bump-regulations-uk>.
- [25] Louis C. Lundstrom. “The Safety Factor in Automotive Design”. In: National West Coast Meeting (1966), p. 6. ISSN: 0148-7191. DOI: 10.4271/660539. URL: <https://doi.org/10.4271/660539>.
- [26] *Speeding and analysis of speed in crash investigation*. Mar. 2023. URL: <https://www.arrivealive.mobi/speeding-and-analysis-of-speed-in-crash-investigation>.
- [27] James Ruppert. *Car servicing: How long should car parts last? part 2*. Apr. 2017. URL: <https://www.motoreeasy.com/magazine/102/Car-Servicing-How-long-should-car-parts-last-Part-2%5C#:~:text=Often%5C%20it%5C%20is%5C%20sections%5C%2C%5C%20such,where%5C%20the%5C%20vehicle%5C%20is%5C%20used..>
- [28] *Grade 10.9 bolts*. 1AD. URL: <https://www.uboltit.com/bolts/hex-bolts/metric-grade-10-9-bolts.html%5C#:~:text=Grade%5C%2010.9%5C%20metric%5C%20bolts%5C%20are,strength%5C%20and%5C%20good%5C%20wear%5C%20resistance..>
- [29] *Specification of SAE J429 grade 8 Fastener*. Nov. 2022. URL: <https://www.high-strength-steel.com/specification-of-sae-j429-grade-8-fastener>.
- [30] *Benefits of Designing Your Own Printed Circuit Board*. (Accessed on 03/16/2023). URL: <https://coruzant.com/tech/benefits-of-designing-your-own-printed-circuit-board/%5C#:~:text=Fewer%5C%20Labor%5C%20Costs%5C&text=Custom%5C%20PCBs%5C%20generally%5C%20require%5C%20less,more%5C%20often%5C%20than%5C%20you%5C%20think..>
- [31] *Single-Phase vs. Three-Phase Power Explanation / Fluke*. (Accessed on 03/16/2023). URL: <https://www.fluke.com/en-us/learn/blog/power-quality/single-phase-vs-three-phase-power%5C#:~:text=Three%5C%2Dphase%5C%20power%5C%20is%5C%20a,use%5C%20a%5C%20three%5C%2Dphase%5C%20supply..>
- [32] *What is VFD, How it works? - VFD working principle*. (Accessed on 03/16/2023). URL: <http://www.vfds.org/what-is-vfd-how-it-works-964803.html>.
- [33] *0900766b813b04e3.pdf*. (Accessed on 03/16/2023). URL: <https://docs.rs-online.com/92fc/0900766b813b04e3.pdf>.
- [34] *Film Capacitors Metallized Polypropylene Film Capacitors (MKP) - B32651 ... B32656*. (Accessed on 03/16/2023). URL: <https://docs.rs-online.com/8176/0900766b81399c64.pdf>.
- [35] *APT13003H*. (Accessed on 03/16/2023). URL: <https://docs.rs-online.com/4a5c/0900766b81517c7b.pdf>.

- [36] *Inside Variable Frequency Drive (VFD) Panel: Configuration, Schematics and Troubleshooting / EEP*. (Accessed on 03/16/2023). URL: <https://electrical-engineering-portal.com/variable-frequency-drive-vfd-panel-configuration-schematics-troubleshooting>.
- [37] *How is a pulse width modulation signal generated?* (Accessed on 03/16/2023). URL: <https://www.vedantu.com/question-answer/a-pulse-width-modulation-signal-generated-class-12-physics-cbse-615d116ddb87cf15af60bec8>.
- [38] *LMV321A-Q1, LMV358A-Q1, LMV324A-Q1 Automotive Low-Voltage Rail-to-Rail Output Operational Amplifiers datasheet (Rev. C)*. (Accessed on 03/16/2023). URL: https://www.ti.com/lit/ds/symlink/lmv321a-q1.pdf?HQS=dis-mous-null-mousermode-dsf-pf-null-wwe&ts=1678931627088%5C&ref_url=https%5C%253A%5C%252F%5C%252Fwww.mouser.co.uk%5C%252F.
- [39] *How is PCB Made in China? - Nova*. (Accessed on 03/16/2023). URL: <https://novaenginc.com/how-is-pcb-made-in-china/%5C#:~:text=The%5C%20PCB%5C%20board%5C%20is%5C%20manufactured,sent%5C%20to%5C%20the%5C%20drilling%5C%20unit..>
- [40] *dcrcw-1762150.pdf*. (Accessed on 03/16/2023). URL: <https://www.mouser.co.uk/datasheet/2/427/dcrcw-1762150.pdf>.
- [41] *A700000006716792.pdf*. (Accessed on 03/16/2023). URL: <https://docs.rs-online.com/a435/A700000006716792.pdf>.
- [42] J. Schutze, H. Ilgen, and W.R. Fahrner. “An integrated micro cooling system for electronic circuits”. In: *IEEE Transactions on Industrial Electronics* 48.2 (2001), pp. 281–285. DOI: 10.1109/41.915406.
- [43] *412FH-RS0 / ebm-papst 400 F Series Axial Fan, 12 V dc, DC Operation, 9m³/h, 800mW, 40 x 40 x 10mm / RS*. (Accessed on 03/15/2023). URL: <https://uk.rs-online.com/web/p/axial-fans/7009231>.
- [44] P. W. Bearman. “Vortex shedding from oscillating bluff bodies”. In: *Journal of Fluids and Structures* 4.2 (1984), pp. 125–159.
- [45] *1 new message*. (Accessed on 03/16/2023). URL: <https://www.renhotecpro.com/product/ev-high-voltage-connector-3-pin-plug-35a-straight-metal-shield-plug-3-6mm-hvil-series/%5C#tab-id-1>.
- [46] Fbs. *The world's most sustainable building material? aluminium*. May 2020. URL: <https://fbsprofilati.it/sustainable-products/%5C#:~:text=Aluminium%5C%20is%5C%20arguably%5C%20the%5C%20most,creates%5C%20primary%5C%20aluminum..>

- [47] ASM Metal Recycling. *Is aluminium environmentally friendly? the Green Metal*. Mar. 2021. URL: <https://www.asm-recycling.co.uk/blog/why-is-aluminium-environmentally-friendly/>#:~:text=Known%5C%20as%5C%20the%5C%20green%5C%20metal,its%5C%20production%5C%20from%5C%20raw%5C%20materials..
- [48] Vincent Doegee. *What is the carbon footprint of steel?* Mar. 2023. URL: <https://www.sustainable-ships.org/stories/2022/carbon-footprint-steel>#:~:text=Steel%5C%20carbon%5C%20footprint%5C&text=The%5C%20IEA%5C%20estimates%5C%20that%5C%20direct,of%5C%20CO2%5C%20per%5C%20ton%5C%20steel.
- [49] SMARTPLY OSB. URL: <https://mdfosb.com/en/products/smartply-osb>.
- [50] Nick Brummel. *How much does a car transmission weigh?* 2019. URL: <https://www.quora.com/How-much-does-a-car-transmission-weigh>#:~:text=That%5C%20will%5C%20vary%5C%20greatly%5C%20depending,passenger%5C%20cars%5C%20and%5C%20light%5C%20trucks..
- [51] Arthur L. Robinson, Alan I. Taub, and Gregory A. Keoleian. “Fuel efficiency drives the auto industry to reduce vehicle weight”. In: *MRS Bulletin* 44.12 (2019), pp. 920–923. ISSN: 1938-1425. DOI: 10.1557/mrs.2019.298. URL: <https://doi.org/10.1557/mrs.2019.298>.
- [52] *What is quad-motor drive? - support center*. URL: <https://rivian.com/support/article/what-is-quad-motor-drive>.
- [53] *Rivian Drive Systems, decoded by Rivian - Rivian Stories*. URL: <https://stories.rivian.com/difference-between-r1-drive-systems>.

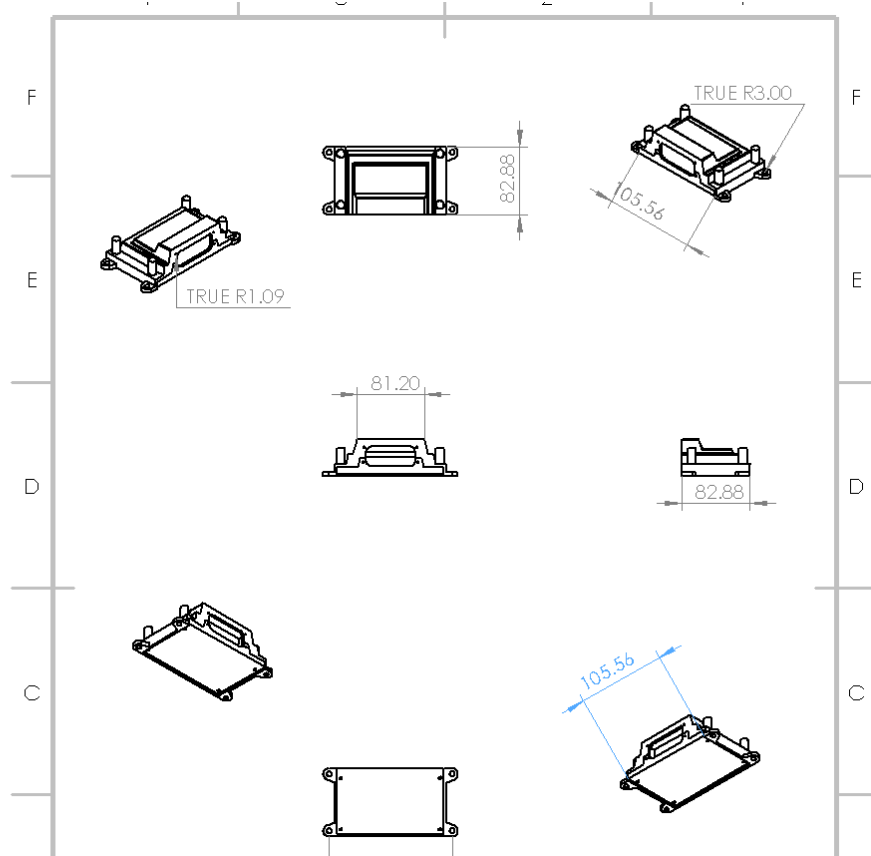
Appendices

Appendix A: Bill Of Materials

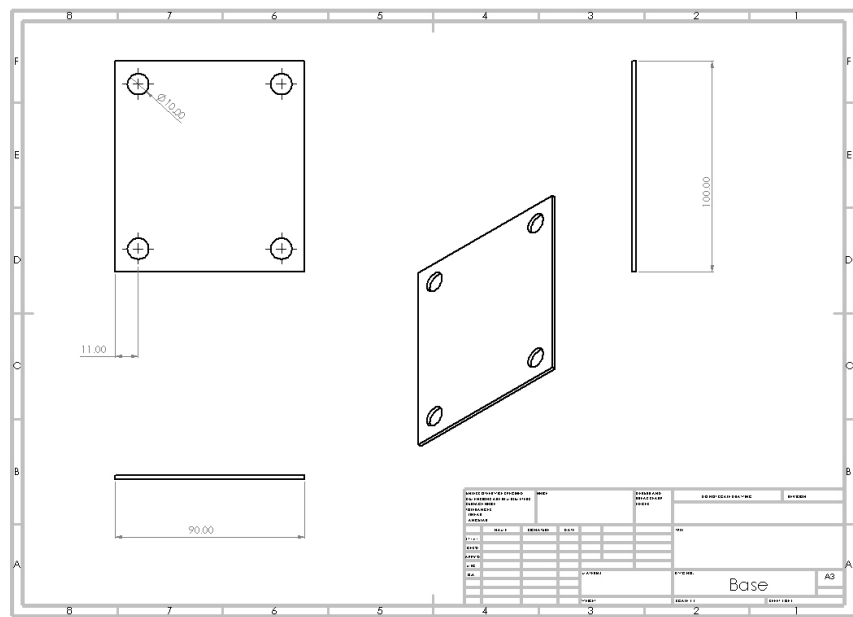
Material/component needed	Price per unit	Number Required	Total Cost
ECU			
Aluminum sheet (AA7075)	£31.21 per AA7075 sheet (20cmx30cm, 2mm thickness)	2	£62.42
Soldering iron	£15.71 per	1	£15.71
Silicone Sealant	£5.49 per bottle	1	£5.49
Silicone thermal adhesive	£83.02 per	1	£83.02
Metric grade 10.9 bolts (M10 x 60mm)	£0.70	4	£2.80
ATSAME54P20A	£6.48	1	£6.48
ATA6561	£0.31	2	£0.52
1-776163-1Connector	£12.43	1	£12.43
Electrolytic Capacitors	£0.502x2 + 0.084x2	2	£1.17
Inductors 5050	£1.04	1	£1.04
Inductors 4040	£0.344 x 2	2	£0.69
3.3 Converter	£4.42	1	£4.42
5 Converter	£3.93	1	£3.93
Ref 195	£3.79 x 2	2	£7.58
AD620	£6.98	1	£6.98
OP213ES	£12.81	2	£25.62
1N5822	£0.11	2	£0.21
SD12_SOD323	£0.26	20	£5.18
HC49 Crystal	£0.22	2	£0.43
32k Crystal	£1.19	1	£1.19
Small Capacitors	£0.01	25	£0.30
Small Resistors	£0.12	30	£3.63
Small Inductor	£0.05	10	£0.53
PCB	£5	1	£5.00
Total			£255.67
4 VFDs			
ebm-papst 400 F series axial fan	£37.45	8	£299.60
AA7075 sheet	£31.21 per AA7075 sheet (20cmx30cm, 2mm thickness)	4	£124.84
Metric grade 10.9 bolts (M10 x 60mm)	£0.70	16	£11.20
Silicone thermal adhesive	£83.02	1	£83.02
Silicone Sealant	£5.49	1	£5.49
Op Amps	£1.38	16	£22.08
1k Resistor	£0.07	4	£0.29
5k Resistor	£0.70	4	£2.78
Diode	£1.64	4	£6.58
Transistor	£0.49	4	£1.96
Total			£546.23
Wiring			
cables - high voltage	£30/m	2m	£60.00
connectors - AMPSEAL	£13.00	1	£13.00
low voltage cable	£15/m	20m	£30.00
connectors - HVLA	£22.00	8	£176.00
Total			£279.00
Running Total			£1,080.90

Full Product Bill of Materials

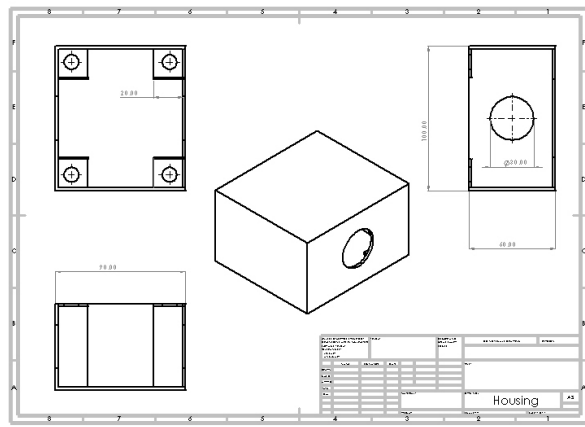
Appendix B: Manufacturing Drawings



Manufacturing Drawing For The ECU Casing.



VFD Housing Base



VFD Case

C: Linear Bicycle Model Assumptions

1. Velocity of the vehicle's centre of gravity is considered constant along the longitude of its trajectory.
2. All lifting, rolling, and pitching motion will be neglected.
3. The mass of the vehicle is assumed to be at the centre of its gravity.
4. Front and rear tyres will be represented a single tyre, one each axle.
5. Aligning torque resulting from the side slip angle will be neglected
6. The wheel-load distribution between front and rear axles is assumed to be constant.
7. The longitudinal forces on the tyres, resulting from the assumption of a constant longitudinal velocity, will be neglected.

D: Reaching Law Derivation

$$\begin{aligned}
 s &= \lambda(x - x_{\text{des}}) = \lambda e \\
 \dot{s} &= \lambda(\dot{x} - \dot{x}_{\text{des}}) = \lambda \dot{e} \\
 \dot{s} &= \lambda(Ax + Bu + C\delta - \dot{x}_{\text{des}}) + d
 \end{aligned}$$

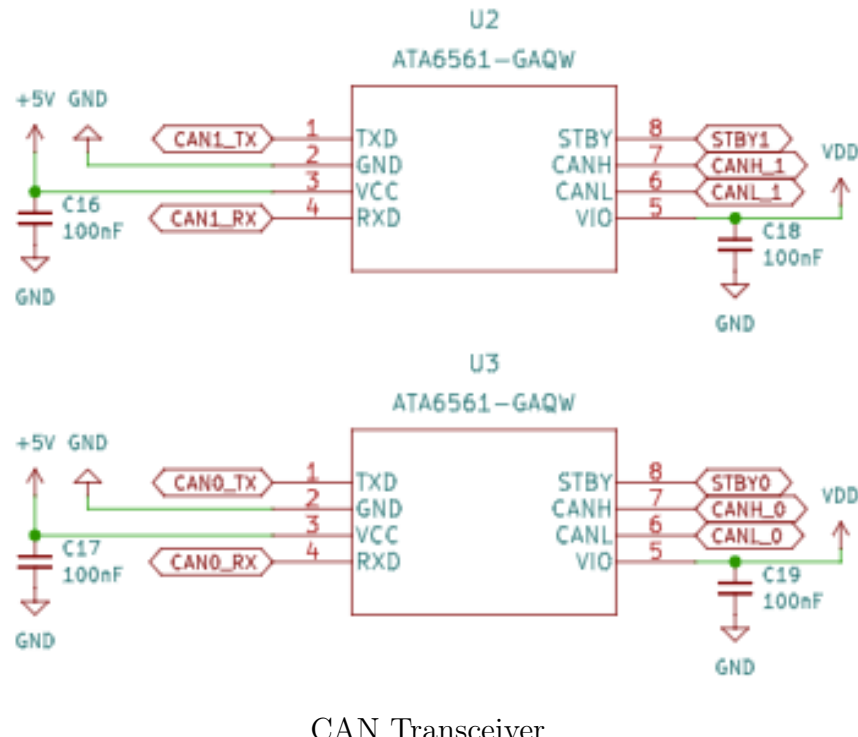
Select u to cancel with \dot{s} :

$$\begin{aligned}
 u &= \beta^{-1}(-Ax - C\delta + x_{\text{des}} + \lambda^{-1}\nu) \\
 \dot{s} &= d + v
 \end{aligned}$$

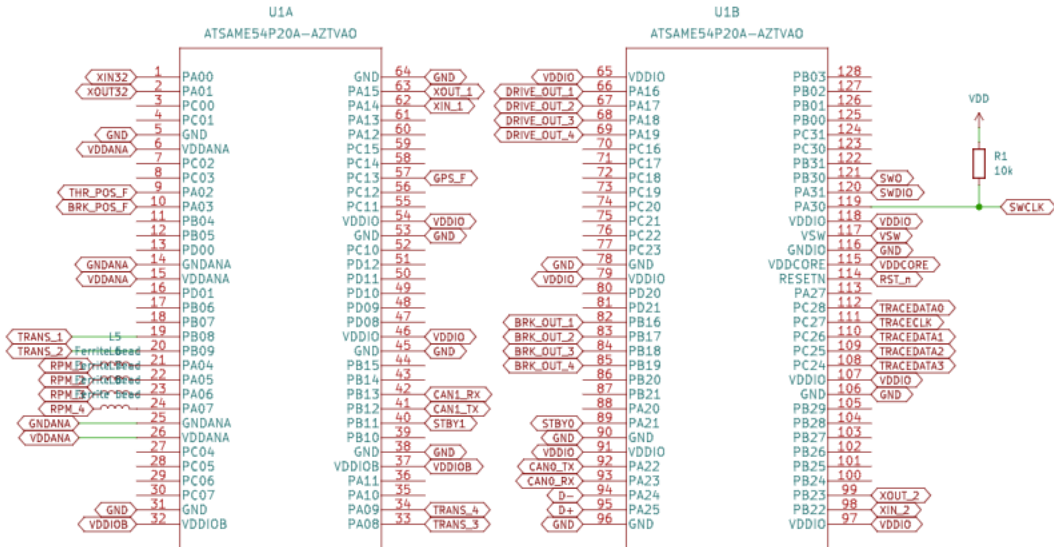
Using Lyapunov Function, σ is maximum disturbance:

$$\begin{aligned}
 s\dot{s} &= s(d + v) \leq s\sigma \text{sign}(s) + sv \\
 u &= B^{-1}(-Ax - C\delta + x_{\text{des}} + \lambda^{-1}(\sigma + n) \text{sign}(s))
 \end{aligned}$$

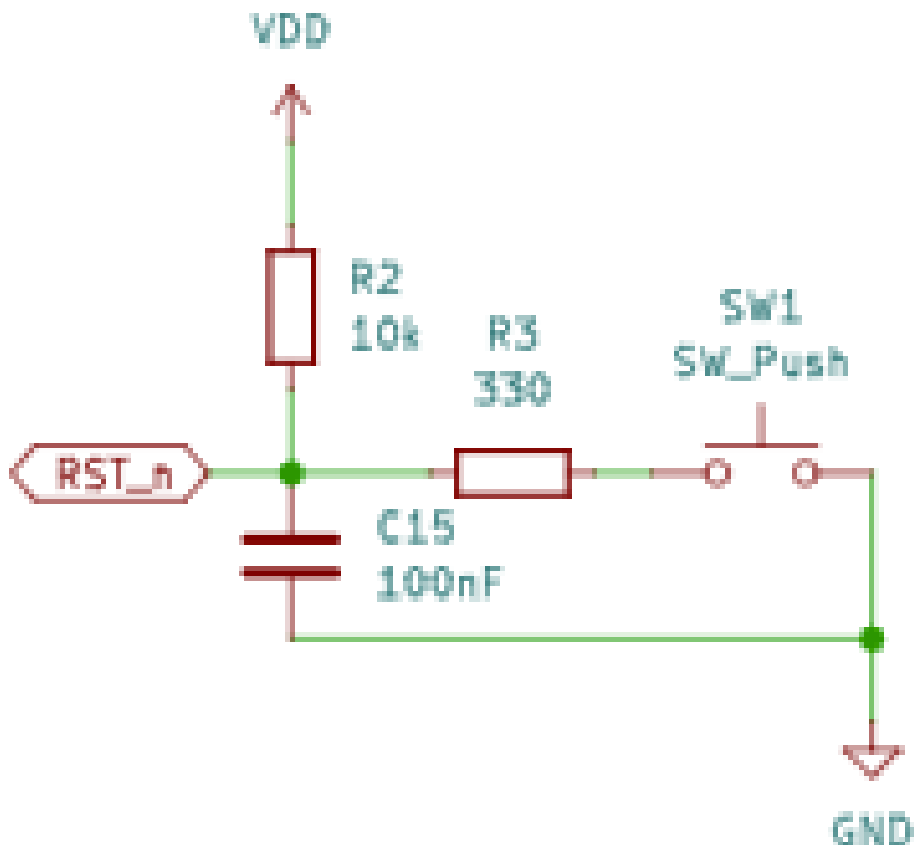
Appendix E: PCB Schematics



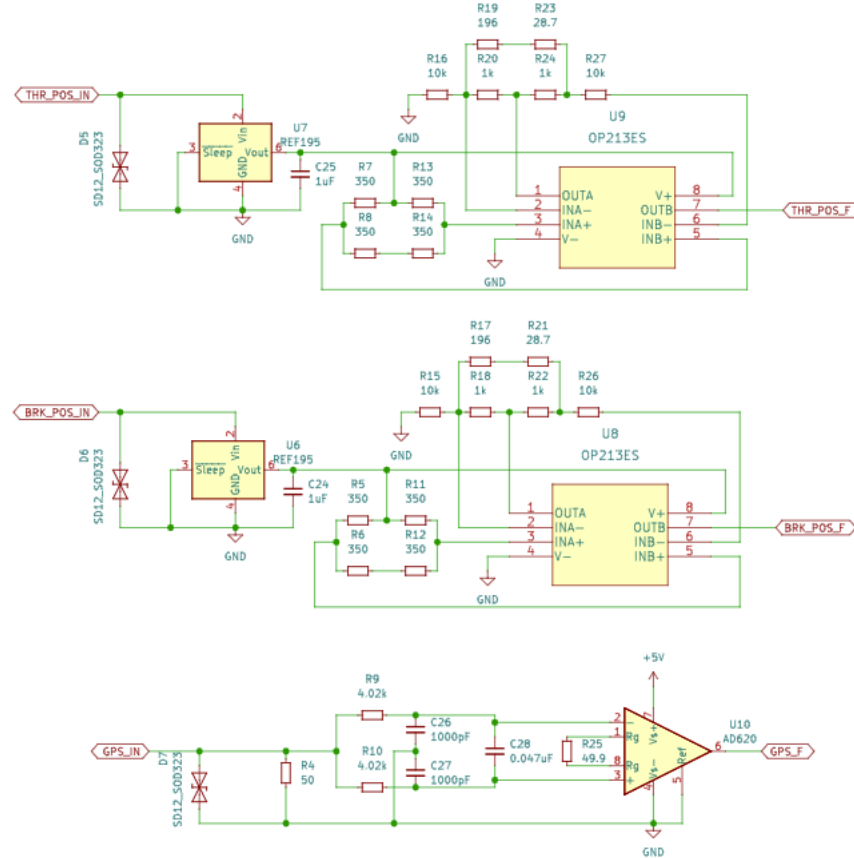
CAN Transceiver



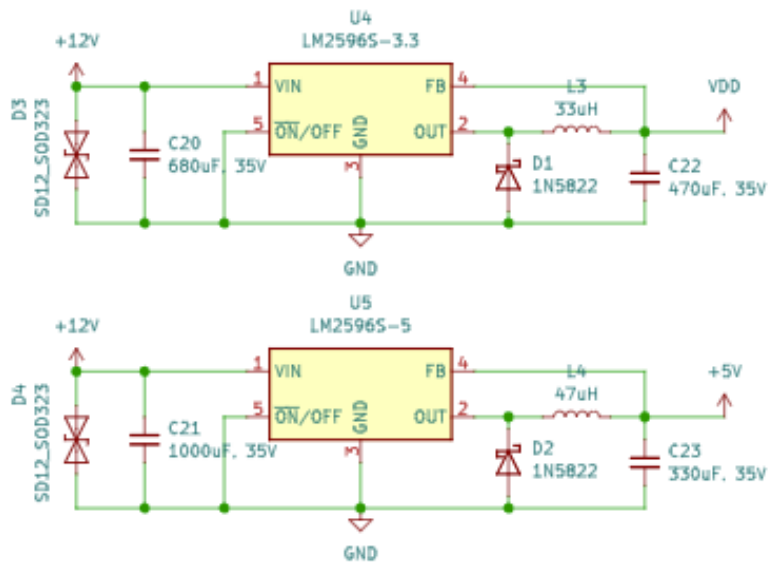
Micrcontroller



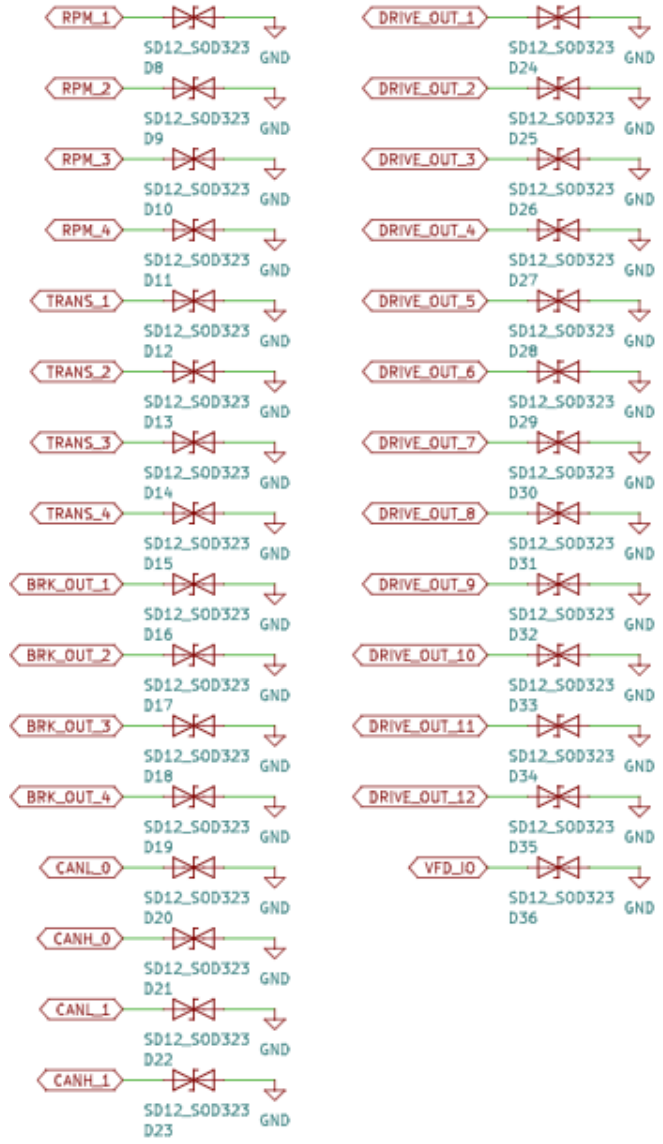
Active Low Reset Circuit



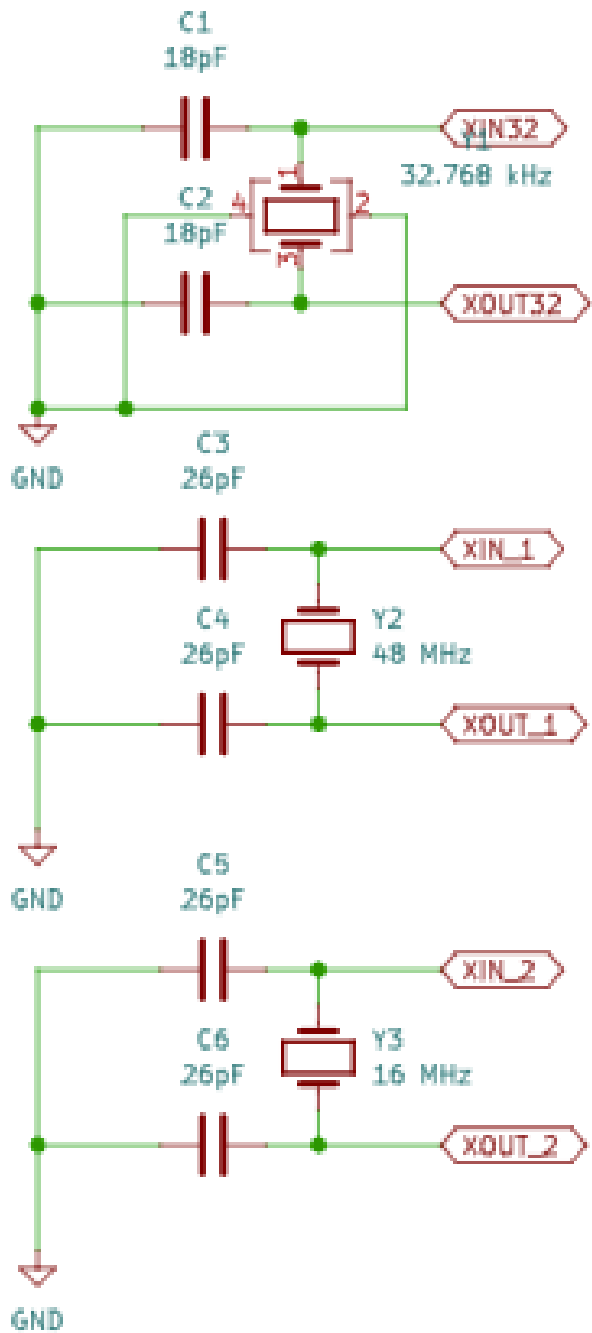
Signal Conditioning



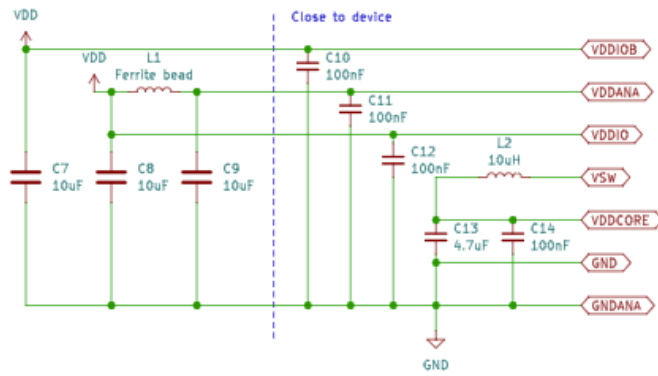
Step-Down Voltage Regulator



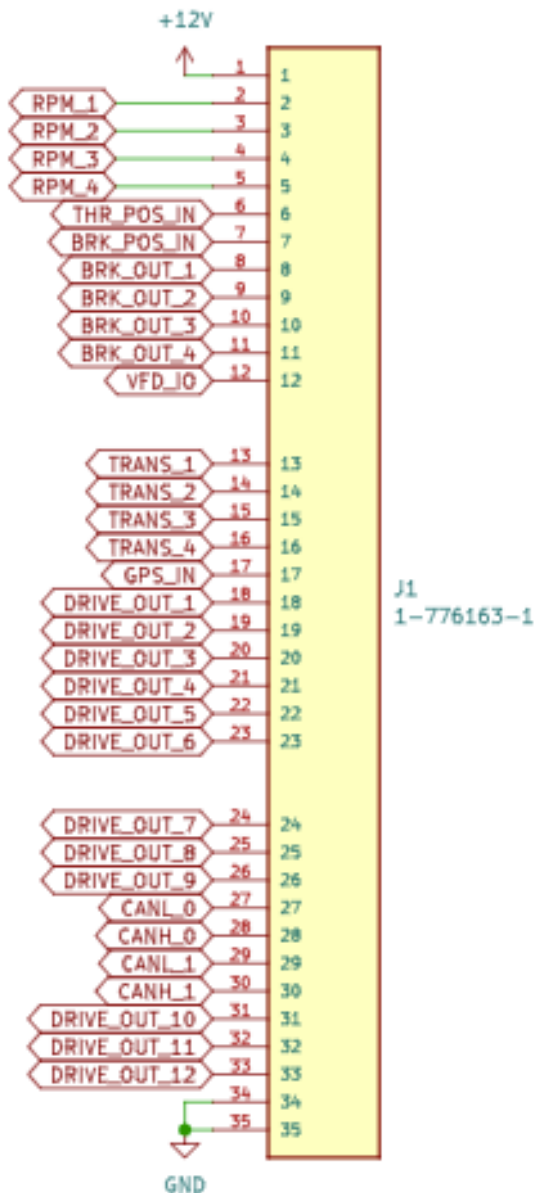
ESD Protection



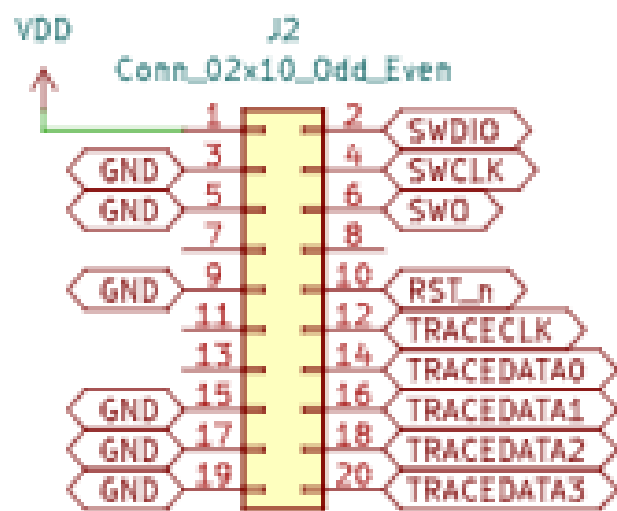
Crystal Oscillators



Power Supply Connection For Switching Regulators



Connector



Cortex Debug and EDM